EUROPEAN COMMISSION

Community Research

SEVENTH FRAMEWORK PROGRAMME

CARBOWASTE

Treatment and Disposal of Irradiated Graphite and Other Carbonaceous Waste

Grant Agreement Number: FP7-211333

Soxhlet Extraction of irradiated graphite

Author(s): J. Ruediger, D. Vulpius, K. Baginski
Forschungszentrum Juelich, IEF-6

Date of first issue of this report : 12/07/2011

Start date of project : **01/04/2008** Duration : **48 Months**

Project co-funded by the European Commission under the Seventh Framework Programme (2007 to 2011) of the European Atomic Energy Community (EURATOM) for nuclear research and training activities		
Dissemination Level		
PU	Public	
RE	Restricted to the partners of the CARBOWASTE project	
CO	Confidential, only for specific distribution list defined on this document	**X**

Distribution list

Person and organisation name and/or group	Comments
WP4 Partners	

CARBOWASTE		
Work package: 4 **Task: :** 4.3	**CARBOWASTE document no:** CARBOWASTE-1107-T-4.3.5-b	**Document type:** T=Technical Report
Issued by: Forschungszentrum Juelich, Germany **Internal no.:** CW1107-T-4-3-5-b		**Document status:** Final

Document title
Soxhlet Extraction of irradiated graphite
Executive summary

Revisions						
Rev.	Date	Short description	Author	Internal Review	Task Leader	WP Leader
00	Dd/mm/yyyy	Issue	Name, Organisation	Name, Organisation *Signature*	Name, Organisation *Signature*	Name, Organisation *Signature*
01	01/06/2011	First issue	Ruediger	Vulpius	Vulpius	von Lensa
02		2nd Issue				

1 0. TABLE OF CONTENTS

1 0. TABLE OF CONTENTS 4
A. Introduction 6
1. Objective 6
2. Experimental Objective 6
B. General 7
1.1. The Chemical Behaviour of Graphite 7
1.2. The Radionuclides Contained in the Samples 9
2. Reactor Graphite (Merlin) 14
2.1. General 14
2.2. Samples 14
3. Reactor Graphite (AVR) 17
3.1. General 17
3.2. The Graphite of the AVR's HTR 18
3.3. Samples 19
C. Experimental section 22
1. Materials and Equipment 22
1.1. Equipment List 22
1.2. Equipment 22
2. Reagents 23
2.1. Selection of Solvents 23
2.2. Reagents Used 23
3. Preliminary Work 25
3.1. Preparation of the Extraction Thimbles 25
4. General Description of the Experiments 26
4.1. Soxhlet Extraction or Liquid Extraction 26
4.2. Separation of ^{90}Sr 30
4.3. Separation of Caesium with Ammonium Molybdophosphate (AMP) 31
• 31
4.4. Detection of Organic ^{14}Carbon 32
4.5. Determination of the Tritium Content (Merlin only): 32
5. Measuring Radionuclide Activity 33
5.1. LSC Measurement 33
5.2.γ Spectrometry 35
D. Results 37
1. Results (Merlin) 37
1.1. Measuring the Total Activity 37
1.2. Results of the γ Spectrometry 42
2. Results (AVR) 47
2.1. Results of the LSC measurements 47
2.2. Results of the γ Spectrometry 49
2.3. Separating the Individual Radionuclides 51
2.4. Comparison of the LSC Values with the γ Spectrometry Values 54
3. Comparison of the Merlin and AVR Results 55
4. Results Relevant to the Storage of the Treated Reactor Graphite 61
E. Summary and Outlook 62
F. Appendix 64

1. List of Figures/Tables and Equations..... 64
1.1. List of Figures 64
- 1.3. List of Equations 66
- 2. Figures: 67
  - 2.1. Figures (Merlin) 67
  - 2.2. Figures (AVR) 69
- 3. Tables: 74
  - 3.1. Tables (Merlin) 74
  - 3.2. Tables (AVR) 78

G. References 82

A. Introduction

1. Objective

This study is aimed at investigating the extent to which contaminated reactor graphite can be decontaminated using solid-liquid extraction. To do so, a series of tests involving the use of inorganic as well as organic solvents will be performed to remove the radionuclides contained in the reactor graphite samples to such an extent that the remaining quantities of radionuclides are below the legally permissible limits. For this reason, it will be necessary to determine or know and compare the individual samples' activity inventory before and after the tests.

The samples analysed in the tests were removed from the decommissioned research reactor FRJ-1, Merlin for short, and the prototype reactor of the Reactor Working Group (Arbeitsgemeinschaft Versuchsreaktor), AVR for short. These reactors are located on or next to the premises of the Forschungszentrum Jülich (Jülich Research Centre) in Staatsforst Stetternich, Germany.

In the run up to the study, the age of the Merlin reactor and the associated lack of accurate information about the reactor graphite samples used proofed to be a problem. The reactor was developed in the United Kingdom in approximately the mid-fifties, and built on the premises of the former Kernforschungsanlage (KFA) Jülich (Jülich Nuclear Research Facility) at the start of the sixties. In contrast to the AVR's high temperature reactor, which was developed in Germany, the materials used in the construction of the FRJ-J had never been an object of investigation and had therefore not been taken into consideration in the subsequent literature.

2. Experimental Objective

This study comprises 2 series of tests. The aim of the first series of tests is to determine which solvents are most suitable for decontaminating reactor graphite using solid-liquid extraction. The samples used for this series of tests originated from the research reactor Merlin.

The findings from these tests are then to be applied in a second series of tests with the aim of decontaminating the more heavily contaminated reactor graphite from the AVR which contains more radionuclides.

B. General

1.1. The Chemical Behaviour of Graphite

The chemical behaviour of non-irradiated graphite

Graphite is resistant to aqueous salt solutions, acids and alkali, but not to strongly oxidising acids. In conjunction with oxidants, concentrated nitric and sulphuric acid will therefore corrode graphite. This process leads to the formation of graphite salts. On contact with chlorine dioxide or dimanganese heptaoxide, these salts can turn into graphite oxide. When fully oxidised, it turns into graphite acid ($C_8O_2(OH)_2$), a compound of OH groups with an only slightly acidic character. At 200 - 300°C, graphite acid releases CO, CO_2 and H_2O and decays into an "extremely unstable graphite oxide with a low oxygen content"[19]. In the presence of vanadium catalysts, graphite reacts with concentrated nitric acid HNO_3 to form mellitic acid $C_6(COOH)_6$, and graphite dissolves in molten metal such as in iron melts.

Since graphite is otherwise very inert towards all solvents, the reaction usually only takes place at the surface. This leads to a kind of surface corrosion. The smaller the grain size of the graphite particles in a sample, the larger the surface that can be wetted with solvent and the greater the number of radionuclides that can be dissolved from the reactor graphite.

Some of substances graphite reacts with that are relevant to the following tests are summarized in table 1 below.

Table 1: Reactions with graphite

Substance	Compatibility or reaction
Air or O_2	Oxidation (negligible below approx. 300°C)
CO_2	Oxidation at approx. 600°C (when irradiated, at approx. 500°C)
H_2	Formation of hydrocarbon at 600°C (when irradiated, at approx. 500°C)
H_2O, $D_2O_{(liquid)}$	No reaction
H_2O, $D_2O_{(vapour)}$	Oxidation at approx. 600°C (when irradiated, at approx. 500°C)
Organic liquids	Generally no reaction
HNO_3	Oxidation to nitrates, which can lead to the formation of mellitic acid (benzenehexacarboxylic acid)
H_2SO_4	Oxidation to graphite hydrogen sulphate in the presence of CrO_3, HNO_3 or $(NH_4)_2S_2O_8$

Important carbon compounds (random selection):

- Carbide (form at temperatures from 800°C)
- Carbonate (form at temperatures from 540°C)
- Oxides (form at temperatures from 600°C)
- Acetates
- Volatile compounds (form at temperatures from 800°C)

The following illustration shows the compounds that graphite can form:

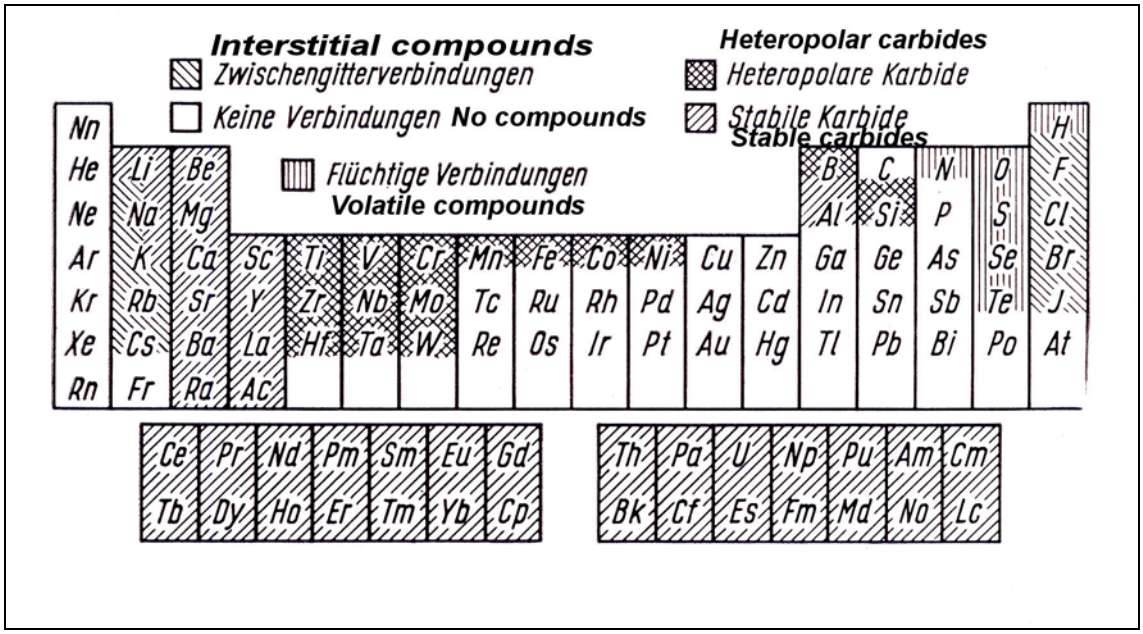

Figure 6: Possible compounds that reactor graphite can form [14]

The Chemical Behaviour of Irradiated Graphite

After being subjected to 4 * 10^{20} n/cm^2 neutron radiation, the graphite's subsequent oxidation in the oxygen gas stream at 250°C to 450°C showed that its activation energy of 2.12 eV when not irradiated dropped to 1.57 eV after radiation. (see curve a in figure 7).

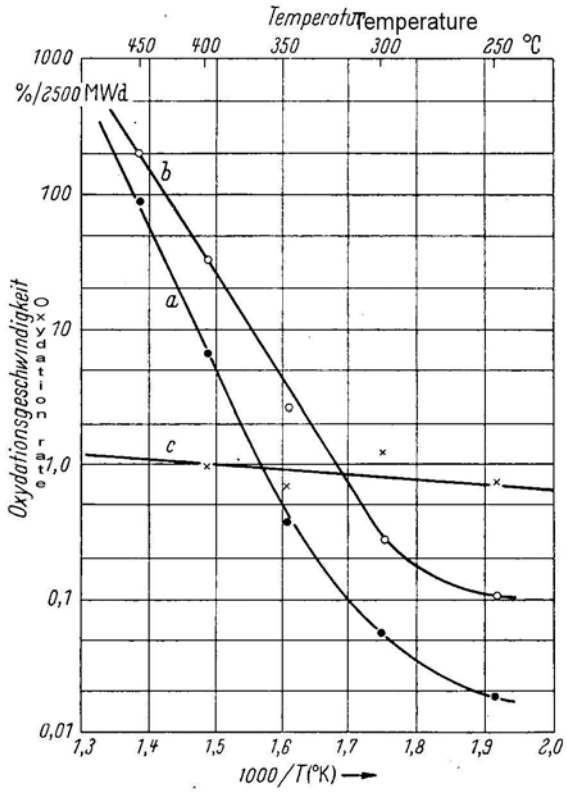

Figure 7: Oxidation speed of graphite [25][2]

Another test showed that this irradiated graphite is oxidized more strongly (curve c) than non-irradiated graphite (curve a) when applying γ radiation ($\Phi = 6*10^{12}$ n/cm^2*s) from a ^{60}Co source. While a temperature treatment of 600°C did not produce any changes in the graphite's oxidation behaviour, a temperature treatment of 2800°C made the oxidation behaviour to return to the normal value.

1.2. The Radionuclides Contained in the Samples

<u>Formation/characteristics of the radionuclides contained in the samples</u>

^{3}H: Tritium

Tritium is a pure β^- emitter with a max. energy of 18.6 keV (average energy of 5.7 keV).

It is created during the following neutron reactions:

- Ternary fission of heavy cores in nuclear fuel (e.g. ^{235}U, ^{238}U)
- Neutron reactions with light elements such as deuterium, ^{3}He (AVR), ^{6}Li, ^{9}Be, ^{10}Be, ^{11}B and ^{12}C, which are formed in coolants (only AVR), moderators and control rods as either material components or contaminants:

[2] (1 MWd = Megawatt day Ξ 24000 kWh. Fully splitting 1 g U-235 releases approx. 1 MWd of energy)

$D\ (n, \gamma)\ ^{3}H$

$^{3}He\ (n, p)\ ^{3}H$

$^{6}Li\ (n, \alpha)\ ^{3}H$

$^{9}Be\ (n, \alpha)\ ^{6}Li\ (n,\alpha)\ ^{3}H$

$^{10}Be\ (n, 2\alpha)\ ^{7}Li\ (n,\alpha)\ ^{3}H$

$^{11}B\ (n, n\alpha)\ ^{7}Li\ (n,n\alpha)\ ^{3}H$

$^{12}C\ (n, \alpha)\ ^{9}Be\ (n,\alpha)\ ^{6}Li\ (n,\alpha)\ ^{3}H$

[6]

As an isotope of hydrogen, tritium has similar characteristics to ^{1}H. It can dissolve in solid materials and diffuse into them. Graphite adsorbs tritium very well. Due to the adsorption efficiency of tritium, the fuel elements of the pebble-bed reactor are coated with graphite as a barrier to prevent the tritium from leaching into the reactor's core or the cooling gas.

Tritium has almost the same characteristics as hydrogen.
In hydrogenous solvents, the radiolysis of tritium can cause tritium to exchange with hydrogen atoms:

$T_2\ (\beta^-, p)\ T + H^+$

$H^+ + T_2 \Leftrightarrow HT + T^+$

$T^+ + H\text{-}X \Leftrightarrow T\text{-}X + H^+$ etc.

This effect can, amongst others, be amplified by other beta emitters in the solution or external beta radiation. The self-labelling of organic compounds with tritium is called Wilzbach labelling [24].

^{14}C:

The ^{14}C isotope is the second most frequent radionuclide in radioactive graphite waste. It is a pure β^- emitter with an energy of 0.156 MeV.

Amongst others, it is created:
primarily when capturing neutrons from nitrogenous compounds in the air, e.g. ^{14}N (frequency 99.63%/cross section$_{n,\ p}$ 1.81 barn):

$^{14}N\ (n, p)\ ^{14}C$

About 99% of the ^{14}C in the samples is formed through this reaction.

During the neutron irradiation of the stable ^{13}C (frequency 1.1%/cross section $_{n,\gamma}$ = 0.0009) in the graphite lattice:

$$^{13}C\ (n, \gamma)\ ^{14}C$$

About 1% of the ^{14}C in the samples is formed through this reaction.

During the neutron irradiation of the stable ^{17}O (frequency 0.039%/cross section $_{n, \alpha}$ = 0.235) in the moderation water

$$^{17}O\ (n, \alpha)\ ^{14}C$$

About 0.04% of the ^{14}C in the samples is formed through this reaction.

^{60}Co: ^{60}Cobalt

^{60}Cobalt is an activation product that is formed when stable ^{59}Co from e.g. metal and concrete reactor parts and graphite contaminants, is irradiated with neutrons.
^{60}C in a sample is an indication of an activation product.

$$^{59}Co\ (n, \gamma)\ ^{60}Co$$

$E_{ß-}$= 0.318 MeV, 0.66 MeV, 1.48 MeV
E_{γ} = 0.347 MeV, 0.826 MeV, 1.173 MeV; 1.332 MeV

^{90}Sr: ^{90}Strontium

^{90}Strontium is created when uranium undergoes nuclear fission with thermal neutrons in reactors.
It is a pure β^- emitter with a half-life of 28.5 years.

$E_{ß-}$= 0.546 MeV

^{133}Ba: ^{133}Barium

^{133}Barium has the longest half-life of all unstable barium isotopes.
^{133}Ba is created during the neutron irradiation of reactor construction material e.g. in the neutron absorbers of the reactor. (Due to their high density, high contents of baryte make concrete highly absorbent to γ rays.)

$$^{132}Ba\ (n, \gamma)\ ^{133}Ba$$

E_{γ} = 0.356 MeV, 0.081 MeV, 0.303 MeV, 0.384 MeV

^{152}Eu, ^{154}Eu and ^{155}Eu: Europium

The europium isotopes ^{152}Eu, ^{154}Eu and ^{155}Eu are uranium and plutonium fission products.
They can also form as the activation products of europium and gadolinium isotopes, e.g. in the contaminants of the reactor's construction materials.

$^{151}Eu\ (n, \gamma)\ ^{152}Eu$

$^{152}Gd\ (n, \gamma)\ ^{153}Gd\ (\beta^{+})\ ^{154}Eu$

$^{154}Eu\ (n, \gamma)\ ^{155}Eu$

^{152}Eu: $E_{\beta-}$= 1.48 MeV, 0.69 MeV E_{γ} = 0.122 MeV, 0.344 MeV, 1.408 MeV; 0.964 MeV

^{154}Eu: $E_{\beta-}$= 0.89 MeV, 0.59 MeV, 0.27 MeV E_{γ} = 0.123 MeV, 1.275 MeV, 0.723 MeV; 1.005 MeV

^{155}Eu: $E_{\beta-}$= 0.247 MeV, 0.185 MeV, 0.152 MeV E_{γ} = 0.086 MeV, 0.105 MeV, 0.045 MeV; 0.060 MeV

- <u>The behaviour of the radionuclides in the reactor graphite</u>

^{3}H:

In Merlin and in the AVR, tritium is formed from the contaminants (usually lithium) during the graphite's irradiation with neutrons or outside the reactor graphite during the nuclear reaction. In the AVR or in HTR, it diffuses through the matrix graphite of the spherical fuel elements into the cooling gas. From there, the tritium can diffuse into the reactor graphite and deposit itself between the carbon atoms in the interstitial lattice sites of the graphite.

Tritium is only noticeably released by diffusion at temperatures over 400°C (see figure 8):

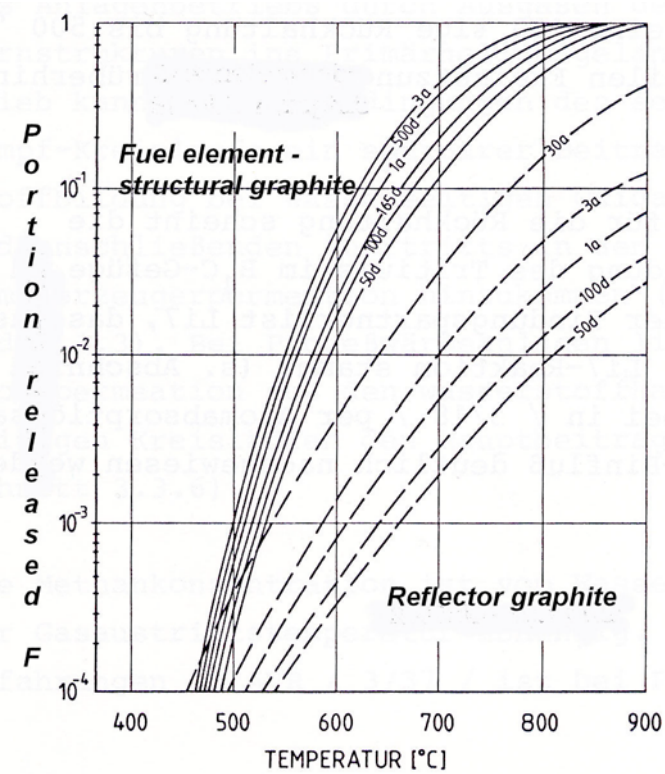

Figure 8: Release of tritium in graphite in dependence on temperature and time [34]

Most of the tritium contained in the AVR reactor graphite was formed as result of the neutron irradiation of the ^{6}lithium contaminations. At the start of the AVR's period of operation, the formation rate was very high

and then continuously fell until the lithium had been fully "burned up". Over a period of 30 operating years, the AVR's operating temperature of up to more than 900°C could have potentially caused around 30 percent of the tritium to be released. This release was counteracted by the sorption of the new tritium that was constantly formed in the cooling gas as a result of the nuclear reactions in the fuel elements and the neutron irradiation of the helium isotope ^{3}He. At a certain point, the quantity of released and newly created tritium started to reach an equilibrium (see figure 9).

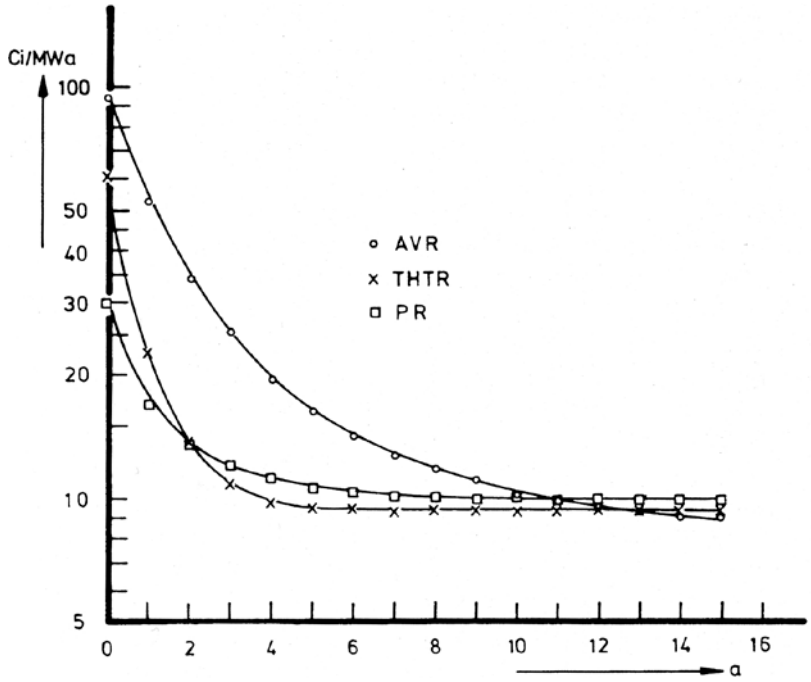

Figure 9: Specific tritium production rate for different HTRs as a function of time [12]

In the AVR, there was furthermore the possibility of the reactor graphite becoming contaminated with tritium during the neutron irradiation of the helium isotope ^{3}He: During the ^{3}He (n, p) ^{3}H reaction, a triton particle[3] receives 0.191 MeV of energy, which is sufficient for hurtling the particle into the graphite structure [6].

^{14}C:

When the reactor graphite is irradiated with neutrons, stable ^{14}N atoms are converted into unstable ^{14}C atoms as a result of a (n, p) - reaction, and ^{14}C is created from ^{13}C ((n, γ) reaction) and ^{17}O ((n, α) reaction). During this process, the activation energy or the kinetic energy of a neutron can dislodge them from the lattice structure. In this case, they will move into the interstitial lattice sites in the graphite. If they deposit in clusters, these clusters can deform the lattice [17].

^{60}Co, ^{133}Ba, ^{134}Cs-134, ^{137}Cs, ^{152}Eu, ^{154}Eu and ^{155}Eu:

[3] Triton particle: Tritium atom, without outer electron; tritium nucleus

It can be assumed that the remaining radionuclides ^{60}Co, ^{133}Ba, ^{134}Cs-134, ^{137}Cs, ^{152}Eu, ^{154}Eu and ^{155}Eu are created through the neutron irradiation of the contaminations in the reactor graphite.

2. Reactor Graphite (Merlin)

2.1. General

Figure 10: Reactor building with extensions seen from the north-west

The buildings of the research reactor FRJ-1 (Merlin), 'Merlin' for short, are located on the premises of the Forschungszentrum Jülich. Merlin has been undergoing demolition since 1996. It used to be a swimming pool reactor that was moderated and cooled with light water and produced a thermal output of 10 MW before being shut down. It was fuelled with 2.7 kg U-235 enriched to 80% and operated from 1962 to 1985. It was primarily used to irradiate samples with neutrons with different energies.

The maximum thermal neutron flux was $8.8 * 10^{13}\ cm^{-2}\ s^{-1}$.

The thermal neutron flux on the front surface of the thermal columns was $1\text{-}2 * 10^{10}\ cm^{-2}\ s^{-1}$. [10]

Its fast neutron flux at thermal column II was $1.8 * 10^{8}\ cm^{-2}\ s^{-1}$. [6]

2.2. Samples

The samples used in this study were thoroughly analysed in 2000. This section briefly details the work performed in preparation of and the results of these analyses.

Sample site of origin:

The samples used in the following tests were removed from the thermal columns during the reactor block's demolition. The thermal columns were used to slow down the fast neutrons that are released during the nuclear reaction to thermal neutrons for test purposes.

The following figure 11 shows the reactor block's structure.

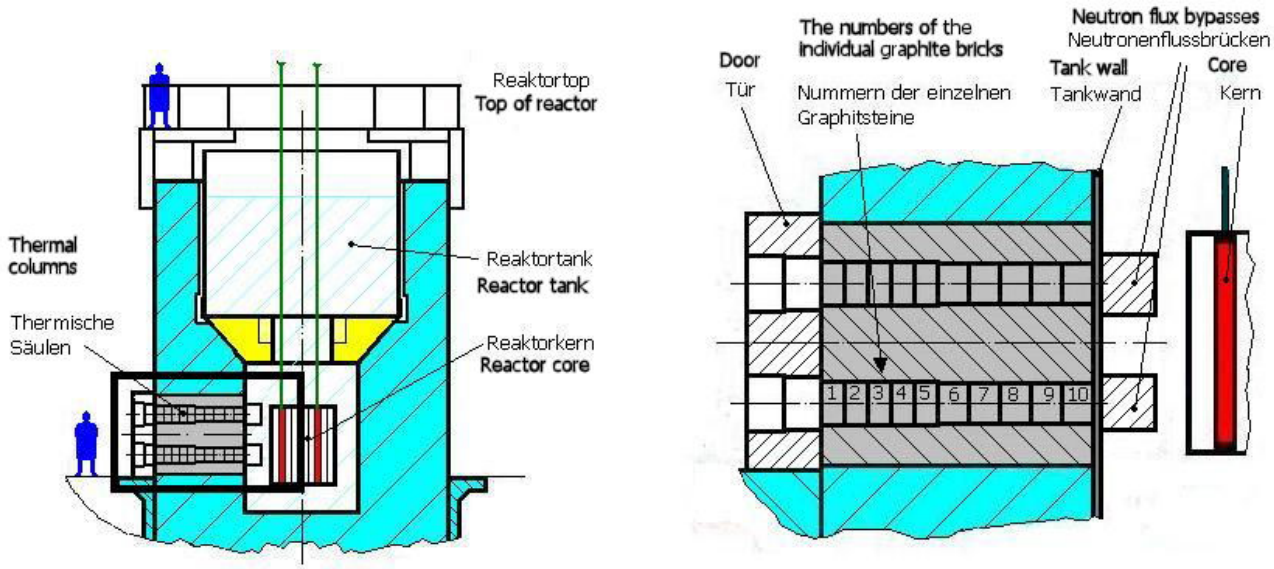

Figure 11: Cross section of the reactor block/ Position of the individual graphite bricks inside the reactor block

Ten individual graphite bricks were removed from the bottom right channel of thermal column II in the reactor block (see figure 11 for structure). A sample was removed from each one of these graphite bricks.

Each of these 10 samples was analysed for radionuclides by LSC and γ spectrometry.
The results of this analysis showed that the samples contain the following radionuclides:

^{3}H, ^{14}C, ^{60}Co, ^{133}Ba, ^{152}Eu, ^{154}Eu and ^{155}Eu

The reactor graphite's total inventory of contaminants was determined using ICP-MS measurements.
(see table 4 in the appendix). There is no other information available about the type and characteristics of the reactor graphite [27].

Sample selection

The analysis of the ten samples described in section 4.3.1 showed that sample T10 of the reactor graphite, from the part of the thermal column that was closest to the reactor's core, contained the greatest number of radionuclides (see figure 12 and table 3 in the appendix).

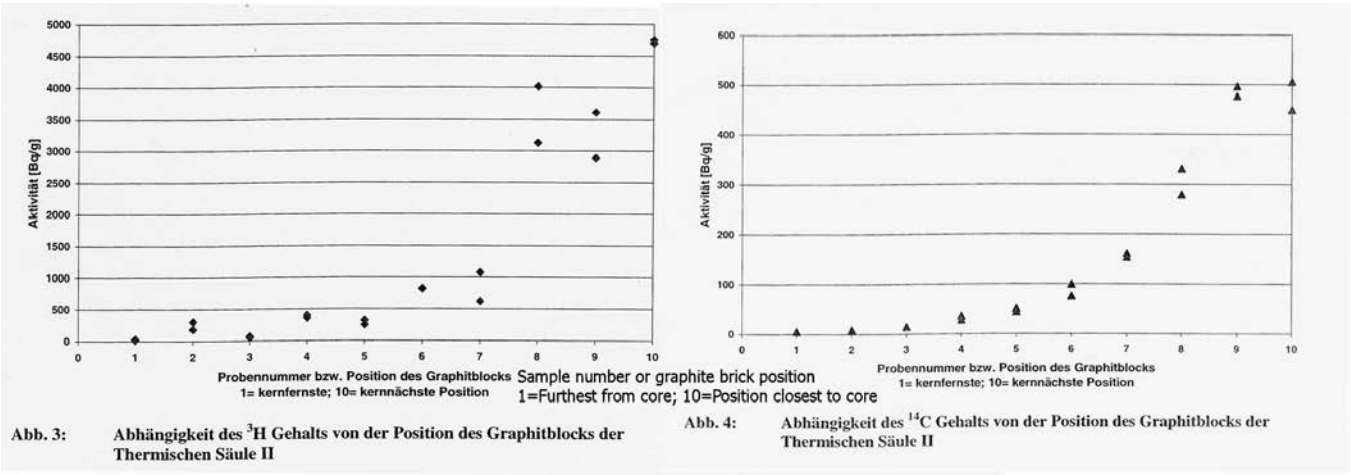

Figure 12: Dependence of the ^{3}H- and ^{34}C content on the position of the graphite brick from thermal column II [27]

This particular sample was consequently selected for the tests that are detailed in the first part of this study. In the following tests, some of the subsamples of this graphite sample were treated with different solvents. There is no information available about the exact procedure used to remove the samples and about the samples' appearance before they were crushed that would make it possible to assess their state and the exact site of origin.

The graphite samples were crushed inside a glove box with a hammer and mortar, which was guided through a stainless steel sleeve, and subsequently sifted. The graphite particles' grain size is ≤ 0.5 mm.

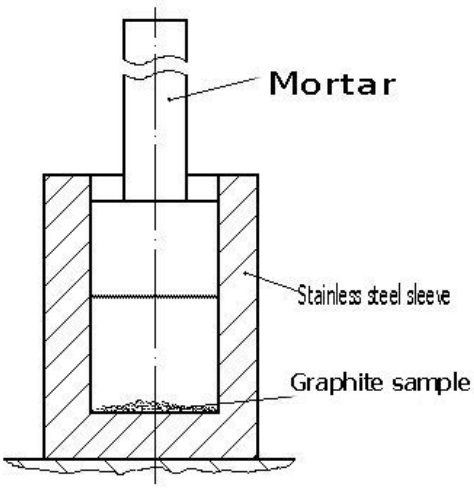

Figure 13: Tools used to crush the samples

3. Reactor Graphite (AVR)

3.1. General

Figure 14: HTR of the AVR with extensions during operation

The research reactor of the Research Reactor Working Group (Arbeitsgemeinschaft Versuchsreaktor) (AVR) in Jülich, which was a high temperature reactor with a thermal output of 46 MW and an electrical output of 15 MW, was started up at the end of 1967 and shut down in 1987. In the AVR, the graphite was used to coat the spherical fuel elements and as the core's reflector material (see figure 15). The isotropic graphite reflector was used to weaken or slow down the radiation (thermal and fast neutron radiation) to such an extent as to prevent it from causing damage to the reactor's other components. During this process, the graphite was exposed to temperatures of up to 950°C and a pressure of 11 bar. Since graphite reacts with O_2 at temperatures above 300°C, and with CO_2 and H_2O around 600°C, the HTR was cooled with helium [22]. The samples were taken from one of the HTR's reflector shields.

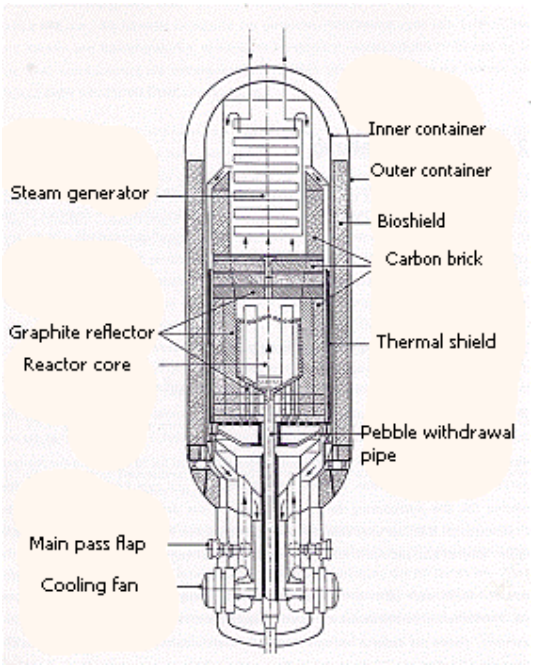

Figure 15: Internal structure of the AVR's high temperature reactor [3]

- **Neutron flux inside the reactor**

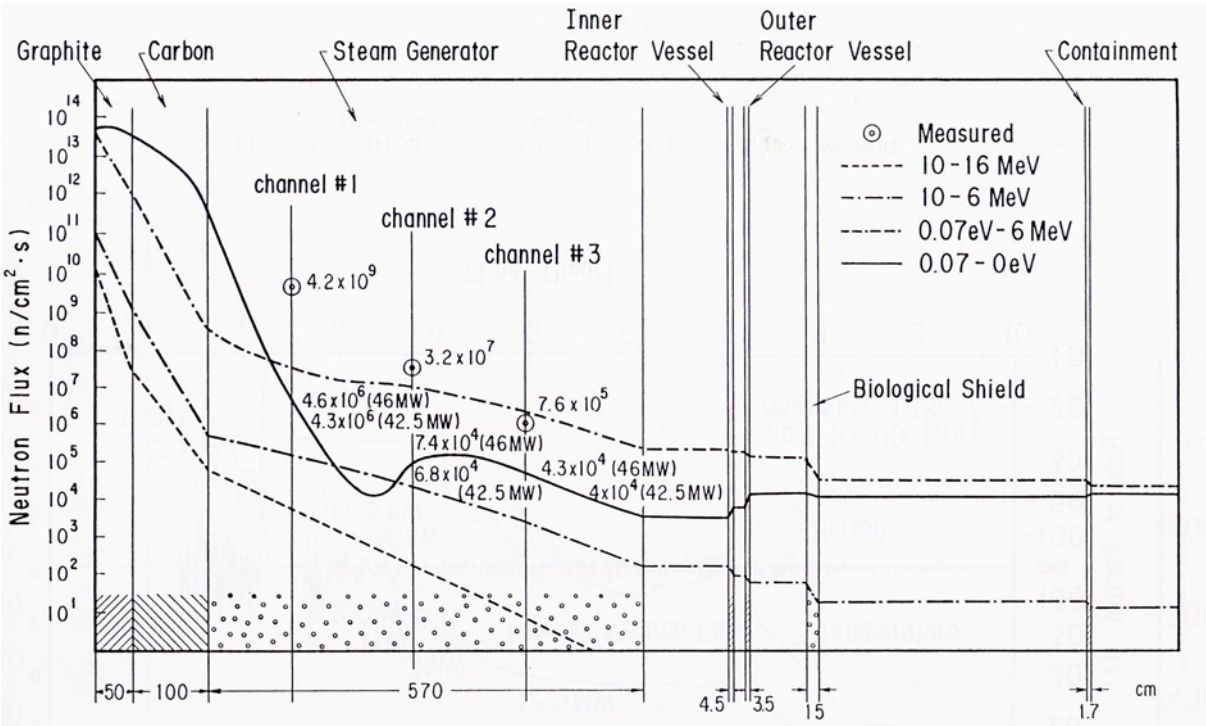

Figure 16: Neutron flux above the ceiling reflector [36]

The illustration at the top (figure 16) shows the calculated reduction in neutron flux at and above the ceiling reflector and the HTR reactor components above the reflector. The left side edge is the bottom side of the reflector that faces the core. The next illustrations, amongst others, show the carbon brick structures, the steam generator in which the measurements that form the basis of the calculations were taken, the double-walled dry well, the biological shield and the reactor's superstructures. All lengths are stated in cm.

In the ceiling reflector's graphite, the calculated maximum energies of the neutron radiation at 10 – 16 MeV have a neutron flux of 10^{10} cm^{-2} s^{-1}. This energy is sufficient for knocking out atoms from the crystal lattice ($E_{Bond.\ Graphite} \leq$ 25 – 60 eV)

3.2. The Graphite of the AVR's HTR

The high temperature reactor of the working group's research reactor (AVR) was built using two types of ARS/AMT graphite manufactured by SIGRI Elektrographit GmbH.

Both of these types of graphite are pitch coke graphites. The binding agent used for this graphite is coal tar pitch and the filler is needle coke (shell coke). The graphites distinguish themselves from one another by the varying degress to which they are compressed during manufacture. The first type of graphite is extruded and was used for the floor and side reflector, the second type was die-pressed during manufacture and was used for the ceiling reflector. The extruded graphite contains a larger percentage of bonding agent than the die-pressed graphite. The first type was furthermore manufactured in two different grain sizes with 1 mm and 4 mm diameters. However, there is no clear indication of whether both types of graphite were used. [8/9]

The total weight of the reflector components is 67 Mg.
Use of graphite in HTR plants [3]:

- Moderator
- Reflector
- Fuel element – matrix material
- High-temperature resistant construction material
- Shielding material
- Filler (with boron) in regulating and control rods
- Nuclear fuel cladding material

The surface of the ceiling reflector was thoroughly examined with a video camera in 1984 during an inspection on the occasion of the AVR's planned conversion. This examination showed that *"there are hardly any changes visible on the outside of the ceiling and top side reflector, with the exception of a few reflector bricks that have shifted ...."* [35]. (see figure 17)
This suggests that the neutron radiation has not led to any visible changes to the surface.

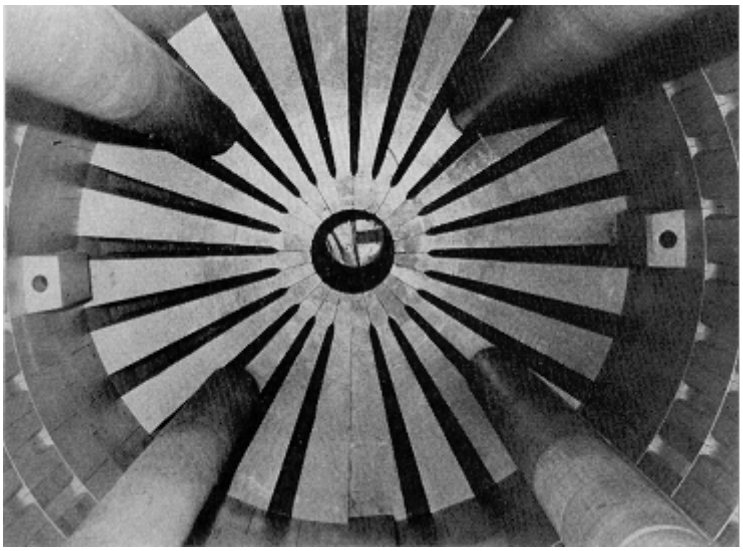

Figure 17: View of the ceiling reflector, the upper part of the side reflectors and the guide pipes of the control rods of the AVR's research reactor before being filled with spherical fuel elements

3.3. Samples

The samples for the second series of tests were taken from the core's graphite jacket. The exact site (ceiling, side or bottom reflector) and location (e.g. surface) from which the samples were removed is confidential. There was therefore no information available on whether the graphite samples were from the extruded or die-pressed reactor graphite or whether the sample was removed directly from the surface. It is

consequently not possible to draw any reliable conclusions regarding the relationship between the samples' location and the analysis results.

The samples available for selection comprised 11 samples from previous test series (AVR analytics (April 2000) and AVR analytics II (August 2000)). These series of tests were performed in order to create a database about the AVR's HTR's activity inventory. The samples for the following tests were selected on the basis of their activity concentrations and dose output. To keep radiation exposure as low as possible, the sample with the lowest dose output of all of the available samples was selected. This sample is sample AVR-G-19.

The selected sample, AVR-G-19, comprised a black, powdered solid material.

Eight subsamples were subsequently removed from this sample and put into a test tube (Ø 8 mm, height 70 mm) (see figure 18) with a stopper. These samples were labelled AVR-1 to AVR-8. The mass of these subsamples ranged from 0.037 to 0.043 g.

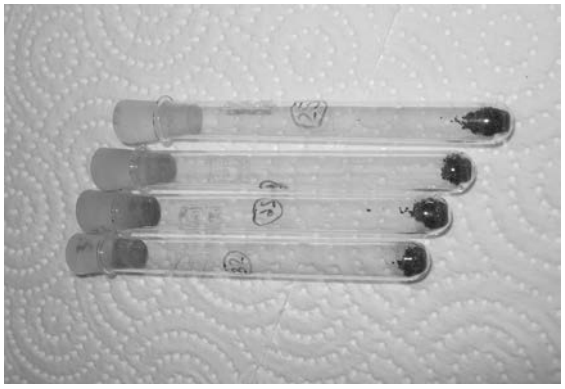

Figure 18: Solid material samples in test tubes

Before the start of the wet chemical tests, each one of these samples was analysed by γ spectrometry and then compared with the previous analysis values. The results of this analysis showed that the samples contained the same radionuclides as shown by the previous measurement, and which are as follows:

^{60}Co, ^{133}Ba, ^{134}Cs, ^{137}Cs, ^{154}Eu and ^{155}Eu

The activity values of samples AVR-1 –AVR-8 deviated in some cases by more than 50% from the reference specimen AVR-G-19 (see figure 19).

This is an indication either of the inhomogenity or the individual samples' different quantitative compositions. This deviation has to be taken into account in the following tests.

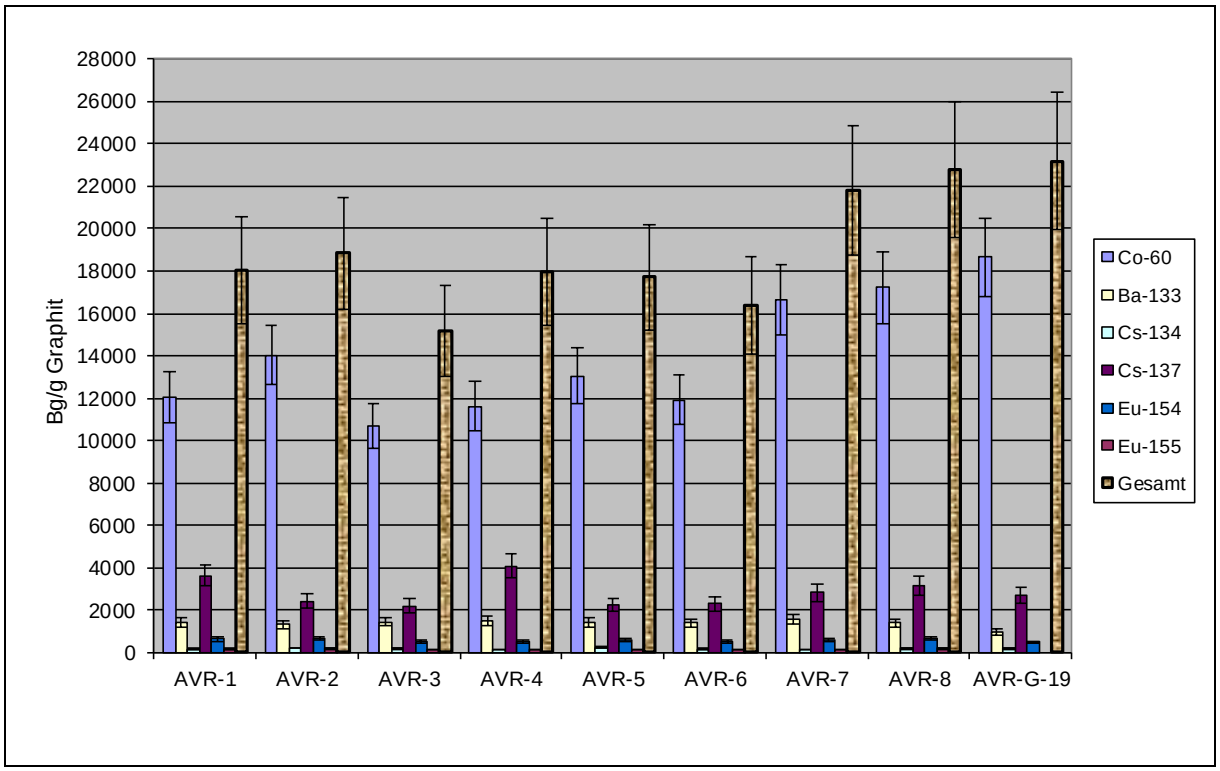

Figure 19: Sample comparison: AVR 1 - AVR 8 with AVR-G-19

(Gesamt = Total)

C. Experimental section

1. Materials and Equipment

1.1. Equipment List

LSC:	Packard Tri-Carb 2200 A.
γ spectrometry:	High Purity Germanium Detector from EG&G Ortec

1.2. Equipment

100-mL single-neck round-bottomed flask
100-mL triple-neck round-bottomed flask
30-mL or 5-mL Soxhlet extractor
30-mL paper or fibre glass extraction thimble
manufactured by Schleicher und Schuell
5-mL fibre glass extraction thimble
manufactured by Schleicher & Schuell 9 x 40 mm
Dimroth condenser (30-mL or 5-mL)

Heating mantle
Hot plate with magnetic stirrer
Laboratory stand
Washing bottle with glass frit
Quartz wool p. a.
Clamps, condenser hoses,
Teflon ground joint sleeves

Other equipment:

- Adjustable pipette max. 1 mL and 5 mL
- Pipette tips manufactured by Eppendorf
- 100-mL PE and glass flasks
- Glass pipettes*
- Measuring cylinders*
- Volumetric flasks*
- Laboratory stands
- Analytical balance Kern 870
- Macherey und Nagel weighing paper
- Zerostat 3 Discwasher (Aldrich)
- 20-mL scintillation measuring glasses
- 10-mL scintillation measuring glasses

*of different volumes

2. Reagents

2.1. Selection of Solvents

The solvents are selected in accordance with their properties and the test results. Amongst others, the ideal solvent would have to have the following properties:

- cost effective
- non-toxic
- removes all of the radionuclides from the graphite, but does not corrode the graphite
- can be separated again from the radionuclides easily and cost effectively
- is inert to the chemical and physical properties of the radionuclides

In order to reduce the number of solvents used, only one representative from the relevant substance groups will be selected from the organic solvents, as, according to the literature, it is not anticipated that there will be large quantities of dissolved activity.
Solvents that are not suitable for Soxhlet extraction or liquid-solid extraction were not considered for selection.
The acids employed in the tests were used at different concentrations.

The solvents for the AVR samples were chosen in accordance with the results of the tests conducted with the Merlin samples. The solvents with the best results were:

6 molar acetic acid, 7 molar nitric acid, 6 molar hydrochloric acid and 4 molar sulphuric acid.

2.2. Reagents Used

inorganic:

Blanket gas:

Argon 5.0

Neutral:

H_2O deionised

Acidic:

In different concentrations:

HCl hydrochloric acid

HNO_3 nitric acid:

H_2SO_4 sulphuric acid

Alkaline:

In different concentrations:

NaOH solution

organic:

Alcohols:

C_2H_5OH ethanol

Ketone (aprotic, dipolar):

CH_3COCH_3 acetone

Carboxylic acids:

CH_3COOH acetic acid 6 M and 12 M

Aromatics:

C_7H_8 toluene

Halogenated hydrocarbons:

CCl_4 tetra chloromethane

1-Bromobutane

Hydrocarbons:

Cyclic hydrocarbons:

C_6H_8 cyclohexane

Aliphatic hydrocarbons:

C_6H_{10} n-hexane

C_5H_8 n-pentane

All of the solvents used are p.a. (per analysis) quality as specified by Merck and Baker. Dilute solutions are produced with the aid of deionised water.

Other chemicals:

Scintillators:

Insta-Gel® Gold from PerkinElmer®: For measuring the organic solvents

Insta-Gel® Plus from PerkinElmer®: For measuring the acidic, slightly alkaline or neutral solvents.

Ion exchanger:

Ammonium molybdophosphate (AMP)

bis-t-cis-Dicyclohexyl-18-crown-6

2.2.1. Radiolysis of the Reagents Used

The radiation emitted by the radionuclides contained in the reactor graphite can on occasion cause the reagents that are being used to undergo radiolysis. This can cause the tritium to become bonded to the solvents used by exchanging hydrogen. In solvents that have a higher boiling point than water, this can make it difficult to separate substances using subboiling (see section 4.5).

The following is a selection of potential reactions:

Nitric acid:

Radical process: $HNO_3 \rightarrow HNO_3^*$

$HNO_3^* \rightarrow \cdot OH + NO_2$

Molecular process: $HNO_3 \rightarrow HNO_3^*$

$HNO_3^* \rightarrow ½\ O_2 + HNO_2$

Sulphuric acid (dilute solutions; indirect radiation effects):

$H_2SO_4 + H^+ \rightarrow H_2 + HSO_4^+$

$H_2SO_4 + OH^- \rightarrow H_2O + HSO_4^-$
or $SO_4^{2-} + OH^- \rightarrow SO_4^- + OH^-$

$HSO_4^- + H^+ \rightarrow H_2SO_4$ (recombination)

$HSO_4^- + OH^- \rightarrow H_2SO_5$ (peroxymonosulphuric acid)

$HSO_4^- + HSO_4^- \rightarrow H_2S_2O_8$ (peroxydisulphuric acid)
or $SO_4^- + SO_4^- \rightarrow S_2O_8^{2-}$

$H_2S_2O_8 + H_2O \rightarrow H_2SO_5 + H_2SO_4$
or $S_2O_8^{2-} + H_2O \rightarrow HSO_5^- + HSO_4^-$

Acetic acid:

$\cdot H + CH_3COOH \rightarrow \cdot CH_2COOH + H_2$

$\cdot OH + CH_3COOH \rightarrow \cdot CH_2COOH + H_2O$

$2\ \cdot CH_2COOH \rightarrow HOOC\text{-}CH_2\text{-}CH_2\text{-}COOH$

3. Preliminary Work

3.1. Preparation of the Extraction Thimbles

The extraction thimbles' material was selected respectively in accordance with the solvents used. For solvents that dissolve paper, a fibre glass extraction thimble was used.

Approximately 500 mg of the powdered reactor graphite (No. 1 in the following figure 20) were placed into one extraction thimble (3) respectively. The extraction thimble was subsequently filled with quartz wool (2) in such a way that the graphite was unable to escape from the thimble.

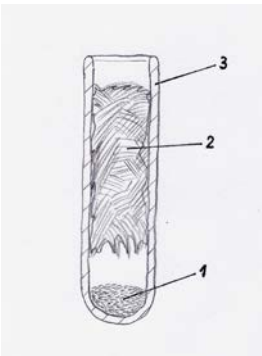

Figure 20: Cross section of an extraction thimble

The tests with the AVR graphite were performed using a 5 mL glass fibre extraction thimble respectively. Approximately 0.04 mg of the powdered reactor graphite respectively were transferred from the test tube into an extraction thimble. In contrast to the Merlin tests, the graphite powder was furthermore covered with a piece of fibre glass, as it had become evident on completion of the tests performed with the Merlin graphite that it was not possible to separate the graphite powder from the quartz wool without a comparatively high loss of powder. The extraction thimble was subsequently filled with quartz wool in such a way that the graphite and the fibre glass were unable to escape from the thimble.
To check the remaining residual amount of graphite, each test tube was subsequently weighed.

Pipetting:
So as to prevent the pipetting from giving rise to any errors, a series of pipetting operations were performed using a precision balance before the actual pipetting and every time the pipetting volume of the adjustable pipettes was changed. To do so, a glass beaker was placed on the balance. Once the balance's measuring scale had been set to zero, the glass beaker was quickly filled with ten times the required volume of deionised water. The weight difference was checked after every single pipetting operation and the total weight was checked at the end of the series of pipetting operations. The measured fluctuations were less than 0.5% in a volume of 0.1 mL, and less than 0.2% in a volume of 1 mL. The reference value used was the density of deionised water at 20°C [21].

4. General Description of the Experiments

Some of the tests and measuring procedures used in this study were made repeated use of.
To avoid any repetition of descriptions within this thesis, the following section contains a detailed description of all of the tests and measuring procedures used.

4.1. Soxhlet Extraction or Liquid Extraction

Background information:
Soxhlet extraction is a distillation-based solid-liquid extraction method. It entails heating the liquid phase to boiling point inside a round-bottomed flask using a heating mantle. The resulting steam travels through the riser pipe into the condenser, where it condenses and drips into the extraction thimble to which the Soxhlet extractor is fitted. The extraction thimble contains the solid material. The extracting agent will continue to rise inside the Soxhlet extractor until it reaches the level of the drain and the solvent flows back into the flask. During the filling phase, the solvent can extract the soluble substances from the solid material. This process is continuously repeated.
Soxhlet extraction has the advantage of being able to achieve a high level of concentration of the substance being extracted using only a small amount of solvent. Its only disadvantage is its high energy consumption.

Experimental set-up:

Merlin:

A Soxhlet extraction apparatus respectively comprises:

- 100-mL round-bottomed flask (triple neck flask when using argon)
- 30-mL Soxhlet extractor
- 30-mL paper or fibre glass extraction thimble - Schleicher & Schuell 22 x 80 mm
- Dimroth condenser
- Heating mantle
- Filter, clamps, stoppers, condenser hoses, Teflon ground joint sleeves

If gas is introduced, the apparatus also includes:

- Glass capillaries
- Washing bottle

Figure 21: Experimental set-up for the Soxhlet extraction for the Merlin graphite

From left: Test apparatus no. 1, 2, 3 and 4. No. 3 and 4 with an argon supply line

AVR:

A Soxhlet extraction apparatus respectively comprises:

- Triple neck flask
- 5-mL Soxhlet extractor
- 5-mL fibre glass extraction thimble - Schleicher & Schuell 9 x 40 mm
- Dimroth condenser
- Heating mantle
- Filter, clamps, condenser hoses, Teflon ground joint sleeves
- Glass capillaries
- 3 washing bottles

Test procedure

Merlin:

Soxhlet extraction was used. The amount of solvent used was 60 mL respectively. The test period was approx. 5 hours. In the tests in which HNO_3 was used as the extracting agent, the resulting gasses were transferred into a water flask filled with 20 mL 0.1 M NaOH by means of an argon stream (p = 1 bar). For comparison, some of the tests were performed without introducing argon. These tests showed that the period of time required to complete each leaching cycle was 2 to 3 times as long when using argon (duration of the extraction process using 4 M HNO_3 approx. 18 min) than it was when not using argon (duration of the extraction process using 4 M HNO_3 approx. 7 min). This increase is due to the triple neck flask's large volume and the longer time needed to heat the flask for each leaching process.

Special incidents observed during the tests

During the 1st test with the 4 molar sulphuric acid, a lot of gas repeatedly formed when the acid flowed back into the round-bottomed flask filled with the hot acid. As a result, part of the liquid from the round-bottomed flask was pushed up as far as the condenser. On these occasions, the vapour coming out of the condenser also increased. As a consequence of these incidents, the amount of solvent that was added to the round-bottomed flask after this test was reduced by 15% compared to the other tests.

Due to these problems, the multiple extraction tests that were subsequently performed were conducted without the use of the Soxhlet extractor. In these tests, the extraction thimble consequently floated in the solvent, which was heated to 100°C with the aid of the heating mantle.

AVR:

a) Soxhlet extraction

The experimental set-up used for the AVR graphite differed from the Merlin tests in the following points:

The volume or the size of the condensers, the Soxhlet extractors and the extraction thimbles were adjusted to the sample volume and were 5-mL instead of 30-mL. The amount of solvent used was 50 mL respectively. The temperature control (3 steps) of the heating mantle was adjusted in accordance with the acids' boiling point.

In each of the tests, the gasses that developed during the tests where transferred into three washing bottles by means of an argon stream (p = 1 bar), which was lead directly to the solvent, which was located in a triple neck flask, through a glass capillary. The first washing bottle was filled with 20 mL 0.1 M HNO_3 for capturing tritium and chloride, the second and third washing bottles contained 20 mL 0.1 M NaOH each for capturing C-14 in the form of CO_2.

b) Liquid extraction with sulphuric acid (differences compared to a) only):
The extraction thimble with the sample was suspended in a Packard vial in the round-bottomed flask. Instead of the heating mantle, a hot plate with a magnetic stirrer was used. The sulphuric acid was thoroughly mixed with the magnetic stir bar. The flask temperature was kept at 80°C by means of a water bath. The water bath's temperature was kept constant with the aid of an adjustable hot plate.

Follow-up work on the sample (Merlin)

Following the completion of the tests, the leaching solutions were, depending on the solvent, filled into either 100-mL glass or PE bottles. An aliquot of the leaching solution was removed and analysed by LSC and γ spectrometry.
The extraction thimbles that were used for solvents with low-volatility at room temperature were furthermore rinsed with deionised water and dried until there was no longer any difference between their weight before and after the tests. After this drying process, the solid material samples were removed from the extraction thimble, the quartz wool residues on the samples removed with a pair of tweezers, the samples rinsed with deionised water to remove the solvent residues and were then transferred into 10 mL Packard vials.
The samples were subsequently carefully heated at 70°C on the hot plate in order to remove the residual moisture until there was no longer any detectable difference in their weight.
After the tests, approx. 0.15 g were taken from each solid material sample respectively, transferred into a test tube and, just as with the liquid samples, measured with a drillhole semiconductor detector measuring station over a measuring time of 5,000 seconds.

Follow-up work on the sample (AVR)

Following the completion of the tests, the leaching solutions were filled into 100-mL PE bottles. An aliquot of each of the leaching solutions was removed and analysed by LSC and γ spectrometry. The solvent contained in the quartz wool from the extraction thimbles was removed with a pipette and added to the leaching solutions. The extraction thimbles were subsequently rinsed with approx. 10 mL deionised water and dried. The liquid used to rinse them was collected and its level of activity determined by LSC. After the drying process, the solid material samples were carefully removed from the extraction thimbles, the quartz wool residues on them removed with a pair of tweezers, the samples rinsed with deionised water to remove the solvent residues and then transferred into measuring test tubes.
They were subsequently placed into a glass beaker and carefully heated at 70°C on a hot plate to remove the residual moisture until their weight remained constant.

4.2. Separation of ^{90}Sr

The quantity of Strontium–90 in the relevant leaching solutions was determined by solid phase extraction. To do so, one column respectively was filled with bis-t-cis-dicyclohexyl-18-crown-6 as the ion exchanger and conditioned with 5 mL of 2 molar HNO_3. Following the expansion of the ion exchanger, the column was rinsed with approx. 2.8 mL of 8 molar HNO_3. The eluate was discarded.

5 mL of the leaching sample solution were transferred into a 20-mL Packard vial. The sample solution was carefully vaporized with the radiant heater and the hot plate until dry, absorbed with 2 mL of 8 molar HNO_3 and applied to the prepared column.

The Packard glass[4]* was subsequently rinsed 2 to 3 times with 1mL of 8 molar HNO_3. The rinsing solution was also applied to the column. Once the sample solution had passed through the column, the column was rinsed with 10 mL of 8 molar HNO_3. The eluate of the rinsing and washing solution was discarded. The ^{90}strontium was subsequently eluated with precisely 10 mL 0.05 molar $HN0_3$. The eluate was collected and homogenised. A sample of 1 mL each of this eluate was transferred into a Packard vial together with 1 mL deionised water and 18 mL Insta-Gel® and homogenized through agitation. The samples' ^{90}strontium content was subsequently determined by measuring their activity by LSC.

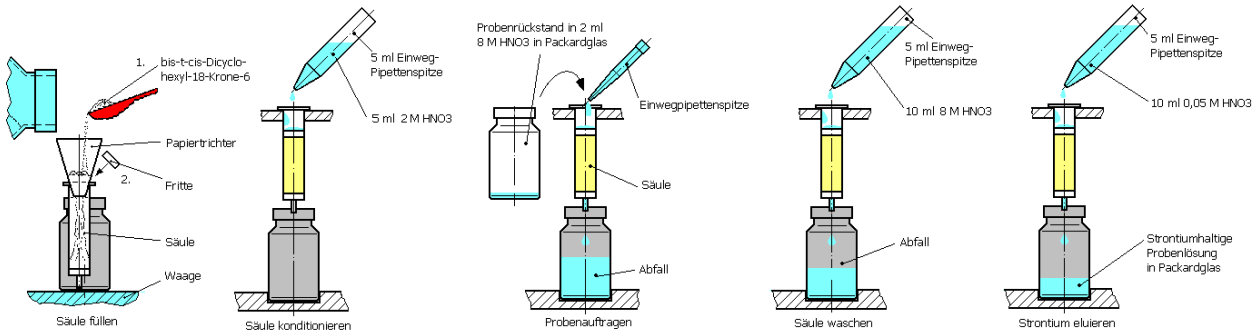

Figure 22: Steps involved in separating ^{90}strontium

bis-t-cis-Dicyclohexyl-18-crown-6	5-mL disposable pipette tip	Sample residue in 2 mL 8 M HNO3 in Packard vial	5-mL disposable pipette tip	5-mL disposable pipette tip
Paper funnel	5 mL 2 M HNO3	Disposable pipette tip	10 mL 2 M HNO3	10 mL 0,05 M HNO3
Frit				
Column		Column		
Balance		Waste	Waste	Strontium-based sample solution in Packard vial
Filling the column	Conditioning the column	Applying sample	Washing the column	Eluting strontium

[4] * For reference, each of these Packard vials were respectively filled with 2 mL HNO_3 and 18 mL Insta-Gel® and analysed for sample residues by LSC. No activity was detected.

Equation 1: ^{90}strontium content of the leaching solution / g graphite

$$A_{90\,\text{strontium/g graphite}}\left[Bq \cdot g^{-1}\right] = \frac{\textit{actvity of sample}\left[Bq\right] \cdot \textit{total}\ \text{volume}\left[mL\right]_{\textit{leach}\ \text{solution}}}{\textit{measuring}\ \text{volume}\left[mL\right] \cdot \textit{mass of graphite}\ \text{sample}\left[g\right]}$$

4.3. Separation of Caesium with Ammonium Molybdophosphate (AMP)

As the peaks of weak γ emitters are covered by the background of the strong γ emitter ^{137}Cs in the γ spectrum, all of the caesium isotopes were removed from the sample solution. This was achieved using the procedure of specific caesium separation by ammonium molybdophosphate (AMP).

To do so, 5 mL of each of the sample solutions were transferred into a 20-mL Packard vial. The sample solutions were carefully vaporised until dry using a radiant heater and hot plate and absorbed in 6.8 mL concentrated HNO_3.

3 g of AMP were weighed in a 25-mL PE narrow mouth bottle and 10 mL of 0.01 molar HNO_3 and the 6.8 mL sample solution added to it. The liquid-solid material mixture was mixed by vigorous agitation. After 24 hours, the solid material had sedimented sufficiently to allow the remaining clear supernatant to be decanted into a 30-mL disposable syringe and to be filtered again through a membrane filter (pore size 0.45 μm) attached to the top of the Packard vial. 0.5 mL of the sample solution was subsequently analysed with a high purity germanium detector that was used as a γ spectrometric detecting device. The solute specific activity was calculated in accordance with equation 2.

Equation 2: Solute specific activity of the AMP sample:

$$\textit{activity}_{\,/\,g\,\textit{graphite}}\left[Bq \cdot g^{-1}\right] = \frac{\textit{activity}_{\textit{AMP sample}}\left[Bq\right] \cdot \textit{total}\ \text{volume}_{\textit{leach}\ \text{solution}}\left[mL\right] \cdot \textit{volume}_{HNO_3}\ \text{used}\left[mL\right]}{\textit{mass graphite sample}\left[g\right] \cdot \textit{volume}_{\textit{leach}\ \text{solution}}\left[mL\right] \cdot \textit{volume}_{\textit{AMP sample}}\left[mL\right]}$$

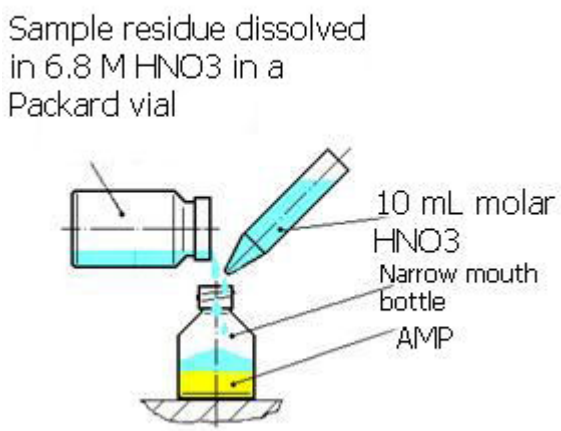

Figure 23: The addition of the sample to the AMP

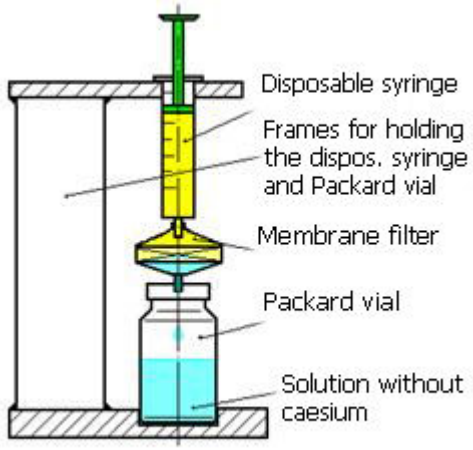

Figure 24: Separation of the sample from the AMP

•

4.4. Detection of Organic ^{14}Carbon

15 mL deionised H_20 and 5 mL or 10 mL of sample were transferred into a triple neck flask. A few drops of phenolphthalein solution were added as an indicator. The solution was neutralised by carefully adding 8 M NaOH solution. The carrier of this solution was 0.3 g of sucrose. To oxidize the organic carbon to CO_2, 7 g of potassium peroxodisulfate were subsequently added to the solution. The entire solution was heated for 3 hours at 70°C. The resulting CO_2 was transferred into three washing bottles through an argon stream.

$$S_2O_8^{2-} \rightarrow SO_3 + O + SO_4^{2-}$$

$$C_{12}H_6O_{12} + 15\ O \rightarrow 12\ CO_2 + 3\ H_2O$$

$$15\ S_2O_8^{2-} + C_{12}H_6O_{12} \rightarrow 12\ CO_2 + 15\ SO_4^{2-} + 15\ SO_3 + 3\ H_2O$$

The first washing bottle was filled with 20 mL of 0.1 molar HNO_3 solution. The 1st washing bottle was used to dissolve unwanted substances such as Cl_2 and ^3H. The 2nd and 3rd washing bottles were filled respectively with 20 mL of 0.1 molar NaOH. This is where the carbon dioxide was bound in the form of Na_2CO_3:

$$CO_2 + 2\ NaOH \rightarrow Na_2CO_3 + H_2O$$

2 mL each of each of the samples were removed from the individual washing bottles and analysed by LSC.

4.5. Determination of the Tritium Content (Merlin only):

Separation of tritium from HTO

In order to determine the free tritium content in the samples, 10 mL of sample were transferred into a glass beaker with a glass pipette. A magnetic stir bar and a glass tripod with a collection container for subboiling samples were added to this glass beaker. The glass beaker was covered with a watch glass. Using a hot plate with an integrated magnetic stirrer, the samples were then heated to 70°C until approx. 1-2 mL of the sample had collected in the subboiling tripod. The activity of the solution collected in the container was established by LSC.

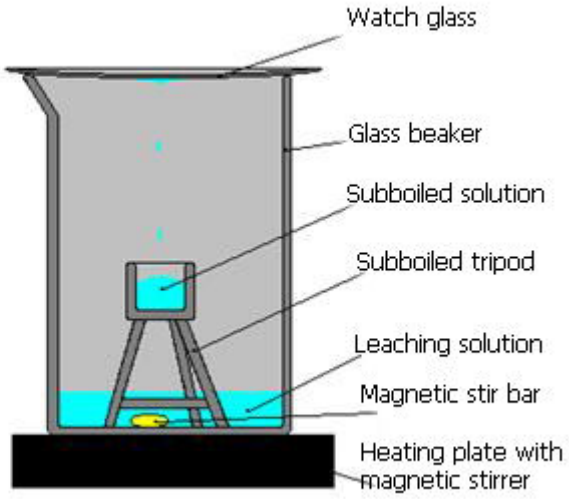

Figure 25: Subboiling apparatus

Evaporation to dryness

2 mL each of a selection of leaching samples were respectively transferred into a 20-mL Packard vial and carefully evaporated to dryness on an adjustable hot plate. The residue was subsequently dissolved again with 2 mL of the same, but fresh solvent to create the most identical measuring conditions possible. The activity was subsequently measured by LSC.

5. Measuring Radionuclide Activity

5.1. LSC Measurement

The samples' β activity was measured with the aid of a LSC device (see figure 26).

Figure 26: Packard sample vials in LSC with open flap

Background information:

Liquid Scintillation Counting technology, LSC for short, can be used to quantitatively determine α and β emitters. As the LSC is also able to detect weak ß emitters, such as the tritium and ^{14}C nuclides contained in the samples, it is, amongst others, also highly suitable for determining the total activity in the liquid samples. When using LSC, a scintillation cocktail that is suitable for the liquid sample's substance group is added. This cocktail contains molecules whose shell electrons can be raised to a higher energy state on stimulation. When these electrons return to their former energy state, they emit energy in the form of photons. The photons then hit a photocathode in the LSC measuring device where they knock out electrons. These electrons are multiplied through a secondary electron multiplier until a measurable pulse is created. The height of this pulse is proportional to the number of primary generated photons and the energy of the radiation.

β emitters have a continuous spectrum, and this spectrum is recorded by the LSC measuring device. Since these spectra are very broad, they generally merge with one another when measured in nuclide mixtures. In order to be able to make accurate quantitative and qualitative statements, it is therefore often necessary to chemically separate the nuclides. Depending on the acid, a concentration of 2-3 mol/L can cause disruptive quenching effects. Quenching effects weaken the energy of the resulting light pulses. This is evident in particular in weak β emitters. As a result, when, e.g. performing LSC measurements, it must always be taken into account that weak β emitters with an energy of ≤ 300 keV, such as tritium and ^{14}C, will have a count rate that is lower than 1. The measuring device records the quenching through the tSIE value (tSIE = spectral index of the external standard). To do so, an external source (Ba-133) is moved to the sample bottle inside the device and the resulting Compton spectrum measured. These tSIE values can be looked up in tSIE value tables which contain the correction values for the count rate and energy shift for the individual nuclides derived from previous standard measurements. These correction values, the background and the count rate can be used to calculate the activity. [37]

Measuring procedure:

Depending on the concentration of the acid, between 0.25 and 2 mL of the leaching solution were transferred to a Packard vial and, where required, thinned with deionised water to a volume of 2 mL; the samples removed from all of the other solvents were 2 mL. 18 mL of the relevant suitable scintillator gel were respectively added to each one of the samples and homogenised through vigorous agitation. The samples' activity was subsequently determined by LSC. The measuring period was 30 min. respectively. The background comprised regular calibration measurements of 47 pulses/min.

The calculation was performed using the following equations:

Equation 3: Activity of the organic solvent samples:

$$A_{\text{sample org. solv.}}[\text{Bq}] = \text{ips}_{\text{sample}}[\text{s}^{-1}] - \text{ips}_{\text{zero sample}}[\text{s}^{-1}]$$

Equation 4: Activity of the aqueous solvent samples:

$$A_{\text{Sample aqueous sol.}}[\text{Bq}] = \frac{(\text{cps}_{\text{sample}}[\text{s}^{-1}] \cdot 60\,\text{s} \cdot 1\,\text{min}^{-1} - \text{imp}_{\text{background}}[\text{min}^{-1}])}{60\,\text{s} \cdot 1\text{min}^{-1}}$$

Equation 5: Activity per mL:

$$A_{\text{mL}}[\text{Bq} \cdot \text{mL}^{-1}] = \frac{A[\text{Bq}]}{\text{sample volume}[\text{mL}]}$$

Equation 6: Total solute activity per g of graphite:

$$A_{/\text{g graphite}} = \frac{A_{\text{mL}}[\text{Bq} \cdot \text{mL}^{-1}] \cdot \text{total volume}_{\text{sample}}[\text{mL}]}{\text{density of solvent}[\text{g} \cdot \text{mL}^{-1}] \cdot \text{mass of graphite sample}[\text{g}]}$$

5.2.γ Spectrometry

The samples of the solvents used in the Merlin tests, which had removed the greatest activity from the reactor graphite, and all of the AVR solvent samples, were additionally examined by γ spectrometry.
The γ spectrometry was performed using a high purity germanium detector (see figure 27).

Background information

High purity germanium detectors are semiconductor detectors with a high purity germanium crystal to which a voltage is applied. In highly simplistic terms, γ quantas knock out pairs of electrons and defect electrons from the crystal lattice. These free charge carriers migrate to the electrons and generate a pulse. This effect can also be observed to a lesser extent without the effects of γ radiation. The noise created during this process creates a background in the spectrum, which can cause weak peaks to be lost. For this reason, the crystal is cooled with liquefied nitrogen to prevent the free charge carriers from moving by themselves. Depending on the pulse height, each pulse is allocated to a channel number that corresponds to the channel width (e.g. 0.5 keV) of a particular energy range e.g. 1332 - 1332.5 keV (^{60}Co).
This information is subsequently converted into a total spectrum through a Multi Channel Analyzer (MCA). As the individual spectra are very narrow and are easy to allocate to the relevant nuclides due to their energies, it is not generally necessary to separate the nuclide mixture, which is very time consuming, for γ spectrometry in order to obtain qualitative results. It is only for weak emitters, whose spectra get lost in the background of strong radiation, that the nuclide mixture has to be separated. In order to obtain accurate quantitative information, it is furthermore necessary to establish the count rate using standards.

Measuring procedure

0.5 mL of a leaching sample respectively was transferred into a test tube (Ø 8 mm, height 70 mm) using a pipette and analysed over a measuring period of 10,000 seconds.

The solid material samples from Merlin were only analysed respectively in test tubes after the tests and over a measuring period of 5,000 seconds. The solid material samples from the AVR were analysed respectively in test tubes before and after the tests over a measuring period of 5,000 seconds.

Figure 27: γ measuring device with open doors

D. Results

1. Results (Merlin)

1.1. Measuring the Total Activity

The total activity was measured by LSC. When comparing the measured values, the differences in the dissolving power of the solvents used in the tests become clearly apparent (see figure 59 in the appendix). In contrast to the acids, all of the other solvents removed only very little or no activity at all.

Water, ethanol and acetone remove only very little activity ($A_s \leq 12$ Be/g graphite) from the graphite samples. All other organic solvents only remove small quantities ($A_s \leq 1$ Be/g graphite) of radionuclides from the reactor graphite (see figure 23). All neutral solvents are therefore not suitable for decontaminating reactor graphite and were not be given any consideration in the next series of tests.

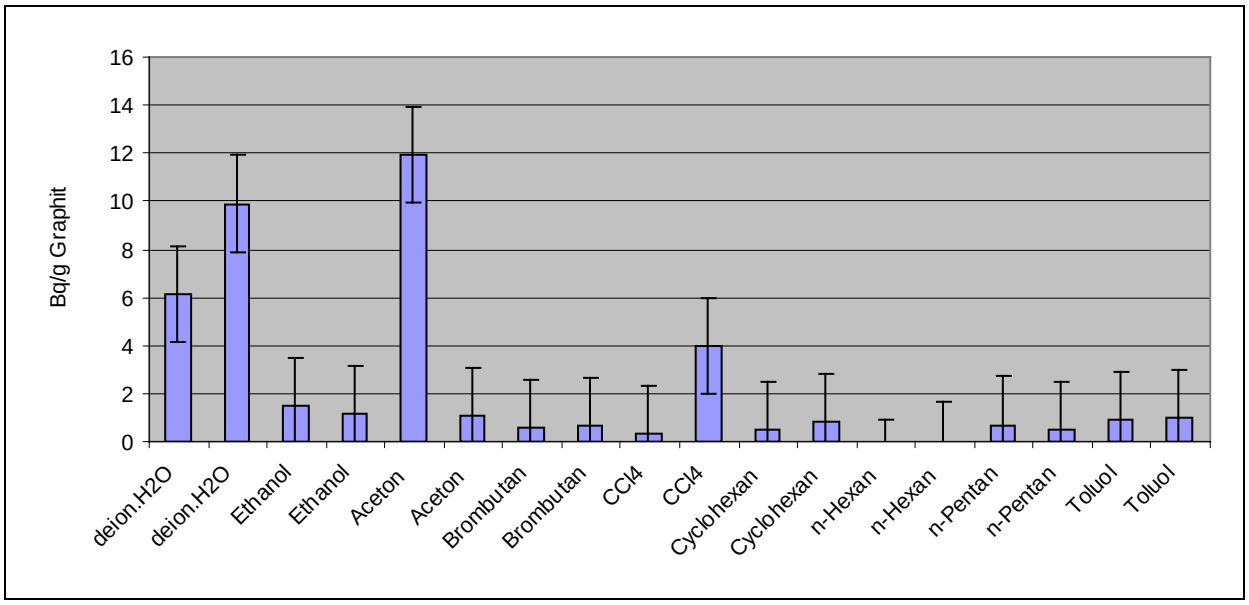

Figure 28: Comparison of the measurement results of the neutral solvents' leaching samples

Hydrochloric acid removes radioactivity from reactor graphite samples in all concentrations. In contrast to the other acids, the results for the sample duplicates fluctuated strongly (see figure 29). This could be the result of the graphite samples' inhomogenity with respect to structure, grain size, position in the reactor and the exact position of the radionuclides in the graphite. As the samples' high level of activity makes measuring errors comparatively minor, measuring errors can be discounted as a potential cause.

In hydrochloric acid, it seems that any increase in concentration will generally result in greater activity removal. However, due to the strong fluctuations in the measured values, this cannot be positively verified with respect to the sample duplicates. As the 6 molar hydrochloric acid removes the highest level of activity, this is also the solvent that will be used for the decontamination tests on the AVR graphite.

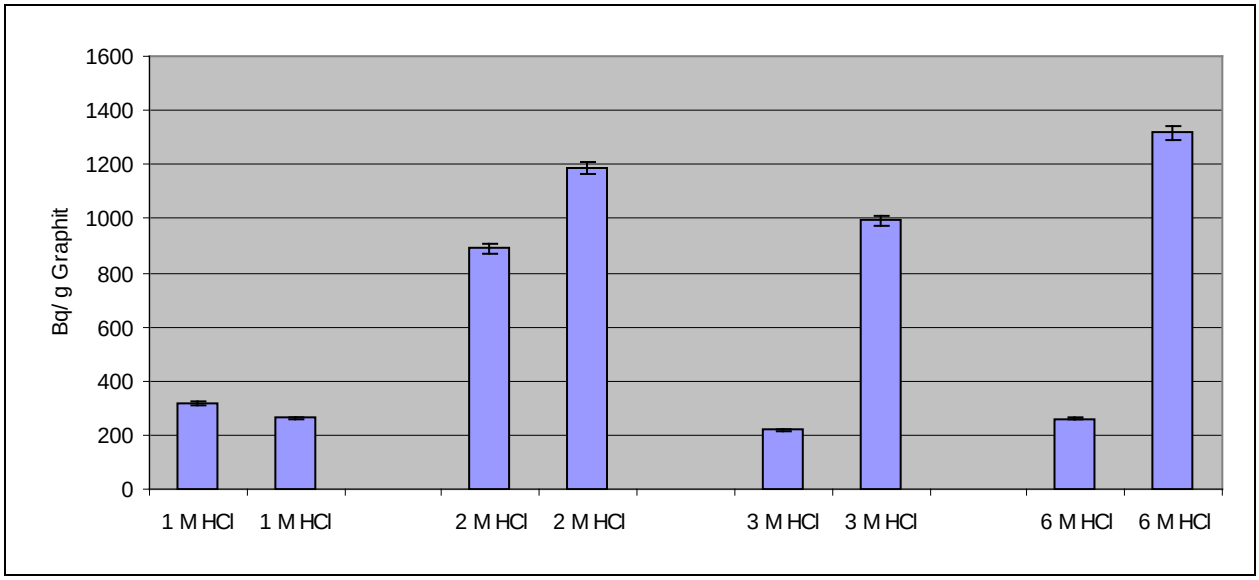

Figure 29: Comparison of the activity of the HCl leaching samples

The tests performed with the nitric acid in different concentrations show that the higher the concentration, the higher the activity in the samples and that the maximum level of activity is being removed at a concentration above 7 mol/L (see figure 30). For this reason, this is the concentration that will be used for the series of tests performed on the AVR graphite.

In the tests in which argon is used, the Soxhlet takes longer to fill and there are consequently fewer leaching processes per test. When comparing the results of these tests to the tests in which no argon is used, it is also evident that performing 2 or 3-times as many leaching processes also increases the level of activity that is removed. This effect decreases as the acid's concentration is increased (see figure 30).

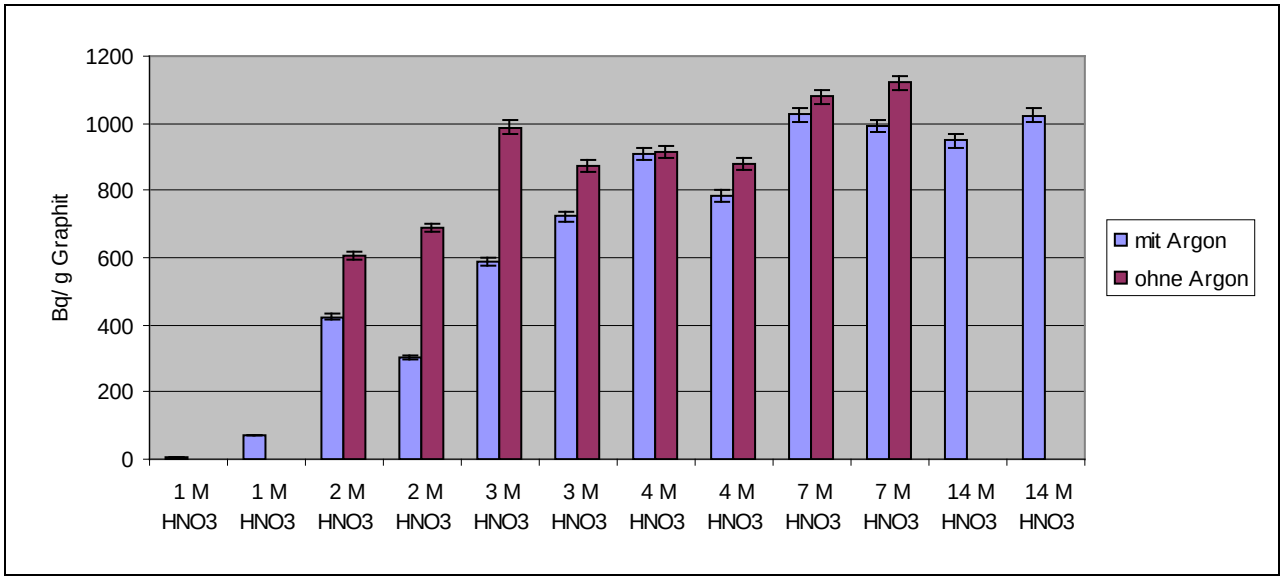

Figure 30: Comparison of the activity of the HNO_3 leaching samples

(with argon)
(without argon)

When leaching Merlin graphite with HNO_3, a small amount (A_s< 3 Be/g graphite) of ^{14}C becomes gaseous. The measured values within the sample duplicates fluctuated very strongly (see figure 31).

This can be explained by the very small measured values, which are subject to significantly larger measuring errors than high measured values.

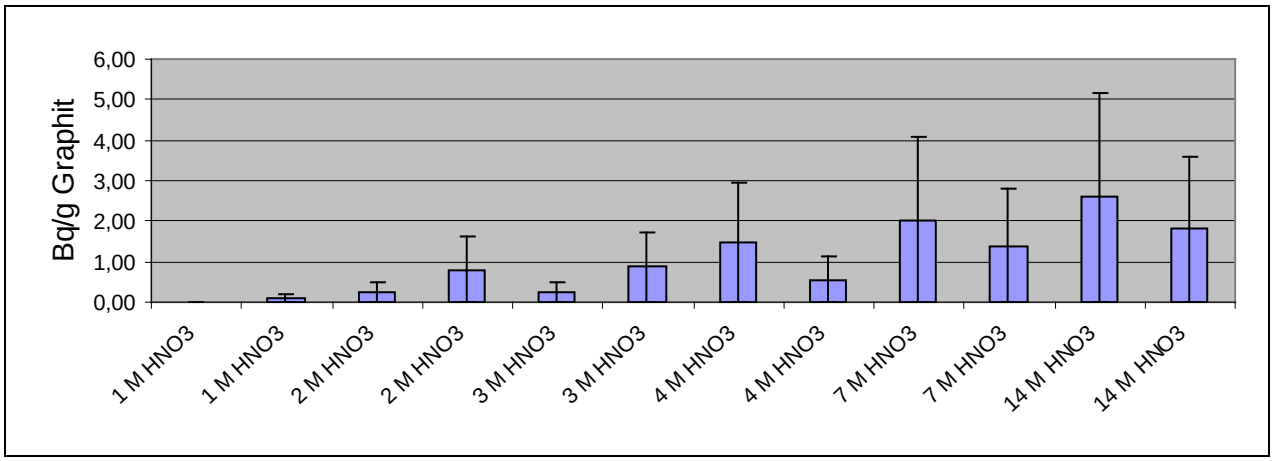

Figure 31: HNO_3 extraction: Activity of the washing bottles' contents

The other acid solvents that were used were acetic acid and sulphuric acid. The comparison of the results shows that increasing the concentration of acetic acid from 6 M to 12 M does not result in an increase in the activity count rate. Due to the problems (see section 4.1, Special incidents) encountered during the extraction using 4 molar sulphuric acid, no other tests with other concentrations will be performed. As with the samples with the nitric acid, the fluctuations of the measured values for the two solvents are significantly smaller within the sample duplicates than those observed for hydrochloric acid (see figure 32).

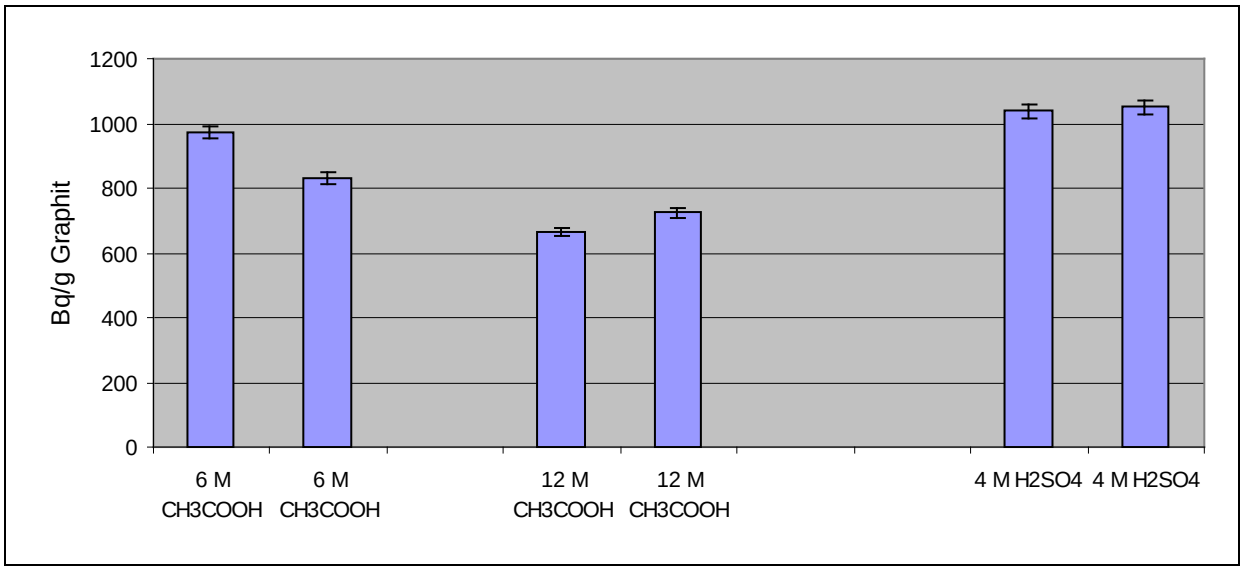

Figure 32: Comparison of the activity of the CH_3COOH and H_2SO_4 leaching samples

In order to ascertain whether repeatedly extracting radionuclides from the same sample using new solvents respectively would remove more total activity than through a leaching test, the same sample duplicate respectively will undergo extraction with the following fresh solvents four or six times for 5 hours each. The acids' concentration is selected in accordance with their effect on the extraction thimbles. The number of extraction tests is chosen in accordance with the respective result obtained from measuring the samples after the extraction.

Solvents used:

1 M HCl	6 M CH_3COOH
1 M HNO_3	4 M H_2SO_4

The test results obtained with the sulphuric acid can only be compared within limits with the other results as, due to the problems described above, their test conditions varied.

In part, the results of the hydrochloric acid and nitric acid extraction tests follow a similar course. The course of the curves of the duplicate hydrochloric acid sample is rather nonconclusive (see figure 33). However, they can be used to draw a few conclusions. In both of the samples, only a small amount of activity was removed from the reactor graphite samples after the 4th leaching process. The sum of the values of the 2nd and 3rd extraction is higher than the measuring result of the 1st extraction and the total sum of all extractions is at least twice as high as the value of the 1st extraction. (In the 1st sample duplicates, by 2.3 times and in the 2nd sample duplicates, by 3.4 times as much). This trend was even more pronounced with the nitric acid. During the 1st extraction, only 1 percent of the total sum achieved by all of the extractions taken together is being removed, and in the second sample duplicate, only 8 percent. The total sum of 813 Bq and 905 Bq of removed activity roughly equates to the values of the single extraction with 4 molar nitric acid.
The higher amount of activity removed from the 2nd hydrochloric and nitric acid samples onwards can be explained by the 3-week break between the 1st and 2nd leaching test, as during that time, the solvent was able to act on the graphite (see figures 33 and 34).

The course of the test curves obtained for acetic acid and sulphuric acid are also similar. The results for the tests performed with CH_3COOH (see figure 35) and H_2SO_4 (see figure 36) show that from the 3rd leaching process onwards, no significant amounts of activity are removed from the samples anymore. The continuous drop in the measured values suggests that the acids with the higher concentrations are able to remove most of the activity from the graphite during the 1st extraction step, in contrast to the weaker acids, which have to be left for a certain period of time to act in order to achieve the same results.

Overall, it can be concluded that the results obtained do not justify the efforts involved in performing multiple extractions. It is consequently more effective to immediately use acids with higher concentrations, which achieve the same results in only one single leaching test.

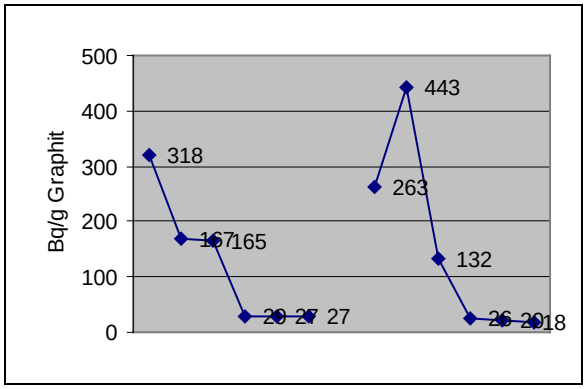

Figure 33: Result of multiple leaching processes using 1 M HCl

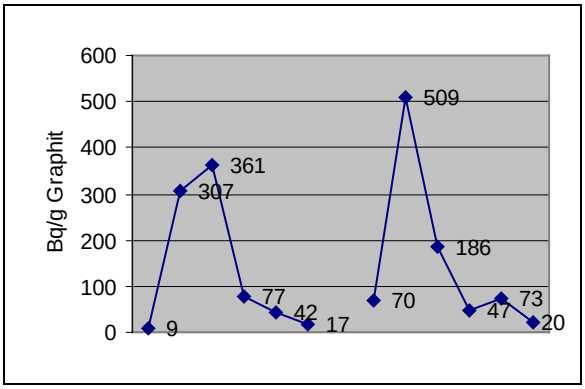

Figure 34: Result of multiple leaching processes using 1 M HNO_3

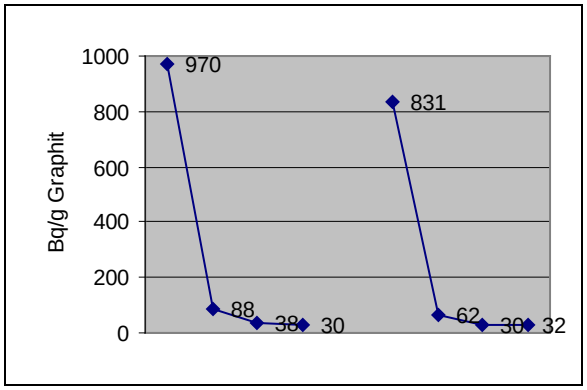

Figure 35: Result of multiple leaching processes using 6 M CH_3COOH

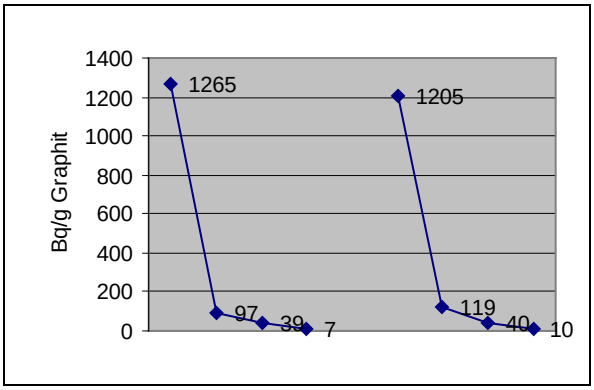

Figure 36: Result of multiple leaching processes using 4 M H_2SO_4

1.2. Results of the γ Spectrometry

Since only the results of the extracting agents that are capable of removing high amounts of activity are of interest for the second series of tests, only the Merlin samples of the solvents with the highest values will be analysed by γ spectrometry.

These are 6 M hydrochloric acid (A_{max} = 1319 Bq/g graphite), 7 M nitric acid (A_{max} = 1026 Bq/g graphite), 6 M acetic acid (A_{max} = 970 Bq/g graphite) and 4 M sulphuric acid (A_{max} = 1051 Bq/g graphite). The 2 M hydrochloric acid samples were also analysed in order to determine the reasons for the high activity of 1185 Bq/g graphite in one of the two sample duplicates. The solid material samples were not analysed by γ spectrometry before the extraction tests. For this reason, the sum of the residual γ activity in the solid material sample and the sum total of the γ activity of the liquid sample are used as a comparison value. This value is comparatively imprecise as, because of the extremely small sample size of 0.5 mL and the count rate of less than 1, it will no longer be possible to measure even relatively large levels of activities like, for example, the ^{154}Eu value of the sample with the 6 molar hydrochloric acid in the following figure 37.

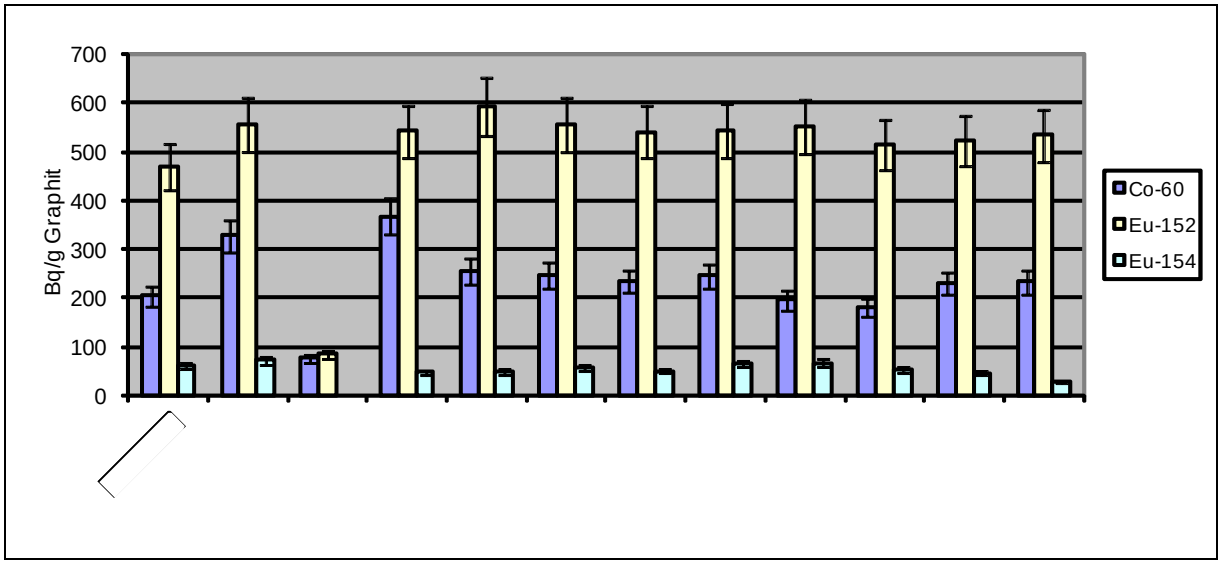

Figure 37: Comparison of the activity of the Merlin leaching samples

In the samples with high total activity, the residual activity of the solid material samples was established after the extraction tests. Just as with the liquid samples, the values of the hydrochloric acid sample duplicates are also not conclusive when comparing the samples with respect to the relationship between the acid's concentration and the samples' activity. I.e. even though one of the 2 M HCl samples has the highest amount of activity, the other also has one of the lowest. The situation with the 6 M HCl sample is similar: Although one of the solid material samples had the lowest values after the leaching, the same also applies to the liquid sample. The results of the liquid samples of the other solvents only fluctuate marginally within the sample duplicates. When taking into account a fluctuation margin that can be explained on the basis of the samples' inhomogenity and a 10 % error of measurement, they are roughly identical. The same can be also be anticipated to apply to the measured values obtained from the duplicate solid material samples. However, there is no positive indication of a relationship between the removed amounts and remaining amounts of activity (see figure 38).

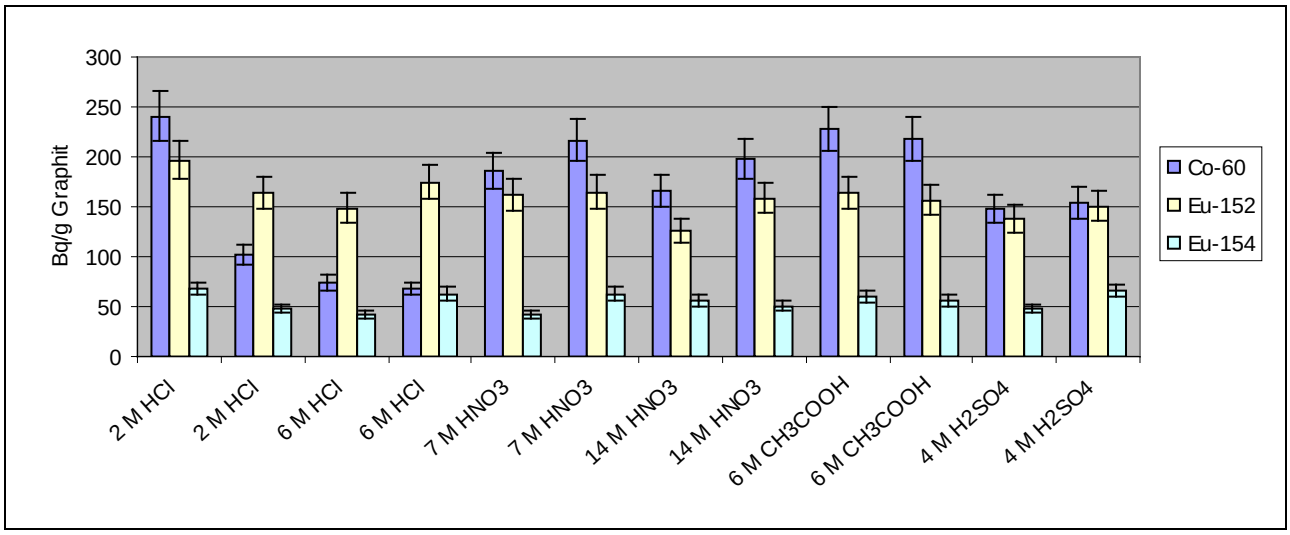

Figure 38: Activity of the solid material samples after the tests

Solubility of the individual nuclides:

^{60}Cobalt:

Comparing the ^{60}Co activity in the liquid samples with the ^{60}Co activity of the sum from the liquid and residual solid sample shows that at least 45% of the ^{60}Co content are removed.

Acetic acid removes approx. 45%, nitric acid removes approx. 55%, sulphuric acid slightly more than 60% and hydrochloric acid up to 85% of the ^{60}cobalt content. These tests also showed that the measured values obtained with the hydrochloric acid sample duplicates fluctuated more significantly than those of the other samples (see figure 39).

^{152}Europium / ^{154}Europium:

Comparing the activity in the liquid sample with the sum total of the activity from the liquid and remaining solid sample shows that, with the exception of 6 M HCl, all other solvents remove at least 70% of ^{152}Eu (see figure 39). The ratio of removed activity to the total activity of ^{154}europium fluctuates between 30 and 65%, with one exception (6 M HCl). 2 M hydrochloric acid, nitric acid and acetic acid reached approx. 50% of the leaching rate. All of the sulphuric acid and the 6 molar hydrochloric acid samples remain below this value (see figure 39).

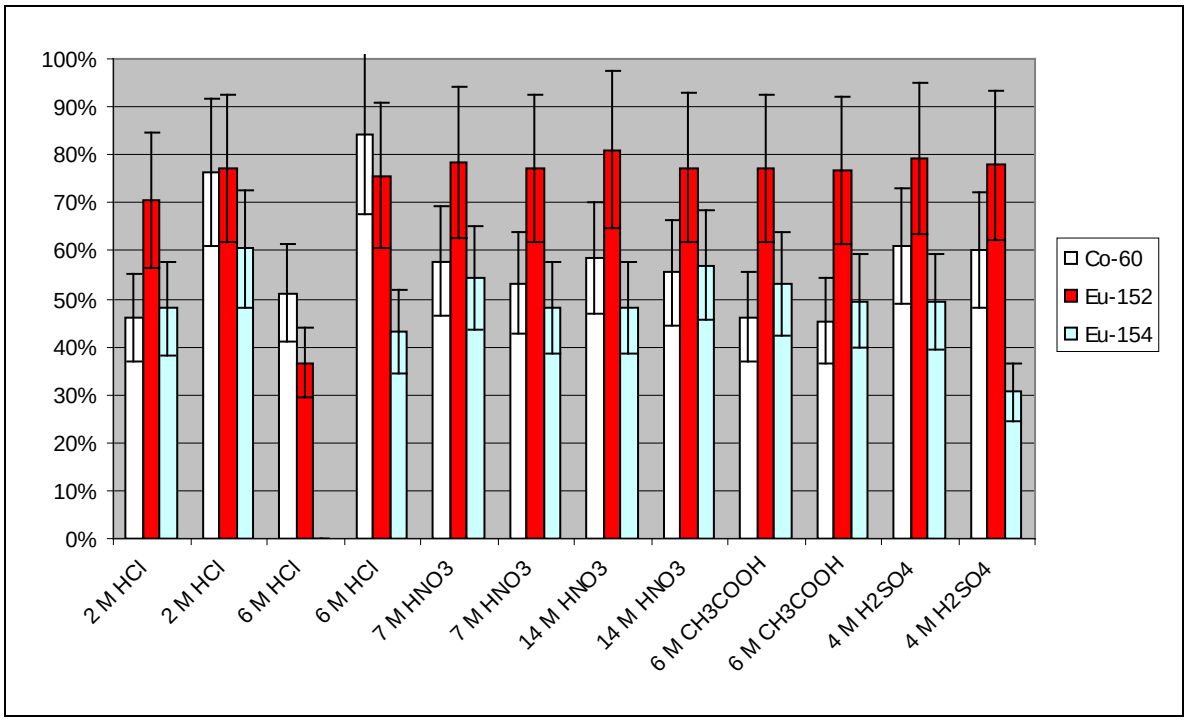

Figure 39: Ratio between activity in liquid sample / activity in sum of all samples

Separation of ^{90}Sr

The very low measured values ($A_s \leq 2$ Bq/g graphite) indicate that the sample solutions do not contain any ^{90}Sr (see figure 60). Since strontium dissolves in water and weak acids, it can be assumed that there are either none or such extremely small amounts of ^{90}strontium in the Merlin reactor graphite that they cannot be measured.

Determining the tritium content

HTO separation / evaporation to dryness

Since, at max. 1.8 Bq/g graphite, the measured activities are too low (see figure 40) and the concentrated acids cannot be used with the selected method of subboiling, the subboiling tests are discontinued. As an alternative, an attempt will be made to evaporate the samples to dryness. The objective is to use the difference between the activity values measured for the evaporated samples and the results of the liquid samples to calculate the amount of free tritium.

Due to the high fluctuations of the measured values (see figure 41), it is not possible to determine whether there are any significant differences between the liquid samples and the evaporated samples. This indicates that the samples only contain a very small amount of free tritium.

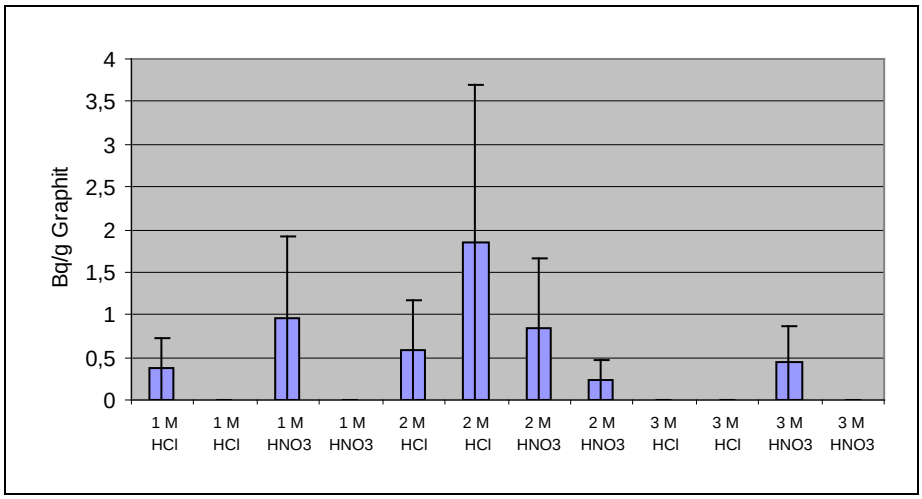

Figure 40: Subboiling tests

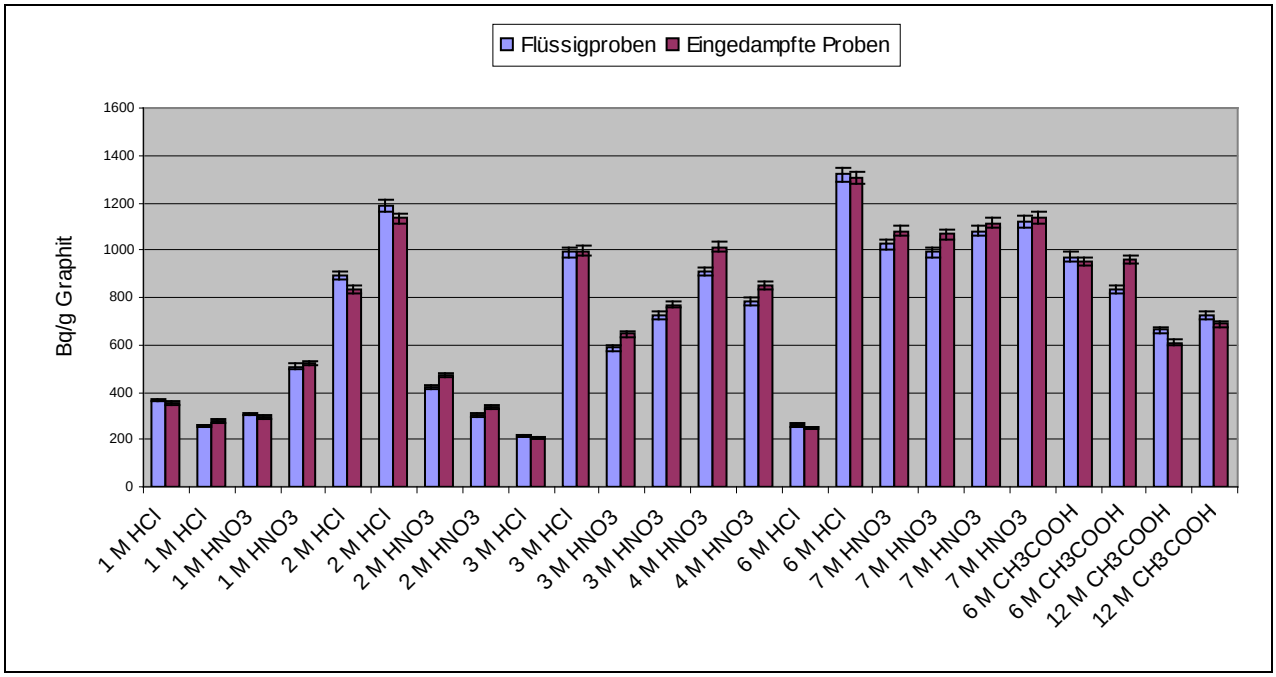

Figure 41: Evaporation test results

(Flüssigproben = liquid samples; Eingedampfte Proben = evaporated samples)

Determination of the samples' ^{14}C and tritium content by comparing the LSC values with the γ spectrometry values

Comparing the activity of the total measured γ spectrometry values and the total LSC values clearly shows that the LSC values are higher than the γ values (see figure 42). As the samples do not contain any ^{90}Sr, it can be assumed that the difference between the LSC- and γ values are caused by bound tritium and ^{14}C in the leaching samples. The ratio between the measured γ values and the LSC values in the liquid samples is predominantly approx. 80% (±20% errors) (see figure 43). This indicates that the ratio between the content of pure β emitters (tritium and ^{14}C) and the γ emitters contained in the liquid samples is roughly the same. The exact total bound tritium and ^{14}C content can only be estimated, but not accurately determined. Since,

because of its low energy, the measured count rate of tritium is only approx. 0.3 and that of ^{14}C only approx. 0.9, the actual total activity will be higher than the measured one.

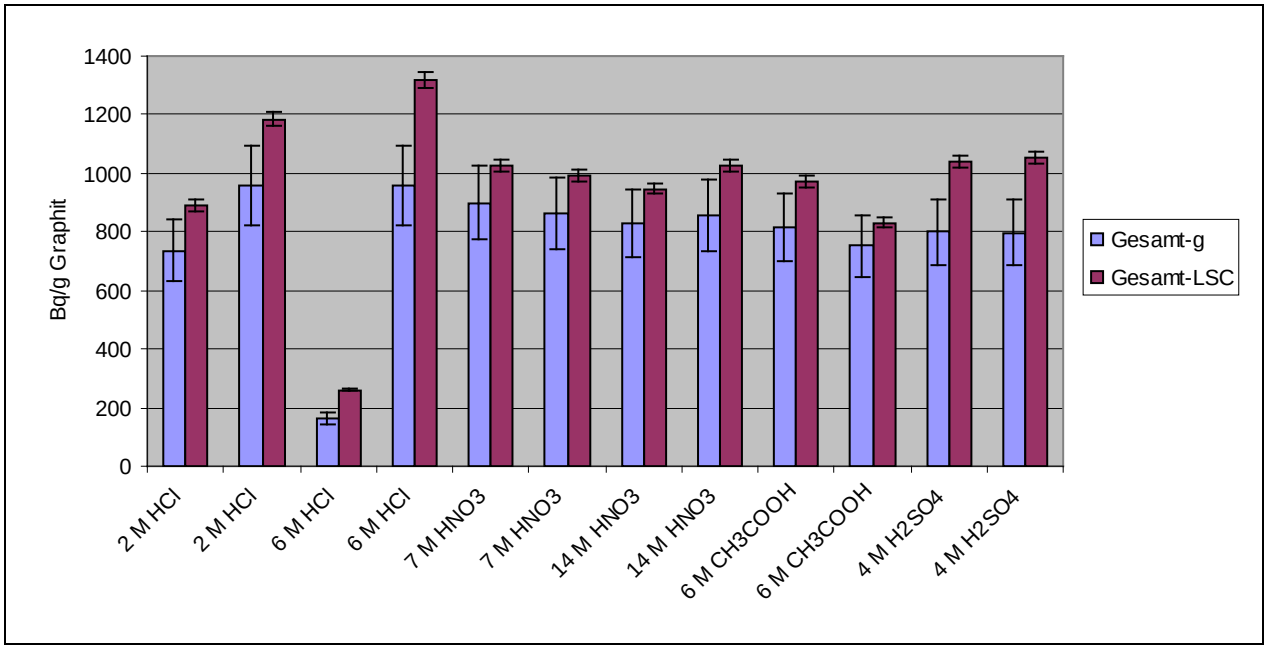

Figure 42: Comparison of the total amount of activity measured by γ spectrometry and the total measured by LSC

(Gesamt = Total)

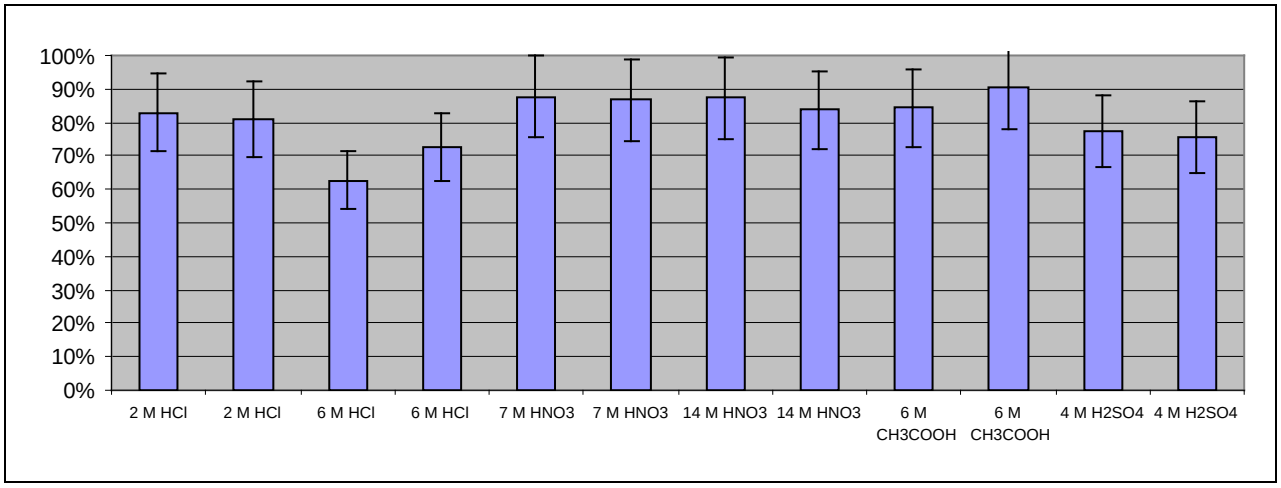

Figure 43: Ratio of the measured γ values to the LSC values of the liquid samples

Detection of organic ^{14}C

Merlin graphite does not contain any organic ^{14}C. Although numerous pulses were measured in some of the samples (see figure 61 in the appendix), an analysis of the spectra (see figures 62 and 69 in the appendix) shows that these measured values are the result of luminescence interference[5] that is caused by organic substances such as, e.g. phenolphthalein. The example spectrum also shows that the peaks of the luminescence interference do not overlap with any other peaks as they are located on the far left of the spectrum.

2. Results (AVR)

2.1. Results of the LSC measurements

2.1.1. Measuring the Total Activity of the Leaching Samples

The values of the total activities within the AVR sample duplicates fluctuated significantly with the exception of the acetic acid samples (see figure 44). The measured values (sum of the results obtained from the 1st and 2nd extraction of the same sample) are between 12,000 and 22,000 Bq; one measured value was 72,000 Bq.

This clearly shows that the acids are also capable of removing more activity from the more heavily contaminated reactor graphite. This is not the result of the significantly higher amount of solvent used in relation to the quantity of reactor graphite (for Merlin 60 mL/ ≈0.5 g graphite Ξ 120 mL/g graphite; for AVR 50 mL/ ≈0.04g graphite Ξ 1250 mL/g graphite). This is made evident on the one hand by the results of the multiple extraction tests performed on the Merlin samples, and on the other, the fact that a significantly lower amount of activity respectively was removed during the 2nd extraction of the same reactor graphite sample than during the 1st extraction (see figure 44).

[5] The chemical reactions that take place in the scintillator solution (chemoluminescence) give rise to individual photons. These are captured by the photoelectron multipliers and can lead to a higher count rate in the low-energy part of the beta spectrum up to an energy of approx. 6 keV.

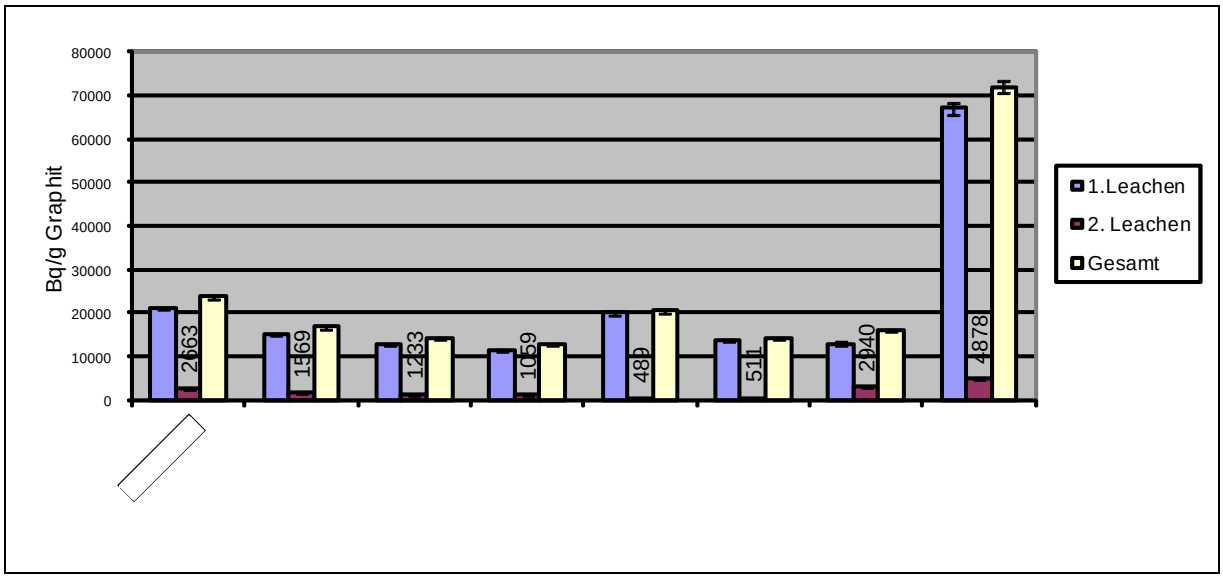

Figure 44: Total LSC result obtained from leaching the same sample twice

(Leachen = Leaching)
(Gesamt = Total)

The lowest decontamination rates were achieved with the acetic acid, while the hydrochloric acid tends to produce better values than the nitric acid. The results obtained with the sulphuric acid are difficult to estimate. On the one hand, the total activity measured for the 1st sample duplicate is the average of all of the values, while, at approx. 72,000 Bq/g graphite, the total activity measured for the 2nd sample duplicate is about three times as high as all of the other results. Comparing the spectrums of the 1st extraction (see figure 63 in the appendix) and the 2nd extraction (see figure 64 in the appendix) of both of the sample duplicates clearly shows how much of the total activity is produced by tritium and how much by ^{14}C. The largest number of pulses were counted within the energy range of these two element's measuring spectra (tritium up to 12 keV; ^{14}C up to 100 keV). This is particularly evident in the spectrum of the sample with the highest activity, sample AVR-14 (2nd sample duplicate, 1st extraction/ see figure 63 below). This spectrum shows that the majority of the activity is caused by tritium.

2.1.2. $^{14}CO_2$ Development during the Extraction

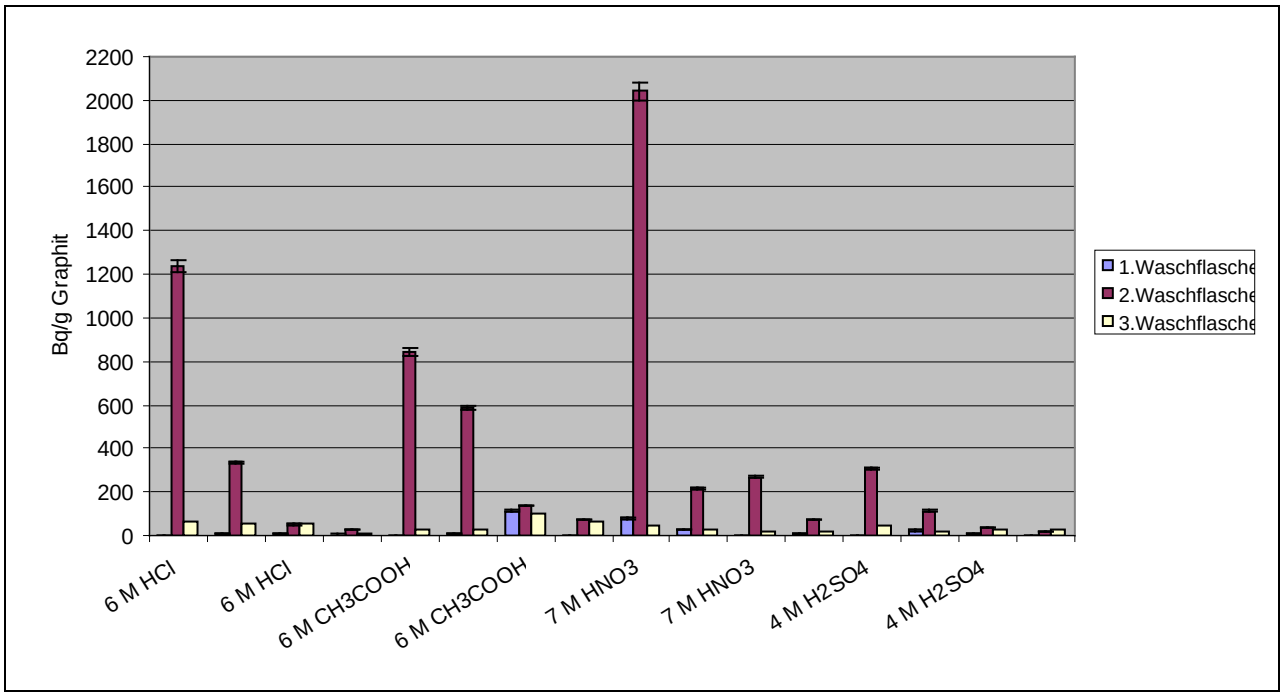

Figure 45: Activity measured in the washing bottles

(Waschflasche = washing bottle)

The activity values within the duplicate samples (see figure 45) (the first two samples respectively are from the 1st extraction, the next two from the 2nd extraction) fluctuate significantly. This is another indication that the samples have inhomogeneous structures. The low number of high values could be due to the fact that the oxidizing acids released a cluster of free ^{14}C atoms in the form of $^{14}CO_2$. The spectra confirm that the activity in the 2nd washing bottles is caused by C-14.

2.2. Results of the γ Spectrometry

2.2.1. Comparison of the Initial Activity and the Residual Activity of the Samples

Comparing the initial activities with the residual activities of the solid material samples shows that the amount of individual nuclides that is removed does not depend on the amount of nuclides contained in the sample. This becomes evident in the case of ^{133}Ba. These values remain nearly unchanged in comparison to the values of the other nuclides (see figure 65 in the appendix).

The ratio between the initial and residual activity of the solid material samples shows that the leaching rates of the individual solvents do not differ to such an extent in relation to the amount of radionuclides that they remove that one particular solvent would stand out from the rest (see figure 47):

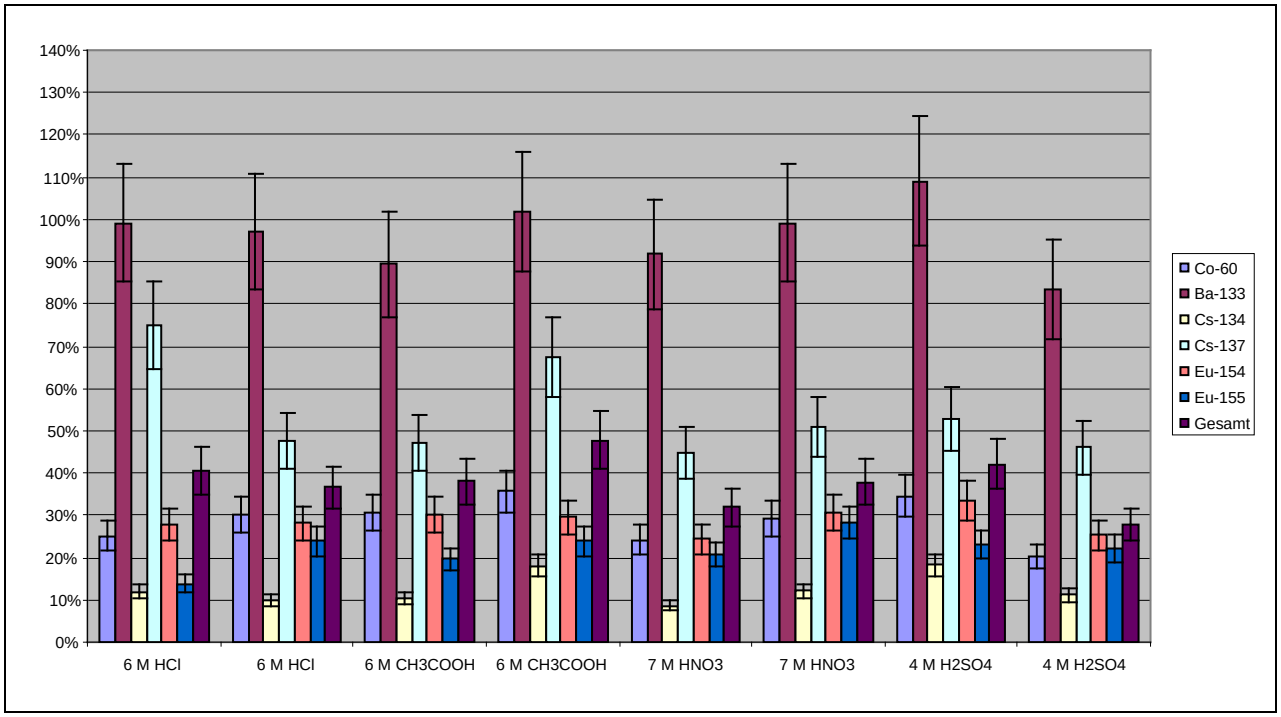

Figure 47: γ activity ratios of the solid material samples before and after leaching.

- In ^{60}Co (A_{before}≈ 12000 – 17000 Bq), the unremoved amount is between 21 and 36%
- In ^{133}Ba (A_{before}≈ 1300 – 1600 Bq), the unremoved amount is between 84 and 100%
- In ^{134}Cs (A_{before}≈ 110 – 230 Bq), the unremoved amount is between 10 and 20%
- In ^{137}Cs (A_{before}≈ 2200 – 4100 Bq), the unremoved amount is between 45 and 75%
- In ^{154}Eu (A_{before}≈ 520 – 660 Bq), the unremoved amount is between 25 and 35%
- In ^{155}Eu (A_{before}≈ 140 – 190 Bq), the unremoved amount is between 15 and 30%

The barium values, some of which are higher than 100%, are an indication of measuring errors. These are at 14% and are due to the measuring device.

2.2.2. Comparison of the γ Activity of the Samples before and after Leaching.

Comparing the solid material samples' γ activity before the tests with the total sum of all of the measuring results from after the tests shows that the initial activity of the nuclides is generally higher in the solid material samples than the total sum of the activity of all samples (residual activity of the solid material samples and all liquid samples) after the tests (see figure 66 in the appendix). The difference of the ^{60}Co values in particular must be taken into account in this respect. ^{60}Co is the nuclide with the highest level of activity and thus contributes to the differences in the measured values. This becomes even more obvious with respect to the ratio between the solid material samples before the leaching and the sum of all values measured after the leaching (see figure 48). Up to 25% of the actual ^{60}Co values remain below the specified value. This cannot be explained in terms of low activity, as was the case in the nuclides, whose small liquid sample size had activity values that were often below the detection level and could therefore not be measured. ^{60}Co is a high-energy emitter, which is why these values can also not be caused by losses from too high a background. The geometric difference between the solid material and liquid samples can also not account for this, as this is taken into account using a correction value. The correction value for ^{60}Co for solid

material samples of up to 0.15 g is 27.6, for liquid samples of a volume of 0.5 mL 27.4. The difference in percentage between the two values is 1%.

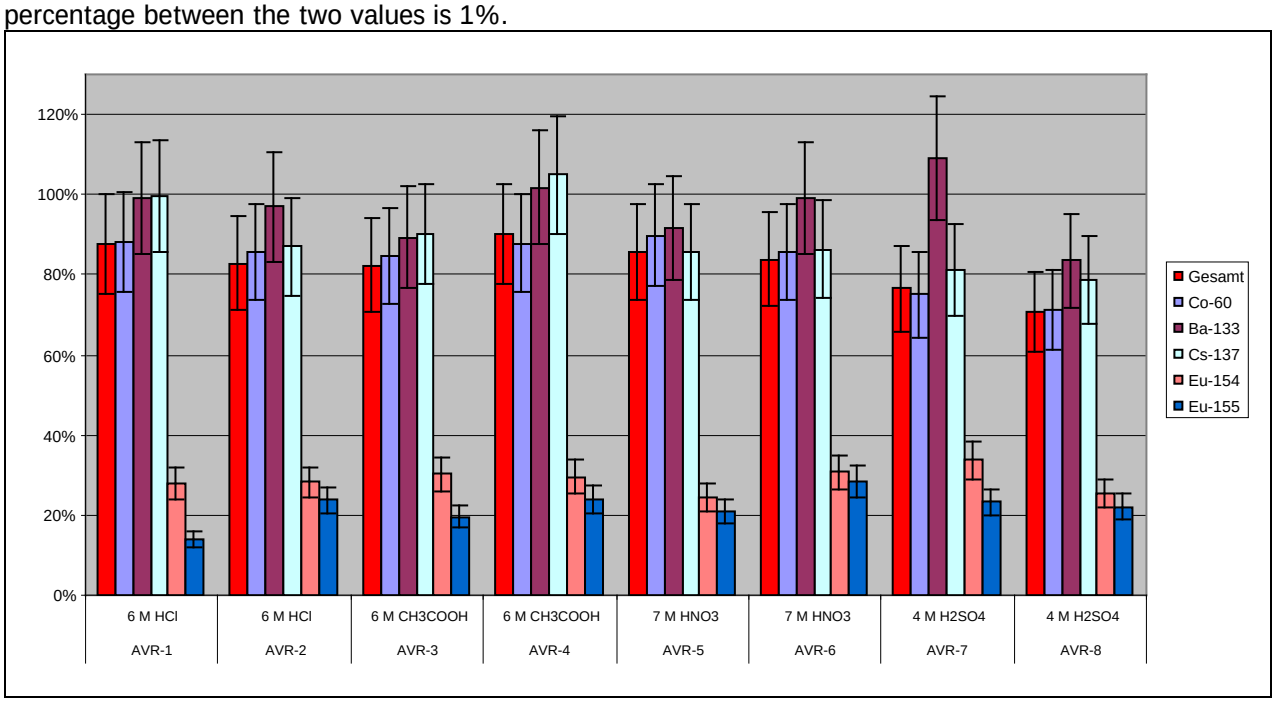

Figure 48: Ratio between activity before the leaching and the sum of all values measured after the leaching

2.3. Separating the Individual Radionuclides

2.3.1 Separation of ^{90}Sr

The spectra of the LSC measurement (see figure 67 in the appendix) clearly show that the measuring error rate is up to 50% high. Amongst others, this is due to the fact that the sample sizes were very small and the measured values (max. 1.86 Bq/sample) are very low. Due to the short measuring time and the comparatively high background of 47 ipm, this leads to highly inaccurate measurements (see figure 49).

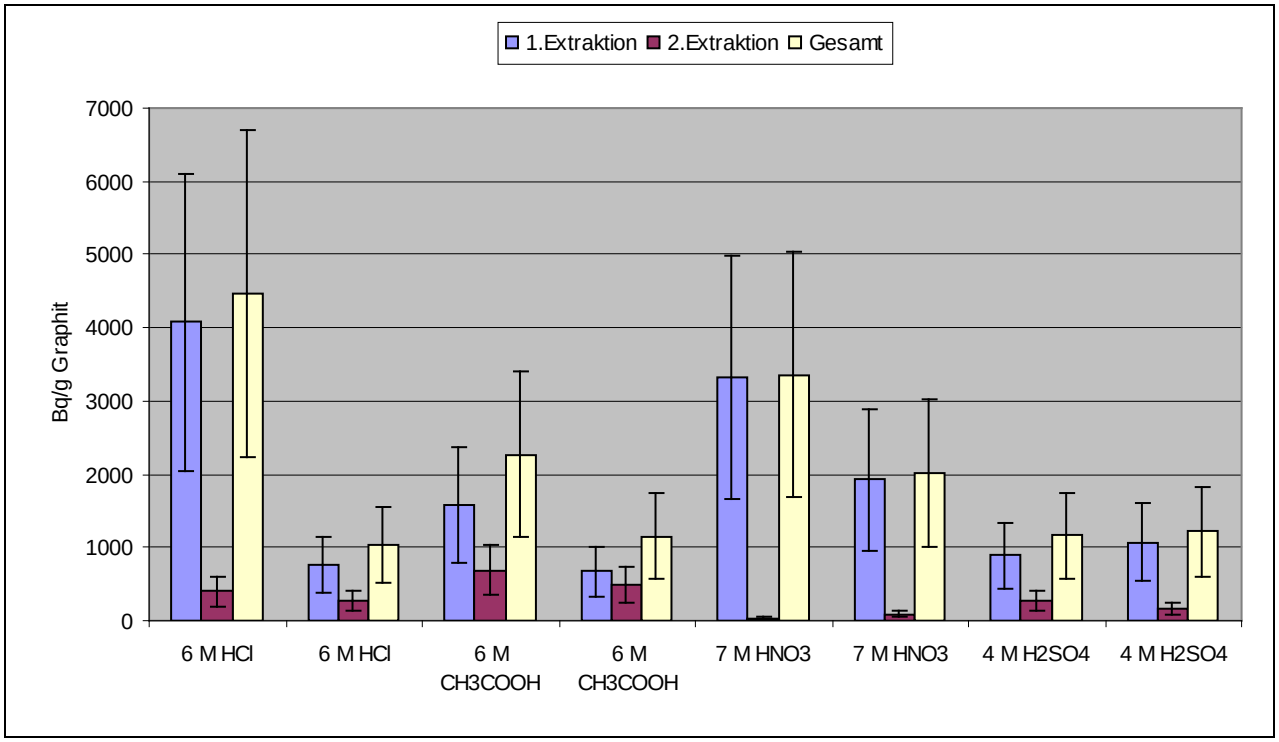

Figure 49: Separation of ^{90}Sr

2.3.2. Separation of Caesium with Ammonium Molybdophosphate (AMP)

Although the results show that the ^{137}Cs has been separated, there is no evidence of any other nuclides apart from ^{60}Co. The differences between the values measured from the AMP samples and the untreated samples are clearly evident. The differences in the ^{60}Co activity values measured for the AMP-samples and the activity of the untreated liquid samples are significantly higher than the value of 4.4% stated in the literature[1]. This can be explained in terms of the low amount of sample solution of 0.5 mL and associated low concentration of the nuclides in the sample, which are below the detection limit (see table 13). The presence of sulphates seems to interfere with the separation, as the cobalt values measured in the sulphuric acid samples after the separation itself are very low (see figure 50).

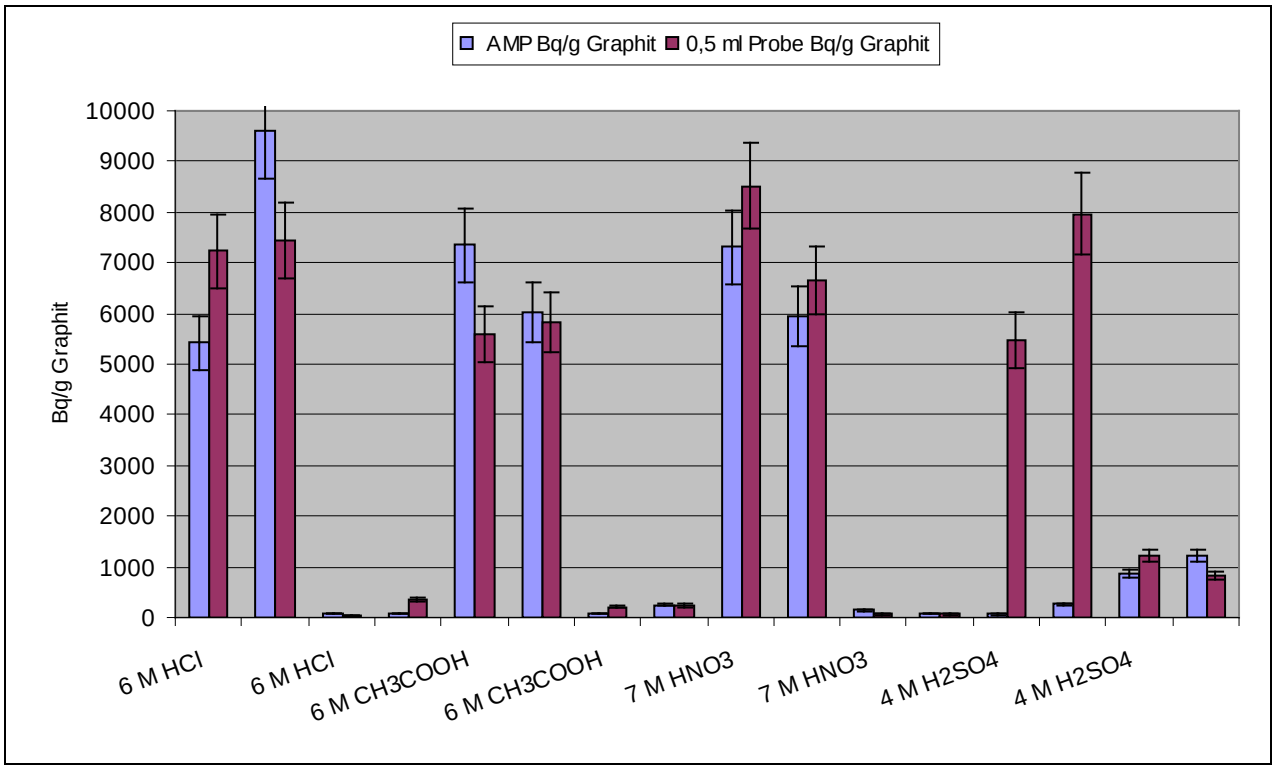

Figure 50: Comparison of the AMP sample and untreated liquid sample Co-60 content

2.3.3. Detection of Organic Carbon

As with the Merlin samples, some of the samples were found to contain numerous pulses that were higher than the background level (see figure 51). However, the samples' spectra show (see figure 68 in the appendix) that these count rates are not the result of ^{14}C, but only of luminescence interference, which is probably caused by low-boiling organic substances (phenolphthalein), that were transferred into the washing bottles. These “ghost peaks” are so far on the left of the energy spectrum that it is clearly evident that they do not cover any other peaks.

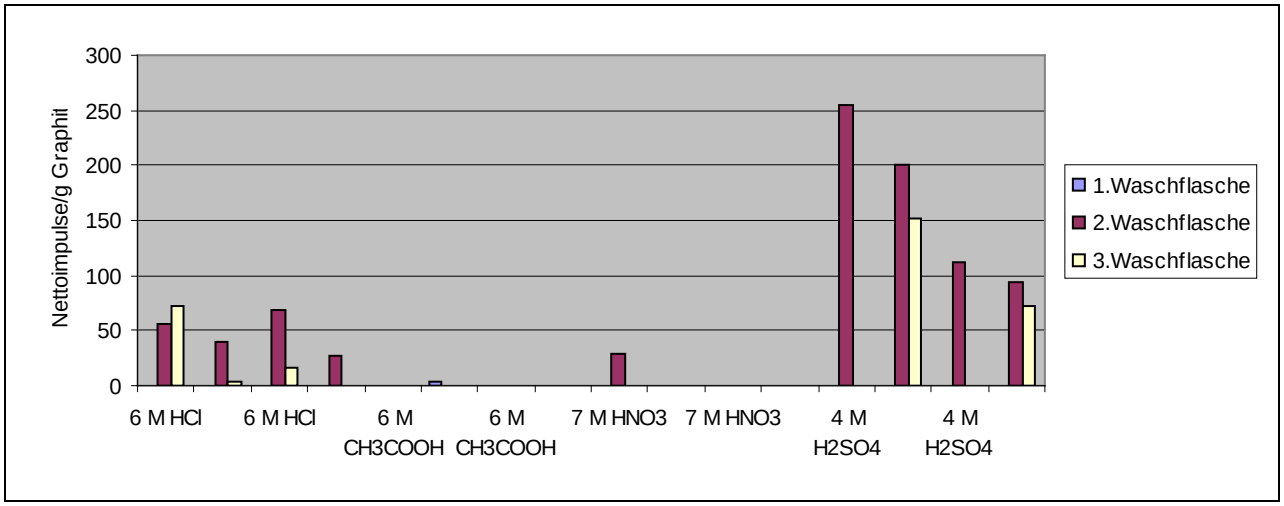

Figure 51: Net pulses measured in the washing bottles

(Waschflasche = Washing bottle)

2.4. Comparison of the LSC Values with the γ Spectrometry Values

It is very difficult to interpret the measured values with respect to the pure β emitters as the majority of the tritium and of the ^{14}C is dissolved in such a way in the leaching solutions that determining or estimating the content is only possible by calculating the difference between the total sum of the LSC values and total sum of the γ values.

When comparing the difference between the γ activities of the solid material samples before and after the leaching (= amount of γ emitting nuclides that has been removed), the total γ activities of all of the liquid samples and the sum total of the measured LSC values, it becomes evident that the values measured by LSC are significantly higher than the two γ values (see figure 52). This is evident in particular when comparing the ratios between the LSC and γ values (see figure 53).

The ratio between the γ values of the liquid samples and the LSC values is between 14% and 60% (± 10% errors). The ratio of the γ values calculated from the difference of the solid material samples before and after the tests and the LSC values is between 23% and 79% (± 10% errors). The pure β emitter (tritium, ^{14}C and/or Sr-90) content fluctuates significantly between the individual samples. Regarding the highest value of over 70,000 Bq measured by LSC, at least 75% of the radionuclides contained in this sample are pure β emitters.

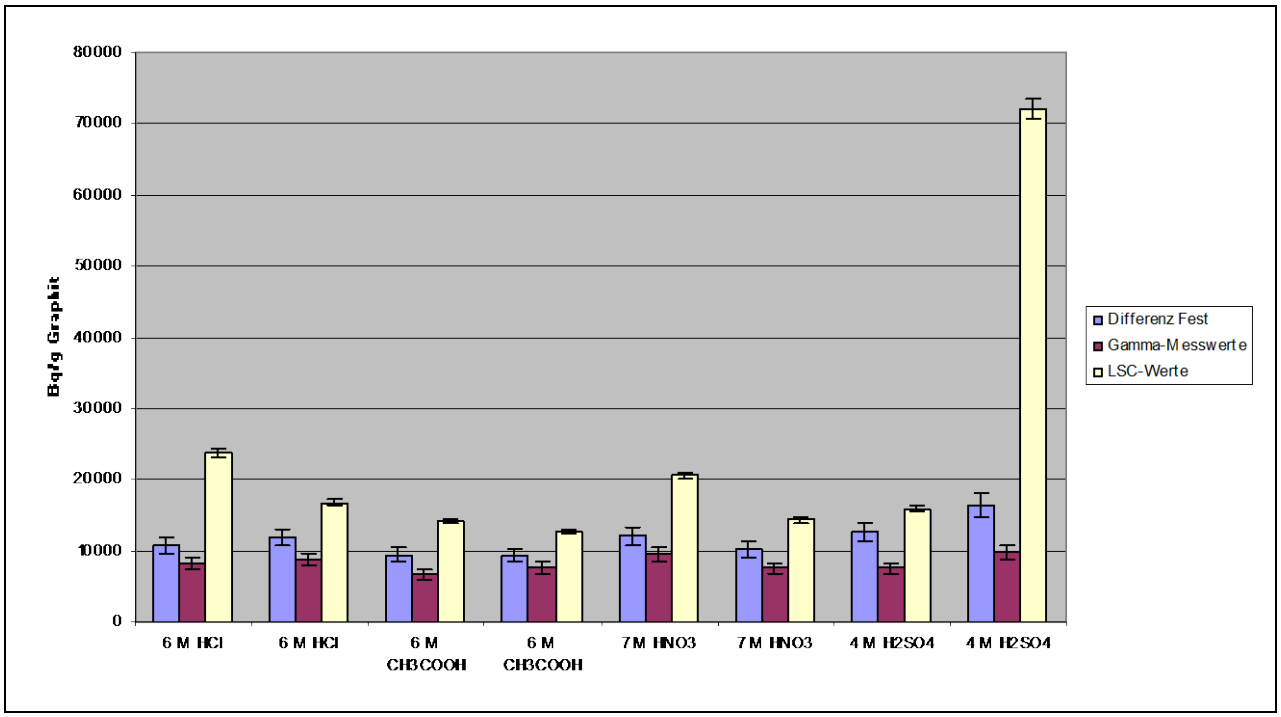

Figure 52: Comparison of the difference between the solid material samples' values before and after leaching, the liquid samples' γ values and the sum total of the LSC values

(Differenz fest = Difference solid)

(Gamma-Messwerte = Gamma measuring values)

(LSC-Werte = LSC values)

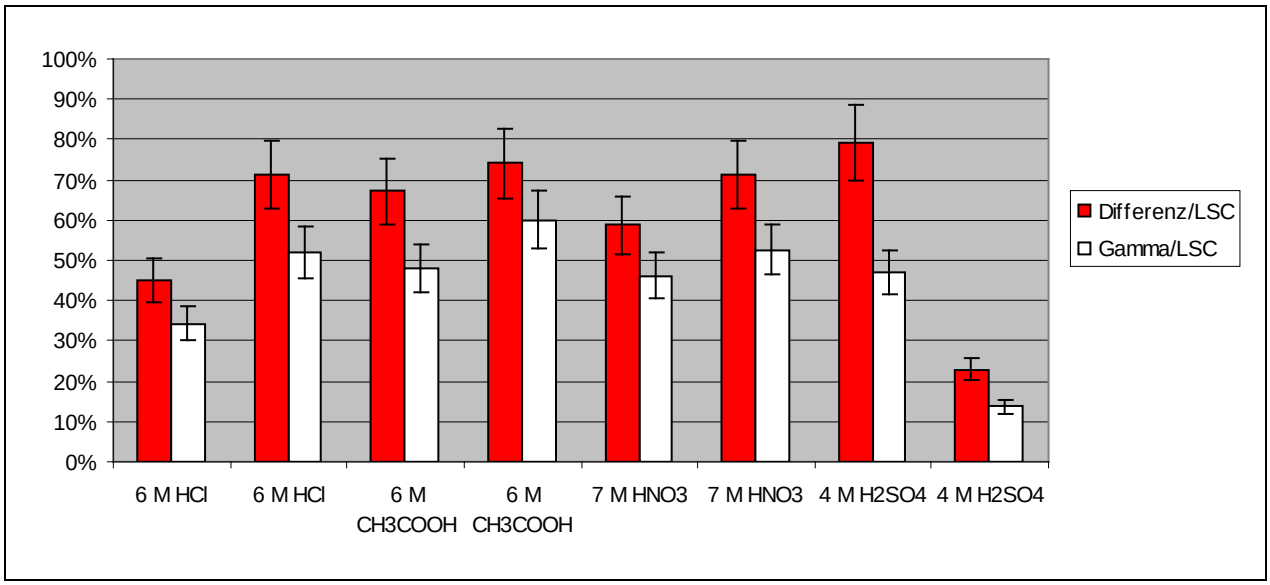

Figure 53: Ratio between the difference between the γ solid material activity before and after the tests and the sum total of the values measured by LSC, and between the γ value of the liquid sample and the sum total of the LSC measured values.

3. Comparison of the Merlin and AVR Results

Pure β emitters:

The percentage of pure β emitters (^{3}H und ^{14}C) in the untreated Merlin graphite samples is more than 71% of the total radionuclide inventory. The percentage measured in the extraction solutions is only 20%.

If one were to assume that the ratio in the leaching solutions is the same as in the untreated leaching solutions, i.e. tritium/^{14}C = 10/1, the actual activity of a sample with a measured activity of 1000 Bq would be calculated by:

e.g. for ^{14}C:

$$A_{14C} = \frac{R_{measured} \cdot \text{percentage}_{\text{pure } \beta \text{ emitter}} \cdot \text{part of } \beta \text{ emitter}_{14C}}{100\% \cdot \text{count rate}_{14C}}$$

Total:

$$A_{total} = A_{14C} + A_{tritium} + A_{\gamma \text{ emitter}}$$

1422 Bq = (1000 * 20% * 0.1/(100% * 0.9) + 1000 * 20% * 0.9/(100% * 0.3)Bq) + 800 Bq

The actual percentage of both nuclides in the total inventory would then not be approx. 20%, but approx. 44%. However, this value would still be lower than the 71% measured for the untreated samples.

The following charts show the calculated values and the ratios between the β emitters and the total inventory:

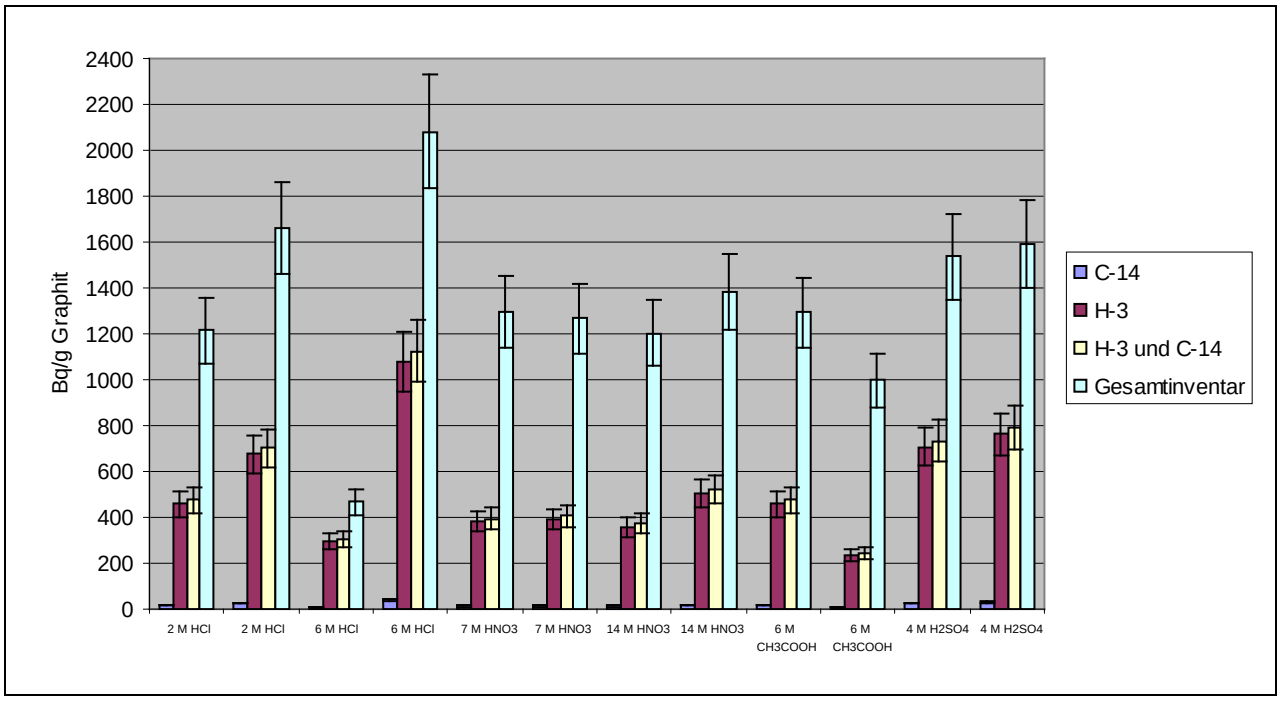

Figure 54: Comparison of the β activities and total activity (hypothesis)

(Gesamtinventar = Total inventory)

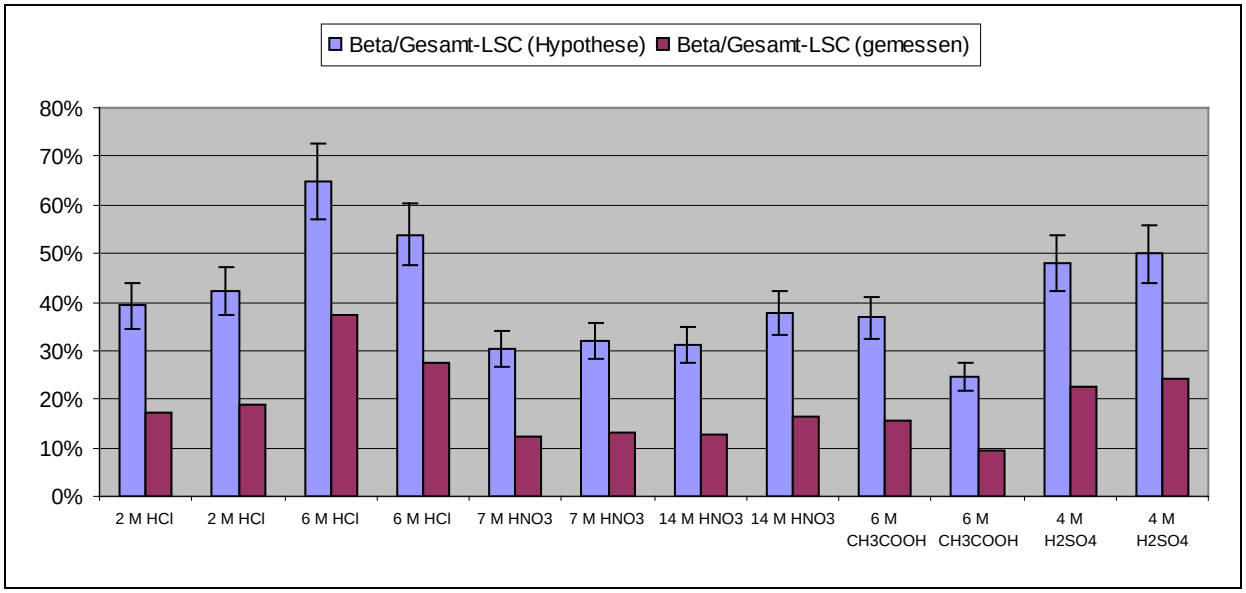

Figure 55: Ratio of pure β emitters and total activity (hypothesis and measured values)

According to the hypothesis, the activity values are nearly twice as high as the measured values. The highest value rises from approx. 1300 Bq/g graphite to just under 2100 Bq/g graphite. The ratios between the activity of the pure β emitters and the total activity generally rise to twice the value. I.e. from values of between 9% and 35% to values of between 25% and 65%. Most of the values are between 30% and 40%.

Regarding the AVR samples, it is furthermore problematic that the quantity of pure ß emitters (^{3}H, ^{14}C and ^{90}Sr) inside the untreated samples is an unknown. For this reason, the radionuclide ratios of known AVR samples were used for comparison. Despite the high differences in activities, the ratio between pure ß emitters and the radionuclide inventory is approx. 95% (see table 8). In the extraction solutions, the measured percentage of pure ß activity is between 20 and 55%, and in the sample with the highest activity, more than 75% (see figure 56). The measured percentage of pure ß emitters in the sample solutions of both series of tests is therefore smaller than their percentage in the untreated solid material samples. However, the actual percentage of pure ß emitters in both series of tests is higher than the measured percentage, as the low count rate of ≤ 1, which is due to the weak energies, also has to be taken into account. This is also evident from the spectra of the LSC measurements.

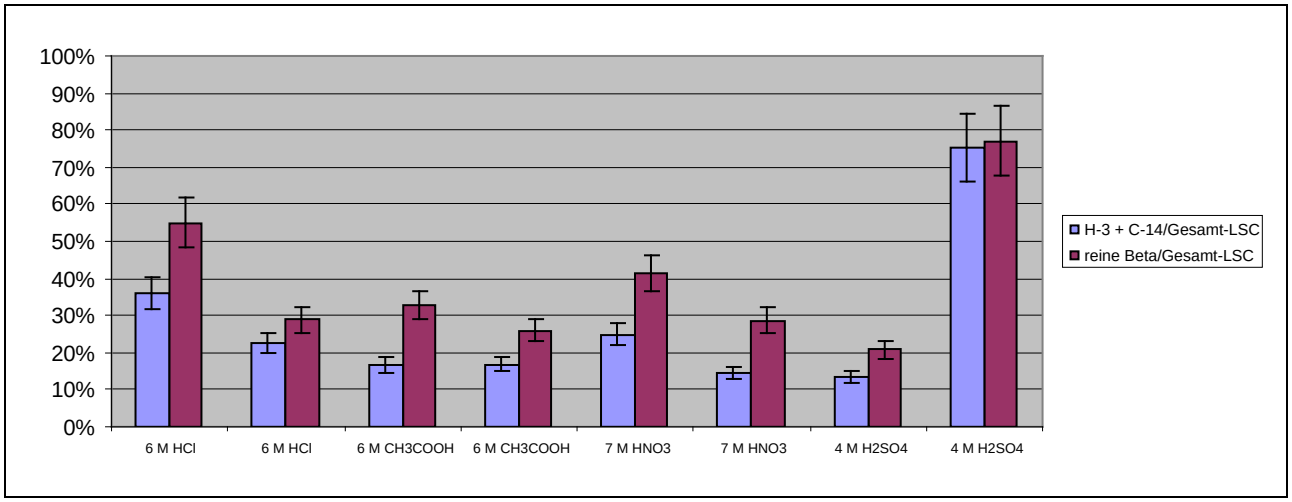

Figure 56: Ratio of the ^{3}H- + ^{14}C content to the total LSC or pure β emitter to the total LSC (measured)

(Pure beta/Total LSC)

If we assume that the ratio of ^{3}H/ ^{14}C is 11 to 1, as is the case in sample AVR-G-8 (see table 8), the resulting graph would look as follows:

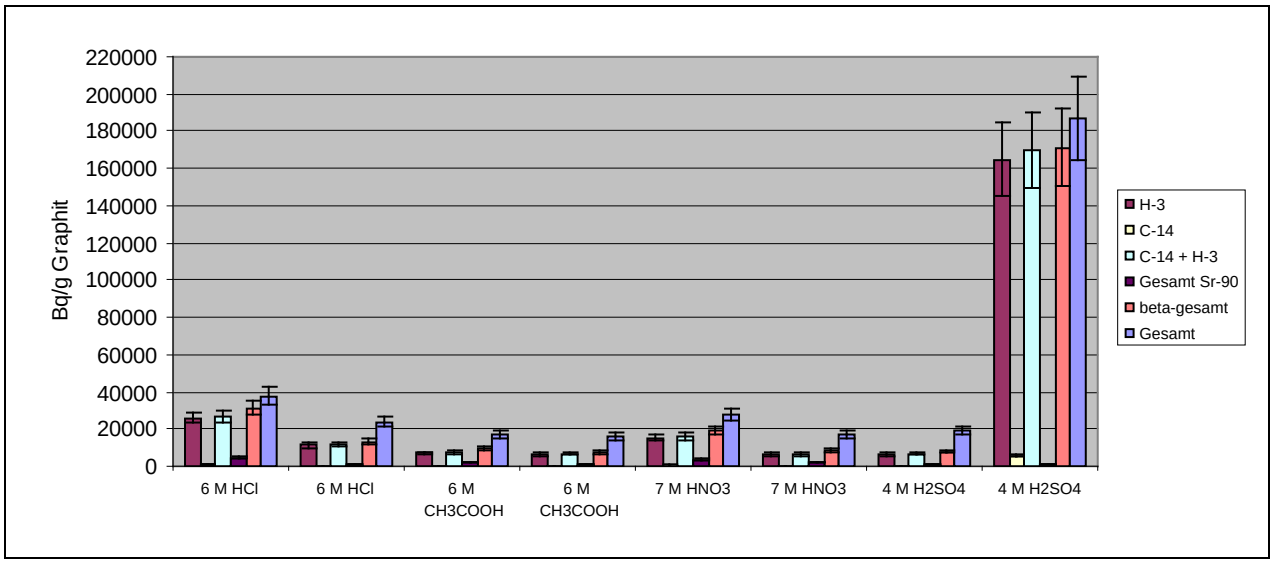

Figure 57: Comparison of the beta activities and the total inventory (hypothesis)

According to the hypothesis, the actual values are 1.5 to 2.5 times as high as the uncorrected measured values. The highest measured value in particular stands out from the rest and increases from approx. 72,000 Bq/g graphite to 185,000 Bq/g graphite. The main reason for this value is the sample's high tritium content. This is clearly shown in the following figure 58:

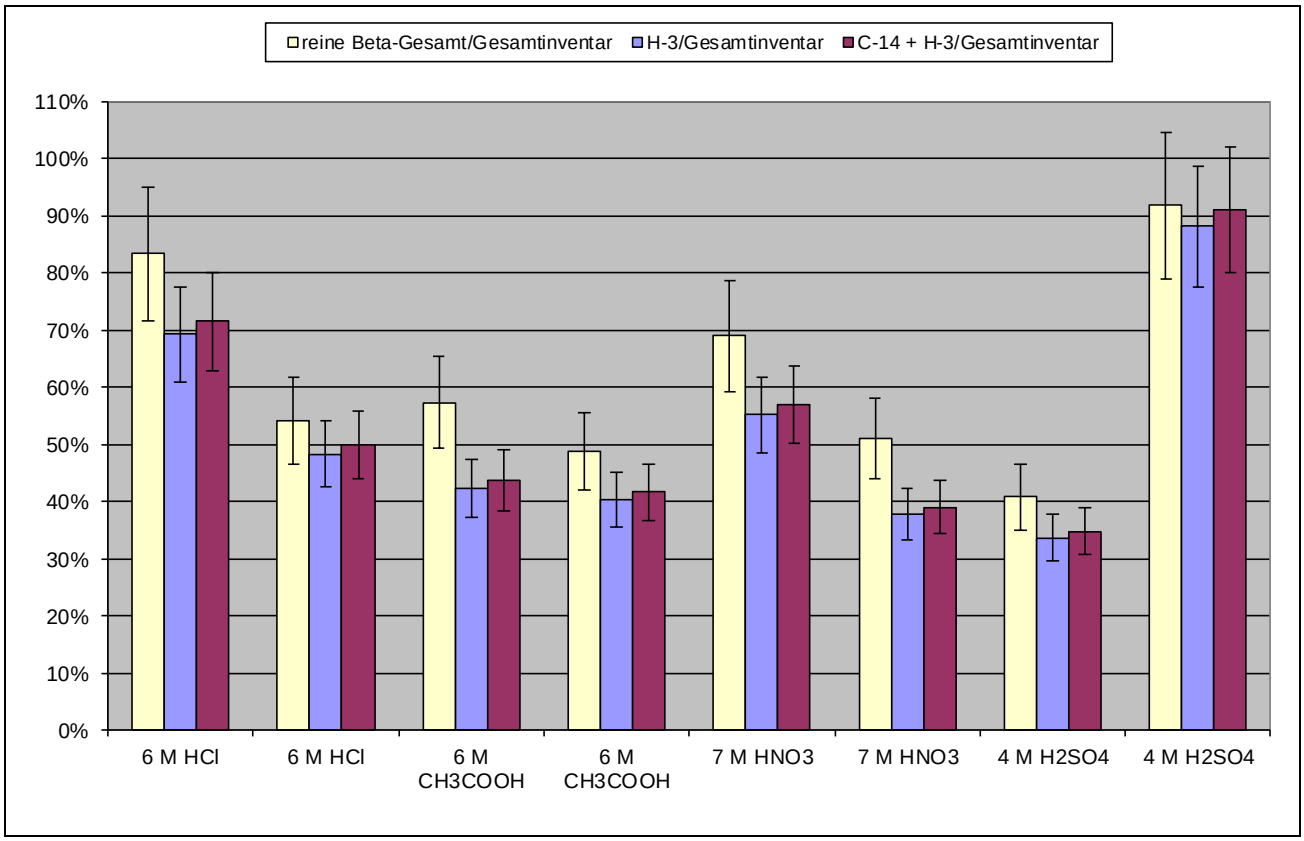

Figure 58: Ratio of the ^{3}H- + ^{14}C content to the total LSC or pure β emitter to the total LSC (hypothesis)

The graph shows that, according to the hypothesis, the total inventory contains up to 92% of pure beta emitters. The sample with the highest activity reaches this value. This sample's total inventory is made up to 88% of tritium. At approx. 41%, the Merlin samples' total inventories contain the lowest percentage of pure ß emitters (mostly 40%).

The comparison shows that more pure ß emitters are usually removed from the AVR graphite than from the Merlin graphite. There may be several reasons for why this percentage is higher in the AVR graphite, such as:

- In contrast to the Merlin graphite, the AVR graphite or the leaching samples contain ^{90}strontium.
- The presumably very high percentage (up to 95%) of pure ß emitters in the AVR graphite
- The higher neutron radiation in the AVR reactor increases the reaction probability and the AVR graphite therefore reacts more easily with the solvents.
- The higher neutron radiation has damaged the graphite lattice to such an extent as to make it easier for the solvents to remove the radionuclides from the graphite.

Tritium ^{3}H:

The leaching solutions and the washing bottles were only found to contain very small amounts of free tritium. The equipment used in this present study is not suitable for analysing the total percentage of removed tritium in the samples.

^{14}Carbon:

Inorganic ^{14}C can only be accurately analysed in the AVR samples in the washing bottles. The highest measured value of 2042 Bq/g graphite amounts to less than 4% of the sample with the lowest known ^{14}C content AVR-G-10 (see table 8). The leaching samples do not contain any organic ^{14}C. As with the tritium, it is not possible to precisely determine the total percentage of ^{14}C in the radionuclide inventory of the leaching samples.

^{90}Strontium:

Only the AVR samples contain ^{90}strontium. The removed amounts are between 14% (lowest value from 4 M sulphuric acid) and 70% (highest value from 6 M hydrochloric acid), compared with sample AVR-G-7, the sample with the lowest known ^{90}strontium content (see table 8).

γ emitters:

Proportionally, the other nuclides, with the exception of ^{133}Ba and ^{137}Cs, were much easier to remove from the reactor graphites than tritium and ^{14}C. One of the reasons for this could be that, in contrast to tritium, these nuclides do not diffuse that strongly into and are absorbed into the graphite lattice's structure, but are located at the boundary surfaces of the graphite lattices. Since ^{14}C, as a carbon isotope, is similarly inert as graphite, it is not as efficiently removed from graphite as other radionuclides.

^{60}Cobalt:

Only the AVR samples contain ^{60}cobalt. The acids used in the tests remove at least 64 % of the ^{60}cobalt. The highest amount is 79%.

Europium isotope ^{152}Eu, ^{154}Eu and ^{155}Eu:

^{152}Eu is removed to at least 70%, ^{154}Eu to between 65 and 75%, and ^{155}Eu is removed to between 70 and 85%.

^{133}Barium:

The maximum amount of ^{133}barium, which is only found in the AVR samples, removed from the samples is 16%. ^{133}barium is therefore the radionuclide of which the smallest amounts were removed from the reactor graphite.

Caesium isotopes ^{134}Cs and ^{137}Cs:

Only the AVR samples contain both of the caesium isotopes. The amount of ^{137}Cs removed is between 25 and 55%. The amount of ^{134}Cs in the solid material sample was measured as being just a small amount over the detection limit. After leaching, these values are below the detection limit for ^{134}Cs. It is therefore only possible to state that ^{134}Cs has been removed.

Hypothesis: As an alkaline earth metal, barium is deposited between the graphite lattice layers just like the alkaline metal caesium. Due to its larger ionic radius, it will be more firmly embedded at this site than caesium and is therefore harder to remove from the graphite.

4. Results Relevant to the Storage of the Treated Reactor Graphite

The Atomic Energy Act does not specify any exact periods of time over which radioactive material can be stored.

Rough estimate of the relevant storage periods of radioactive material:

- Intermediate fuel element storage: 1 – 5 years
- Intermediate storage: approx. 5 – 40 years
- Final storage: approx. after the 40th year

Since it is not yet possible to foresee the date from which on there will be a final storage facility for radioactive waste available in Germany, it is not yet possible to specify for how long the waste that is intended for storage in a final storage facility will be stored in an intermediate one.

The waste from the FRJ-1:

With the exception of europium-152, the radionuclides in the samples from the FRJ-1 would have decayed to such an extent after having been stored in an intermediate facility for approx. 40 years, that they could be disposed of as industrial waste (see table 14). However, since the ^{152}Eu in each of the samples will be higher than the permitted limit after the extraction tests even after 40 years, the treated reactor graphite from Merlin would also have to be put into final storage.

The waste from the AVR:

Depending on the (carrier) quantity and half life, some radionuclides (^{134}Cs and ^{155}Eu) decayed to such an extent during intermediate storage (approx. 40 years) that their levels of radioactivity were below their respective permissible levels.

However, it would be absolutely vital for radionuclides that are particularly problematic (e.g. ^{60}Co), which have a lower permitted limit because of their higher levels of radiotoxicity, to be separated in order to be able to dispose of the reactor graphite as industrial waste.

The amount of activity of ^{133}Ba alone that is removed during the tests is so low that the samples always stay well above their permissible limit of 30 Bq/g. The methods used in the tests are not suitable for effectively lowering the samples' activity levels, which means that the treated reactor graphite has to be moved into a final storage facility even after a forty years of intermediate storage.

E. Summary and Outlook

The aim of this study was to decontaminate radioactive reactor graphite samples by Soxhlet extraction or liquid-solid extraction with a view to potentially removing the need for this radioactive graphite to be put into final storage.

The solvents used in this study were water, various organic solvents and inorganic or organic acids in different concentrations.

The above aim was pursued by performing two series of tests. The first series of tests using less severely contaminated reactor graphite was aimed at selecting suitable solvents. The second series of tests was aimed at establishing the effect of the selected solvents on more severely contaminated reactor graphite samples.

The samples for the first series of tests were originated from Forschungszentrum Jülich's research reactor Merlin. These samples come from the thermal columns where they were exposed to neutron radiation. They contained the following radionuclides: ^{3}H, ^{14}C, ^{60}Co, ^{133}Ba, ^{152}Eu, ^{154}Eu and ^{155}Eu. Their total activity at the time of the tests amounted to approx. 8,000 Bq/g graphite. The samples used for the second series of tests were provided by the Reactor Working Group (Arbeitsgemeinschaft Versuchsreaktor) Jülich, AVR for short, and come from the AVR's high temperature reactor. This reactor graphite was used as reflector material. These samples had consequently been exposed to a higher level of neutron radiation than the Merlin samples. They contained the following radionuclides ^{3}H, ^{14}C, ^{90}Sr, ^{60}Co, ^{133}Ba, ^{134}Cs, ^{137}Cs, ^{154}Eu and ^{155}Eu. At the time of the tests, the γ activity amounted to approx. 23,000 Bq/g graphite.

The first series of tests showed that, with the exception of the acids, all of the other solvents that were used only removed very little of the radioactive inventory from the Merlin reactor graphite samples (approx. 0.5 g per sample) (highest level of activity removed 12 Bq/g graphite). The best results were obtained with the acids with the higher concentrations. (Highest level of activity removed 1300 Bq/g graphite).

The extracting agents used for the second series of tests were 6 M hydrochloric acid, 7 M nitric acid, 6 M acetic acid and 4 M sulphuric acid. In an effort to keep radiation exposure as low as possible, the samples were used in significantly smaller quantities (approx. 0.04 g).

The results of the two series of tests showed that the methods used, i.e. Soxhlet extraction or liquid-solid extraction, are not extremely effective in decontaminating reactor graphite. Compared to the other nuclides, tritium and ^{14}C in particular, which contribute the highest level of activity in the samples (in the Merlin samples ≈ 71% of the total radionuclide inventory, AVR samples ≈ 95% of the total radionuclide inventory) are the two nuclides of which the lowest amount is removed from the graphite. The amount of tritium and ^{14}C that is removed from the less contaminated Merlin graphite is proportionally lower than that removed from the AVR graphite (44% up to 92%).

Using strong acids, all of the other radionuclides, with the exception of ^{133}barium, are comparatively easy to remove from the reactor graphite. However, they were still not removed to a sufficient extent, as both the treated Merlin reactor graphite as well as the graphite from the AVR were still contaminated to such an

extent after an intermediate storage period of 40 years that both of them would have to be disposed of in a final storage facility.

Further tests will be needed to clarify to what extent a smaller grain size and therefore a larger reaction surface might have a better decontamination effect in reference to certain nuclides.

It would furthermore also be of interest to perform these tests with more heavily contaminated reactor graphite or reactor graphite that has been exposed to a higher neutron radiation dose, as the structure of such graphite would have undergone more significant changes or damage as a result of the higher neutron radiation, or would have been disrupted due to the higher percentage of radionuclides, than that of the reactor graphites used in the present tests. This in turn could result in significantly higher leaching rates.

Furthermore, the extent to which consecutive extractions with different acids will lead to better results should also be investigated. It should also be considered whether to investigate the use of catalysts, e.g. vanadium catalysts, and/or a combination of different solvents.

F. Appendix

1. List of Figures/Tables and Equations

1.1. List of Figures

Figure 1-5: Does not apply

Figure 6: Possible compounds that reactor graphite can form [14] 6

Figure 7: Oxidation speed of graphite [25] 7

Figure 8: Release of tritium in graphite in dependence on temperature and time [34] 10

Figure 9: Specific tritium production rate for different HTRs as a function of time [12] 11

Figure 10: Reactor building with extensions seen from the north-west 12

Figure 11: Cross section of the reactor block/ Position of the individual graphite bricks inside the reactor block 13

Figure 12: Dependence of the 3H- and 34C content on the position of the graphite brick from thermal column II [27] 14

Figure 13: Tools used to crush the samples 14

Figure 14: HTR of the AVR with extensions during operation 15

Figure 15: Internal structure of the AVR's high temperature reactor [3] 15

Figure 16: Neutron flux above the ceiling reflector [36] 17

Figure 17: View of the ceiling reflector, the upper part of the side reflectors and the guide pipes of the control rods of the AVR's research reactor before being filled with spherical fuel elements 17

Figure 18: Solid material samples in test tubes 18

Figure 19: Sample comparison: AVR 1 - AVR 8 with AVR-G-19 19

Figure 20: Cross section of an extraction thimble 24

Figure 21: Experimental set-up for the Soxhlet extraction for the Merlin graphite 26

Figure 22: Steps involved in separating 90strontium 29

Figure 23: The addition of the sample to the AMP 30

Figure 24: Separation of the sample from the AMP 30

Figure 25: Subboiling apparatus 31

Figure 26: Packard sample vials in LSC with open flap 32

Figure 27: γ measuring device with open doors 34

Figure 28: Comparison of the measurement results of the neutral solvents' leaching samples 35

Figure 29: Comparison of the activity of the HCl leaching samples 36

Figure 30: Comparison of the activity of the HNO3 leaching samples 36

Figure 31: HNO3 extraction: Activity of the washing bottles' contents 37

Figure 32: Comparison of the activity of the CH3COOH und H2SO4 leaching samples 37

Figure 33: Result of multiple leaching processes using 1 M HCl 39

Figure 34: Result of multiple leaching processes using 1 M HNO3 39

Figure 35: Result of multiple leaching processes using 6 M CH3COOH 39

Figure 36: Result of multiple leaching processes using 4 M H2SO4 39

Figure 37: Comparison of the activity of the Merlin leaching samples 44
Figure 38: Activity of the solid material samples after the tests 40
Figure 39: Ratio between activity in liquid sample / activity in sum of all samples 41
Figure 40: Subboiling tests 42
Figure 41: Evaporation test results 42
Figure 42: Comparison of the total amount of activity measured by γ spectrometry and the total measured by LSC 43
Figure 43: Ratio of the measured γ values to the LSC values of the liquid samples 43
Figure 44: Total LSC result obtained from leaching the same sample twice 44
Figure 45: Activity measured in the washing bottles 45
Figure 47: γ activity ratios of the solid material samples before and after leaching 46
Figure 48: Ratio between activity before the leaching and the sum of all values measured after the leaching 47
Figure 49: Separation of 90Sr 48
Figure 50: Comparison of the AMP sample and untreated liquid sample Co-60 content 49
Figure 51: Net pulses measured in the washing bottles 49
Figure 52: Comparison of the difference between the solid material samples' values before and after leaching, the liquid samples' γ values and the sum total of the LSC values 50
Figure 53: Ratio between the difference between the γ solid material activity before and after the tests and the sum total of the values measured by LSC, and between the γ value of the liquid sample and the sum total of the LSC measured values 51
Figure 54: Comparison of the β activities and total activity (hypothesis) 52
Figure 55: Ratio of pure β emitters and total activity (hypothesis and measured values) 52
Figure 56: Ratio of the 3H- + 14C content to the total LSC or pure β emitter to the total LSC (measured) 53
Figure 57: Comparison of the β activities and total inventory (hypothesis) 53
Figure 58: Ratio of the 3H- + 14C content to the total LSC or pure β emitter to the total LSC (measured) 54
Figure 59: Overview of all of the measuring results from the Merlin leaching samples 63
Figure 60: Measuring result of the 90Sr separation 64
Figure 61: Net pulses washing bottles 64
Figure 62: Spectrum 1st sample H2SO4, 3rd washing bottle 64
Figure 63: Spectra AVR-13 and 14 (1st extraction of the H2SO4 samples) 65
Figure 64: Spectra AVR-15 and 16 (2nd extraction of the H2SO4 samples) 65
Figure 65: Comparison of the activity of the individual nuclides of the solid material samples before and after leaching 66
Figure 66: Comparison of the activity of the solid material samples before the tests with the sum of all measuring results after the tests (plus "ng") 67
Figure 67: Example spectrum separation of 90Sr 68
Figure 68: Example spectrum 2nd washing bottle of the 1st H2SO4 sample 68

Figure 69: Spectra AOC 13.2, 14.2, 14.3 and 15. 68

1.2. List of Tables

Table 1: Reactions with graphite 5
Table 2: Wigner energy generated inside the graphite as a result of neutron radiation (left). Energy stored in the graphite that remains after annealing at 1000°C (right) 69
Table 3: Radionuclides in sample T10 (Merlin) 69
Table 4: ICP/MS measurement data (Merlin) 71
Table 5: Extraction thimble material (Merlin) 72
Table 6: Sample weight γ spectrometry (Merlin) 72
Table 7: LSC: Leaching samples measuring results 73
Table 8: Radionuclides in the HTR samples (all measured values are in Bq/g) 74
Table 9: Comparison oh the activity in the samples AVR-1 to AVR-8/AVR-G-19 74
Table 10: Analysis results from ICP/MS measurements for AVR-G-19 75
Table 11: Tare, gross and net weight of the measuring tubes or samples before the test (AVR) 75
Table 12: Tare, gross and net weight of the measuring tubes or samples after the test (AVR) 75
Table 13: Result of the γ spectrometry Cs-137 separation using AMP (AVR) 76
Table 14: Comparison of the activity of the nuclides with the permissible limits for disposal (Merlin) 76
Table 15: Comparison of the activity of the nuclides with the permissible limits for disposal (AVR) 76
Table 16: AVR leaching results 77

- ## 1.3. List of Equations

Equation 1: ^{90}strontium content of the leaching solution/g graphite 29
Equation 2: Solute specific activity of the AMP sample 30
Equation 3: Activity of the organic solvent samples 33
Equation 4: Activity of the aqueous solvent samples 33
Equation 5: Activity per mL 33
Equation 6: Total solute activity per g of graphite 33

- 2. Figures:
- 2.1. Figures (Merlin)

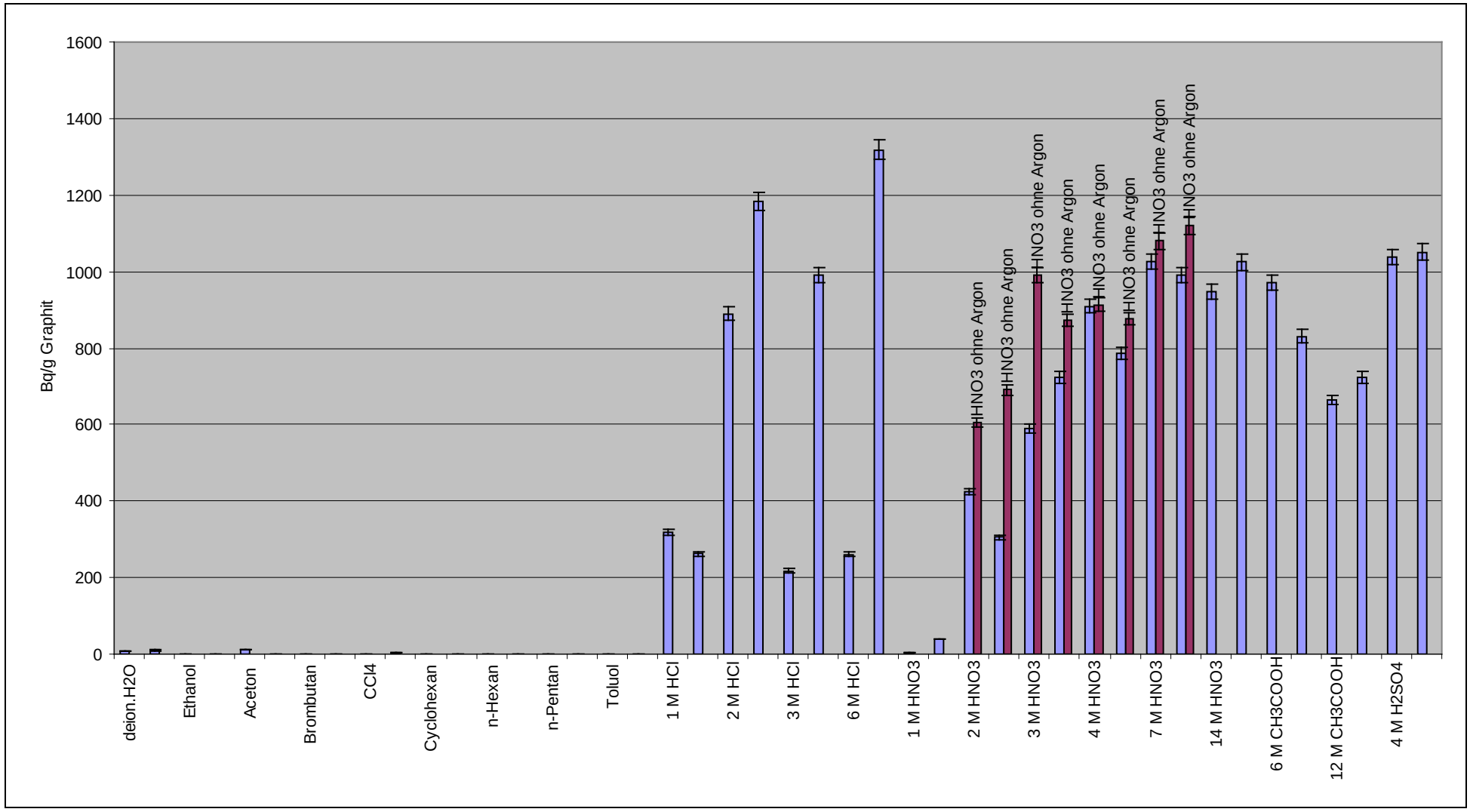

Figure 59: Overview of all of the measuring results from the Merlin leaching samples

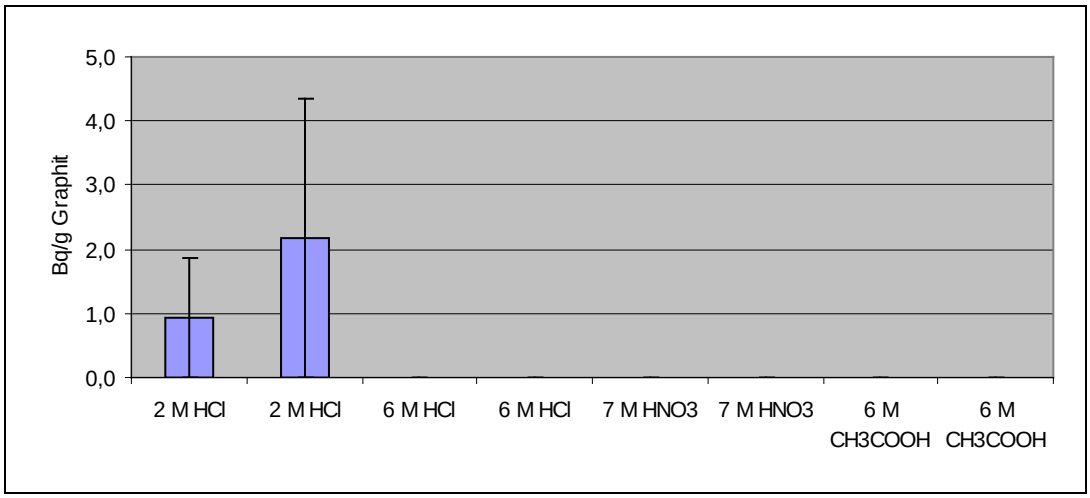

Figure 60: Measuring result of the ^{90}Sr separation

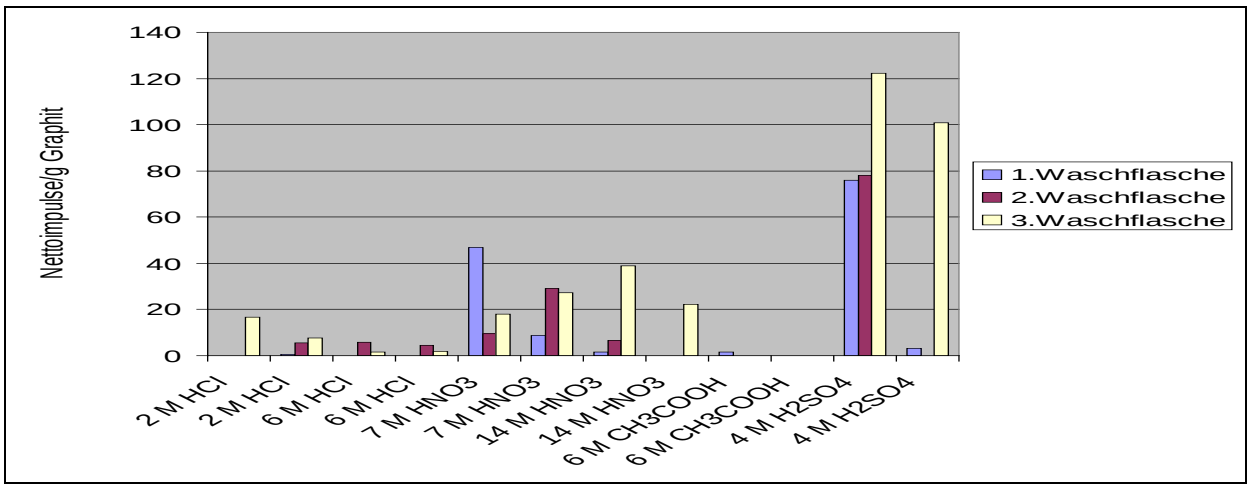

Figure 61: Net pulses washing bottles

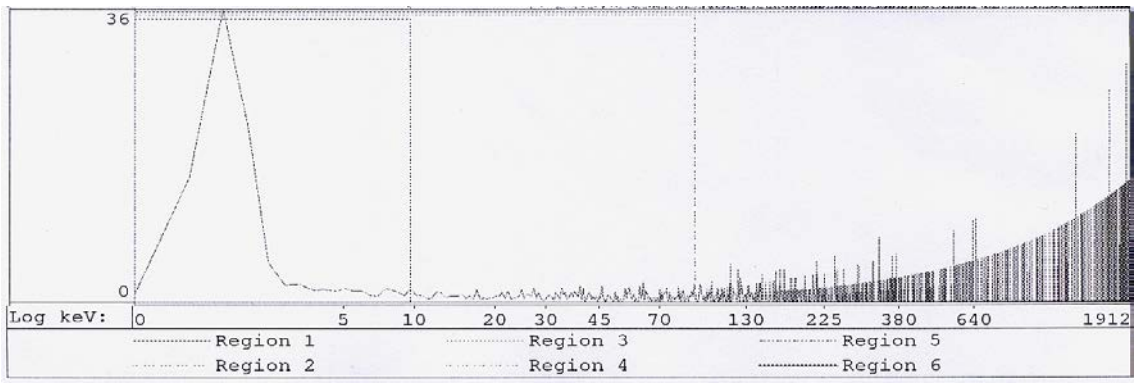

Figure 62: Spectrum 1st sample H_2SO_4, 3rd washing bottle

- 2.2. Figures (AVR)

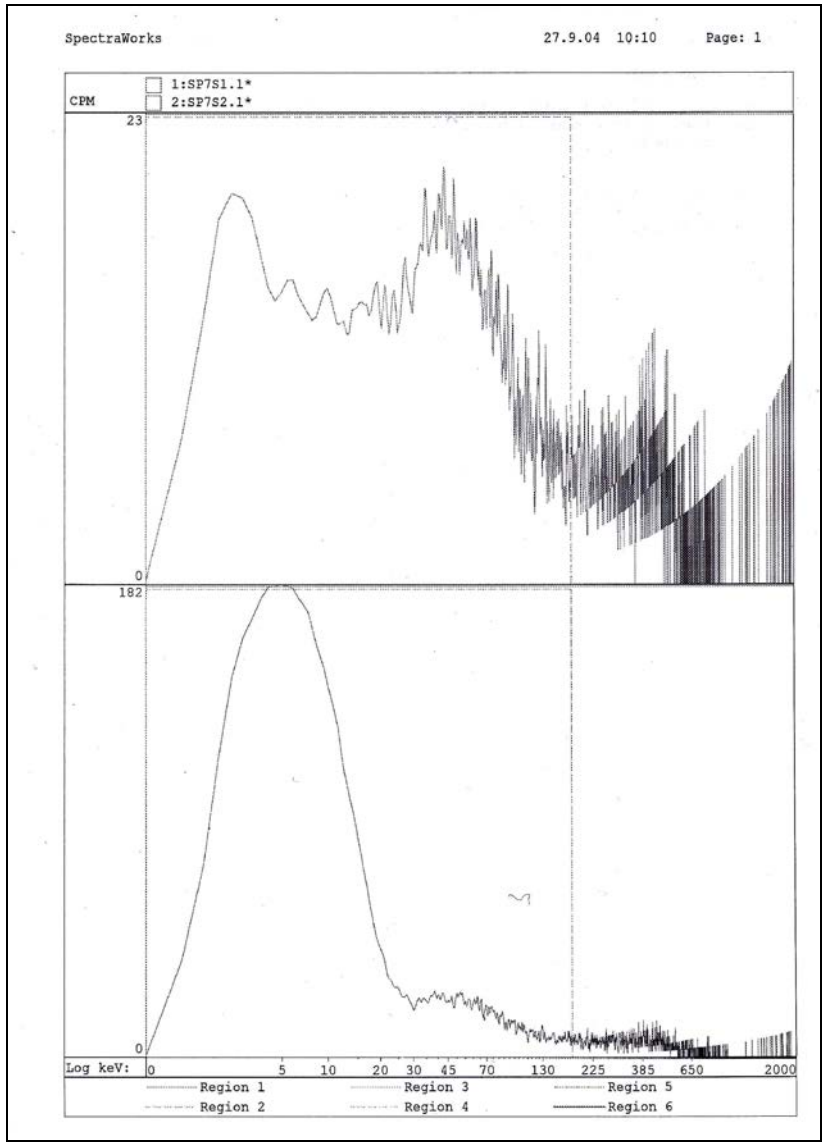

Figure 63: Spectra AVR-13 and 14 (1st extraction of the H_2SO_4 samples)

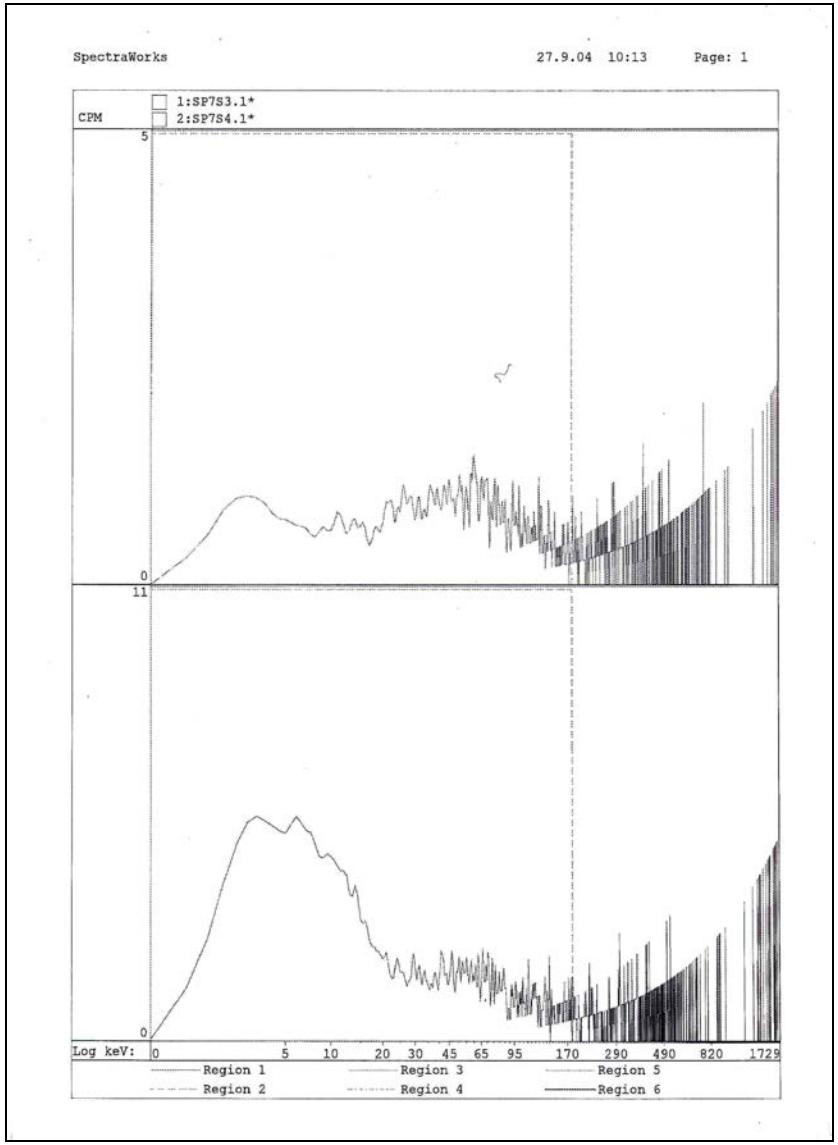

Figure 64: Spectra AVR-15 and 16 (2nd extraction of the H_2SO_4 samples)

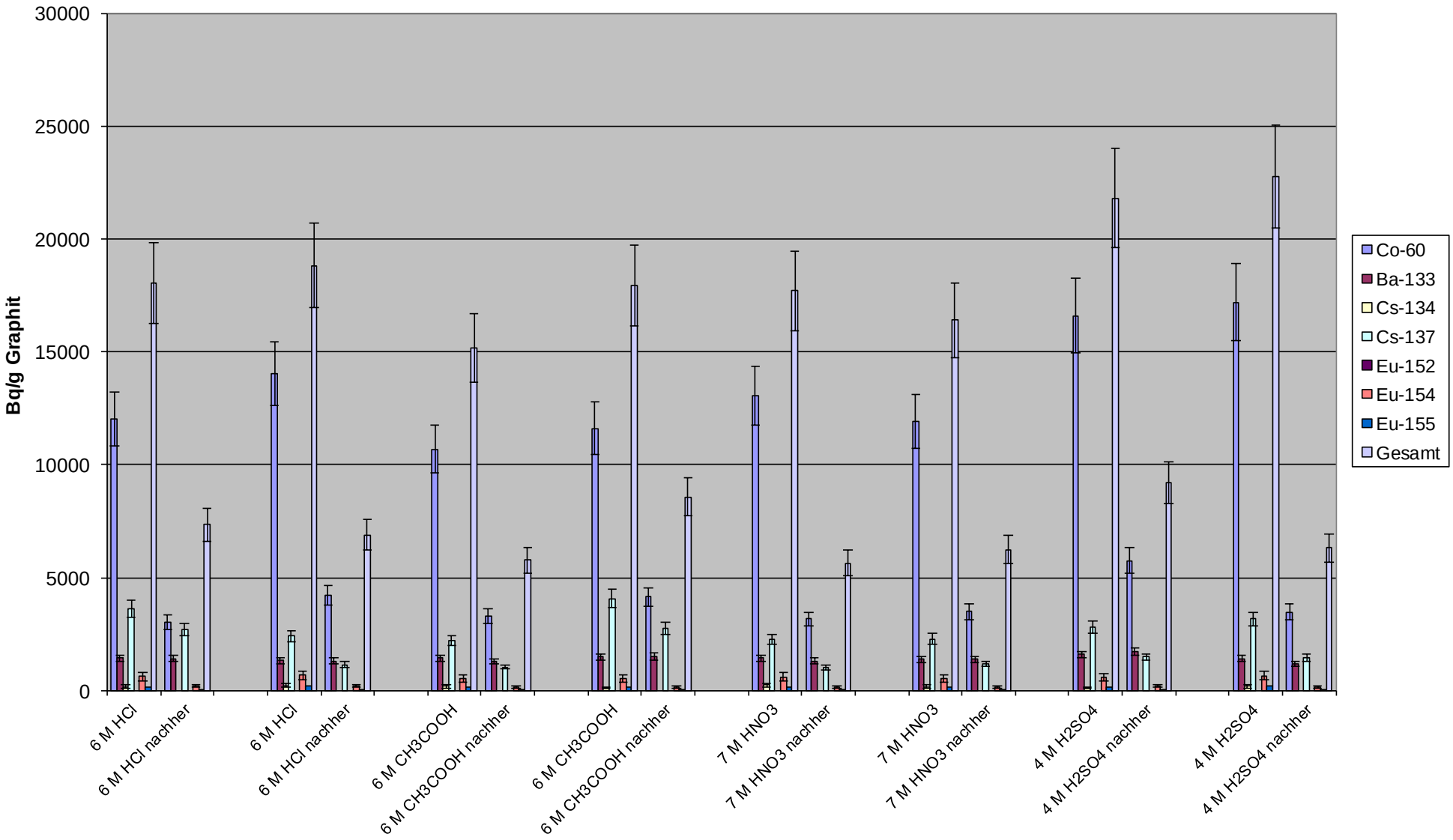

Figure 65: Comparison of the activity of the individual nuclides of the solid material samples before and after leaching

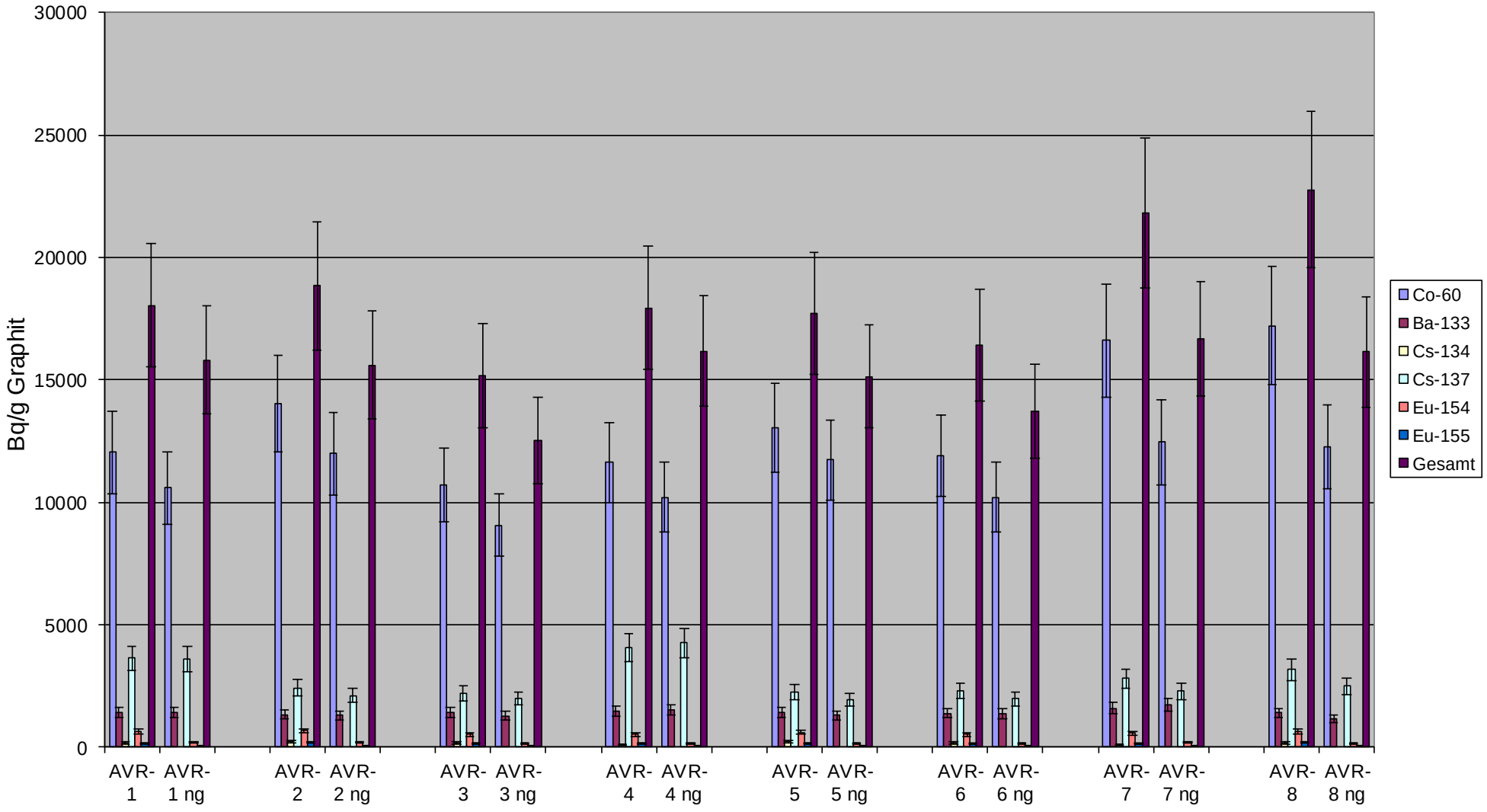

Figure 66: Comparison of the activity of the solid material samples before the tests with the sum of all measuring results after the tests (plus "ng")

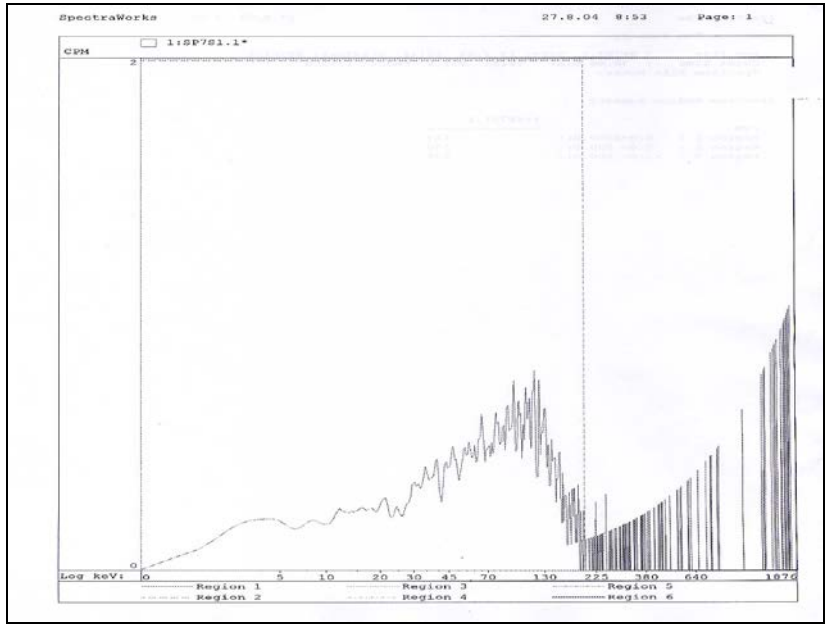

Figure 67: Example spectrum separation of ^{90}Sr

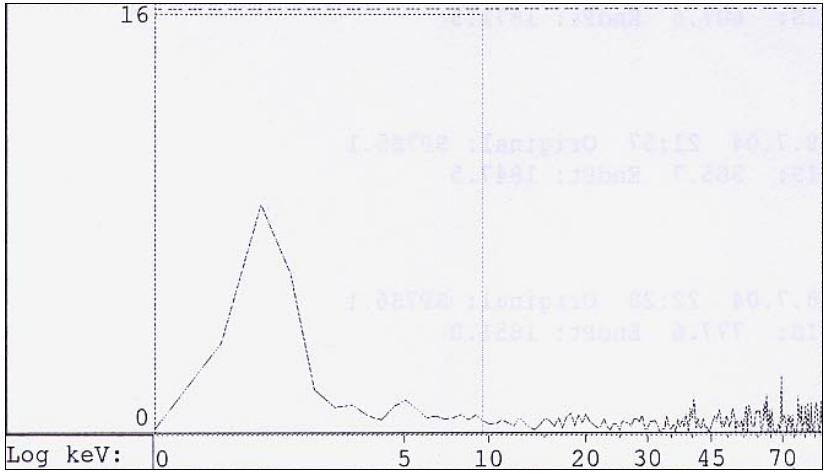

Figure 68: Example spectrum 2nd washing bottle of the 1st H_2SO_4 sample

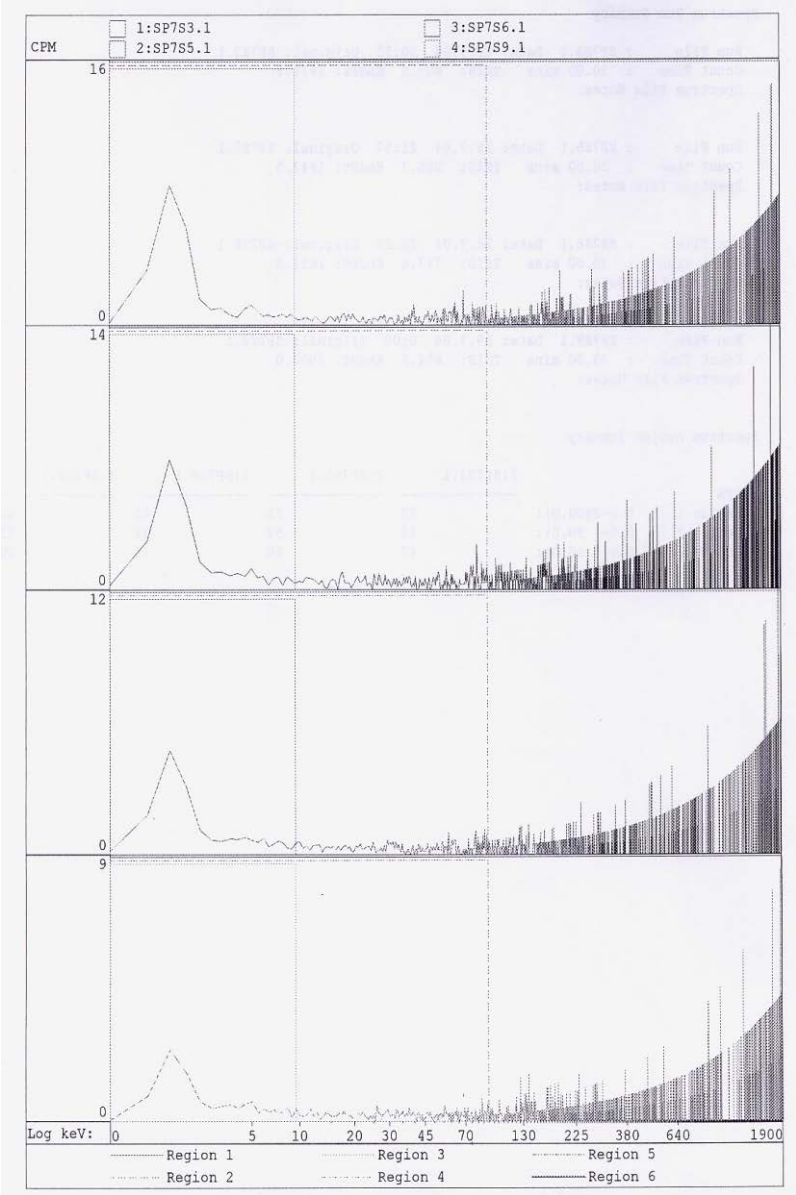

Figure 69: Spectra AOC 13.2, 14.2, 14.3 and 15.

- 3. Tables:
- 3.1. Tables (Merlin)

Table 2: Wigner energy generated inside the graphite as a result of neutron radiation (left). Energy stored in the graphite that remains after annealing at 1000°C (right)

Irritation temperature	Dose [*n*/cm²]	Wigner energy [cal/g]
30°C	$5 \cdot 10^{20}$	250
	$10 \cdot 10^{20}$	400
	$15 \cdot 10^{20}$	500
193°C	$5.3 \cdot 10^{20}$	61
230°C	$5.7 \cdot 10^{20}$	55
252°C	$4.8 \cdot 10^{20}$	49

Irritation dose	Stored energy [cal/g]	Stored energy after ignition [cal/g]
$2.5 \cdot 10^{20}$	160	~5
$5 \cdot 10^{20}$	260	30
$10 \cdot 10^{20}$	390	100
$15 \cdot 10^{20}$	480	180
$20 \cdot 10^{20}$	540	250

[15]

Table 3: Radionuclides in sample T10 (Merlin)

Nuclide	Decay	Product	State	HWZ	Sample [Bq/g]	
					TS 10/1	TS 10/2
H-3	ß-	He-3	stable	12.33a	4700	4760
C-14	ß-	N-14	stable	5370a	505	449
Fe-55	ε	Mn-55	stable	2.73a	<0.05	<0.003
Co-60	ß-	Ni-60	stable	5.2714a	983	956
Ba-133	ε	Cs-133	stable	10.51a	5.83	4.71
Eu-152	ε	Gd-152	stable	13.537a	986	959
Eu-154	ß-/ß+ e	Gd-154/Sm-154	stable	8.593a	89.8	88.3
Eu-155	ß-	Gd-155	stable	4.76a	5.74	5.51
Total - α					<0.003	<0.003
Total - β,γ					2210	-*

* not measured

Table 4: ICP/MS measurement data (Merlin)

	TS 6/2 [µg/g]	Error [%]	TS 7/2 [µg/g]	Error [%]	TS 8/2 [µg/g]	Error [%]	TS 9/2 [µg/g]	Error [%]	TS 10/2 [µg/g]	Error [%]
Al	2,68	20	1,75	20	0,77	20	2,52	20	3,37	20
As	0,02	20	<0,04		<0,04		0,02	20	0,04	30
Ag	<0,04		<0,04		<0,04		<0,04		<0,04	
Ba	3,52	20	6,94	20	4,64	20	5,67	20	4,49	20
Be	0,03	15	<0,04		<0,04		<0,04		<0,04	
Ca	21,24	35	9,56	40	19,93	40	19,86	45	201,18	25
Co	0,05	15	<0,04		<0,04		<0,04		0,19	20
Cd	0,06	30	<0,04		<0,04		0,04	20	0,11	25
Cr	0,18	15	<0,04		<0,04		0,09	20	1,09	20
Cu	0,84	20	0,04	20	0,05	20	0,08	20	0,07	20
Li	0,30	20	0,21	20	0,38	20	0,19	25	0,50	20
Mg	1,04	20	0,99	20	<0,04		1,41	20	1,28	20
Mn	0,13	15	<0,04		<0,04		0,05	20	0,05	20
Mo	0,19	15	0,28	20	0,18	20	0,03	20	0,14	25
Na	17,73	20	13,99	20	9,65	20	18,80	20	24,71	20
Ni	1,52	20	3,83	20	2,40	20	2,49	20	30,60	20
Pb	0,43	20	0,04	20	0,10	20	0,56	20	1,60	20
Sb	<0,04		<0,04		<0,04		<0,04		<0,04	
Se	<0,04		<0,04		<0,04		<0,04		<0,04	
Sr	0,92	20	1,13	20	0,87	20	1,50	20	5,58	20
Tl	<0,04		<0,04		<0,04		<0,04		<0,04	
U	<0,04		<0,04		<0,04		<0,04		<0,04	
V	18,07	20	12,92	20	41,97	20	26,47	20	94,52	20
Zn	1,14	20	<0,04		0,09	20	0,98	20	4,96	25
Ce	0,33	20	0,18	20	0,47	20	0,25	20	0,12	20
Dy	0,04	25	0,03	25	0,07	20	0,04	25	<0,04	
Er	<0,04		<0,04		0,04	20	<0,04		<0,04	
Eu	<0,04		<0,04		<0,04		<0,04		<0,04	
Gd	0,06	20	0,04	30	0,11	20	0,06	20	<0,04	
Ho	<0,04		<0,04		<0,04		<0,04		<0,04	
La	0,15	20	0,08	20	0,22	20	0,11	20	0,06	25
Lu	<0,04		<0,04		<0,04		<0,04		<0,04	
Nd	0,23	20	0,14	20	0,33	20	0,21	20	0,07	20
Pr	0,04	20	<0,04	15	0,06	20	0,03	20	<0,04	
Sm	0,04	30	0,04	20	0,05	25	0,07	20	0,04	30
Sc	<0,04		<0,04		<0,04		0,03	20	<0,04	
Tb	<0,04		<0,04		<0,04		<0,04		<0,04	
Th	<0,04		<0,04		<0,04		<0,04		<0,04	
Tm	<0,04		<0,04		<0,04		<0,04		<0,04	
Yb	<0,04		<0,04		<0,04		<0,04		<0,04	
Y	0,24	20	0,12	20	0,39	20	0,18	20	0,07	17
Hf	<0,04		<0,04		<0,04		<0,04		<0,04	
W	0,06	25	0,06	20	<0,04		0,04	25	<0,04	
Sn	<0,04		<0,04		<0,04		<0,04		<0,04	
Nb	<0,04		<0,04		<0,04		<0,04		<0,04	
Zr	<0,04		<0,04		<0,04		<0,04		<0,04	
Ti	<0,04		<0,04		<0,04		<0,04		3,26	20
Pd	<0,04		<0,04		<0,04		<0,04		<0,04	
Cs	<0,04		<0,04		<0,04		<0,04		<0,04	
Rb	<0,04		<0,04		<0,04		<0,04		<0,04	
Ga	0,17	20	0,34	20	0,22	20	0,28	20	0,22	20
K	<0,04		<0,04		<0,04		<0,04		<0,04	

[27]

Table 5: Extraction thimble material (Merlin)

Test Nos.	Tests	Solvent	Duration of an extraction process	Sleeve material	Scintillator
1, 2, 29 u. 30	4	deion.H_2O	ca. 9 min	Paper	Insta-Gel Plus
3, 4, 31 u. 32	4	Ethanol	ca. 7 min	Paper	Insta-Gel Gold F
5, 6, 33, 34, 59, 60, 63, 64, 71, 72, 75, 76, 79 u. 80	14	1 M HCl	ca. 8 min	Paper	Insta-Gel Plus
7,8, 35, 36, 61, 62, 65, 66, 73, 74, 77, 78, 81 u. 82	14	1 M HNO_3	ca. 8 min	Paper	Insta-Gel Plus
9 u. 10	2	2 M HCl	ca. 9 min	Paper	Insta-Gel Plus
11, 12, 49 u. 50	4	2 M HNO_3	ca. 30 min*/ ca. 7 min	Paper	Insta-Gel Plus
13 und 14	2	3 M HCl	ca. 9 min	Paper	Insta-Gel Plus
15, 16, 45 u. 46	4	3 M HNO_3	ca. 30 min*/ ca. 7 min	Paper	Insta-Gel Plus
17 u. 18	2	Cyclohexane	ca. 4 min	Paper	Insta-Gel Gold F
19, 20, 47 u. 48	4	4 M HNO_3	ca. 25 min*/ca. 6 min	Fibre glass	Insta-Gel Plus
21 u. 22	2	Acetone	ca. 6 min	Paper	Insta-Gel Gold F
23 u. 24	2	n-Hexane	ca. 4 min	Paper	Insta-Gel Gold F
25 u. 26	2	Brombutane	ca. 3 min	Paper	Insta-Gel Gold F
27 u. 28	2	n-Pentane	ca. 4 min	Paper	Insta-Gel Gold F
37 u. 38	2	6 M HCl	ca. 9 min	Fibre glass	Insta-Gel Plus
39, 40, 51 u. 52	4	7 M HNO_3	ca. 20 min*/ ca. 6 min	Fibre glass	Insta-Gel Plus
41 u. 42	2	CCl_4	ca. 4 min	Paper	Insta-Gel Gold F
43 u. 44	2	14 M HNO_3	ca. 30 min	Fibre glass	Insta-Gel Plus
53, 54, 83 - 88	8	6 M CH_3COOH	ca. 8 min	Paper	Insta-Gel Plus
55 u. 56	2	12 M CH_3COOH	ca. 5 min	Paper	Insta-Gel Plus
57, 58, 89 - 94	8	4 M H_2SO_4	ca. 8 min	Fibre glass	Insta-Gel Plus
67 - 70	4	Toluene	ca. 3 min	Paper	Insta-Gel Gold F

* when adding argon

Table 6: Sample weight γ spectrometry (Merlin)

Test	Solvents	Tare [g]	Gross [g]	Net [g]
solid - 9	2 M HCl	2.6929	2.796	0.1033
solid - 10	2 M HCl	2.6861	2.782	0.0961
solid - 37	6 M HCl	2.7067	2.804	0.0976
solid - 38	6 M HCl	2.6733	2.773	0.1001
solid - 39	7 M HNO3	2.6656	2.769	0.1037
solid - 40	7 M HNO3	2.7037	2.799	0.0949
solid - 43	14 M HNO3	2.7366	2.84	0.1031
solid - 44	14 M HNO3	2.6851	2.785	0.1
solid - 53	6 M CH3COOH	2.6934	2.805	0.1111
solid - 54	6 M CH3COOH	2.7732	2.88	0.1063
solid - 57	4 M H2SO4	2.7269	2.831	0.1042
solid - 58	4 M H2SO4	2.7069	2.798	0.091

Table 7: LSC: Leaching samples measuring results

No.	Test.-No.	Flask	[mL]		Scintillator	tSIE	[cps]	[Bq]/mL	[Bq]	[Bq] Flask	Graphite [g]	[Bq] Flask/g Graphite
29	29	deion.H2O	2	neutral	Instagel Plus	403	0.97	0.09	0.19	3.11	0.5042	6.16
30	30	deion.H2O	2	neutral	Instagel Plus	395	1.07	0.14	0.29	4.92	0.4973	9.90
31	31	Ethanol	2	organic	Gold F	671	0.92	0.03	0.05	0.73	0.4963	1.47
32	32	Ethanol	2	organic	Gold F	658	0.91	0.02	0.04	0.58	0.5015	1.17
21	21	Acetone	2	organic	Gold F	550	1.07	0.19	0.38	5.96	0.4989	11.95
22	22	Acetone	2	organic	Gold F	555	0.73	0.02	0.04	0.53	0.5024	1.06
25	25	Brombutane	2	organic	Gold F	583	0.71	0.01	0.02	0.30	0.5019	0.59
26	26	Brombutane	2	organic	Gold F	581	0.71	0.01	0.02	0.34	0.4995	0.67
55	41	CCl4	2	organic	Gold F	12	0.50	0.01	0.01	0.16	0.5023	0.32
56	42	CCl4	2	organic	Gold F	21	0.60	0.06	0.11	1.98	0.4975	3.97
17	17	Cyclohexane	2	organic	Gold F	778	0.67	0.01	0.02	0.25	0.4997	0.49
18	18	Cyclohexane	2	organic	Gold F	781	0.68	0.02	0.03	0.42	0.4976	0.84
23	23	n-Hexane	2	organic	Gold F	779	0.64	-0.02	-0.03	-0.53	0.5038	-1.05
24	24	n-Hexane	2	organic	Gold F	776	0.66	-0.01	-0.01	-0.17	0.5022	-0.34
27	27	n-Pentane	2	organic	Gold F	803	0.67	0.02	0.03	0.35	0.4977	0.69
28	28	n-Pentane	2	organic	Gold F	796	0.66	0.01	0.02	0.26	0.4981	0.52
97	67	Toluene	2	organic	Gold F	798	0.70	0.02	0.03	0.46	0.4963	0.92
98	68	Toluene	2	organic	Gold F	782	0.70	0.15	0.03	0.50	0.4997	0.99
33	33	1 M HCl	1	acidic	Instagel Plus	342	5.50	4.72	4.72	160.26	0.5033	318.42
34	34	1 M HCl	1	acidic	Instagel Plus	348	4.41	3.63	3.63	132.07	0.5031	262.51
9	9	2 M HCl	1	acidic	Instagel Plus	317	13.57	12.79	12.79	449.10	0.5047	889.83
10	10	2 M HCl	1	acidic	Instagel Plus	335	18.90	18.12	18.12	599.28	0.5057	1185.05
13	13	3 M HCl	1	acidic	Instagel Plus	235	5.90	5.12	5.12	109.03	0.5003	217.92
14	14	3 M HCl	1	acidic	Instagel Plus	292	16.16	15.38	15.38	497.95	0.5020	991.92
51	37	6 M HCl	1	acidic	Instagel Plus	344	2.88	4.19	2.10	130.58	0.5004	260.95
52	38	6 M HCl	1	acidic	Instagel Plus	340	10.60	19.63	9.82	659.60	0.5002	1318.72
35	35	1 M HNO3	2	acidic	Instagel Plus	251	1.02	0.12	0.24	2.83	0.5029	5.62
36	36	1 M HNO3	2	acidic	Instagel Plus	269	2.47	0.84	1.69	19.60	0.5023	39.01
11	11	2 M HNO3	2	acidic	Instagel Plus	168	14.31	6.76	13.53	211.20	0.4988	423.42
12	12	2 M HNO3	2	acidic	Instagel Plus	188	9.39	4.30	8.61	153.29	0.5027	304.94
15	15	3 M HNO3	1	acidic	Instagel Plus	212	9.77	8.99	8.99	293.39	0.4986	588.43
16	16	3 M HNO3	1	acidic	Instagel Plus	224	10.66	9.88	9.88	360.70	0.4990	722.85
19	19	4 M HNO3	1	acidic	Instagel Plus	191	13.75	12.97	12.97	454.68	0.5001	909.17
20	20	4 M HNO3	1	acidic	Instagel Plus	193	11.43	10.65	10.65	395.09	0.5037	784.37
53	39	7 M HNO3	0 . 5	acidic	Instagel Plus	226	8.63	15.69	7.85	512.07	0.4989	1026.41
54	40	7 M HNO3	0 . 5	acidic	Instagel Plus	227	7.95	14.33	7.17	496.91	0.5010	991.83
57	43	14 M HNO3	0.25	acidic	Instagel Plus	262	4.63	15.39	3.85	475.94	0.5023	947.53
58	44	14 M HNO3	0.25	acidic	Instagel Plus	267	4.27	13.95	3.49	513.25	0.5009	1024.66
73	53	6 M CH3COOH	1	acidic	Instagel Plus	373	15.94	15.16	15.16	484.39	0.4992	970.34
74	54	6 M CH3COOH	1	acidic	Instagel Plus	370	11.84	11.06	11.06	411.87	0.4956	831.06
75	55	12 M CH3COOH	0 . 5	acidic	Instagel Plus	362	6.60	11.63	5.82	329.51	0.4962	664.07
76	56	12 M CH3COOH	0 . 5	acidic	Instagel Plus	364	6.00	10.43	5.22	364.61	0.5037	723.86
77	57	4 M H2SO4	1	acidic	Instagel Plus	325	10.76	19.95	9.98	511.39	0.4930	1037.30
78	58	4 M H2SO4	1	acidic	Instagel Plus	335	9.21	16.85	8.43	520.73	0.4955	1050.92

- ## 3.2. Tables (AVR)

Table 8: Radionuclides in the HTR samples (all measured values are in Bq/g)

Nuclide	AVR-G-7	AVR-G-8	AVR-G-9	AVR-G-10	AVR-G-11	AVR-G-12	AVR-G-13	AVR-G-14	AVR-G-15	AVR-G-18	AVR-G-19
H-3*	1600000	884000	1600000	1200000							
C-14*	104000	95000	135000	63000							
Cl-36	23	21	27	24							
Ca-41	290	320	1230	EKG							
Fe-55	27000	18500	12800	255000							
Ni-59	3200*	2700*	5750*	107000*							
Ni-63	*	*	*	*							
Sr-90*	5750	7150	6850	931000							
Mo-93	EKG	EKG	EKG	EKG							
Sn-126	EKG	EKG	EKG	EKG							
Sm-151	EKG			400							
Na-22	EKG										
Co-60	32000	27000	42500	410000	23638	7865	69886	82298	378155	1772000	31193
Sb-126	EKG	EKG	EKG	EKG	EKG	EKG	EKG	EKG	EKG	EKG	EKG
Ba-133	850	1140	1690	1700	EKG	2439	2240	EKG	1817	4228	1275
Cs-134	470	580	930	EKG	804	652	796	238	EKG	10436	694
Cs-137	780	1940	2250	4400	12851	3818	7203	2843	4664	5754	2986
Eu-152	100	650	EKG	EKG	EKG	EKG	EKG	EKG	EKG	EKG	EKG
Eu-154	860	560	440	9700	679	665	1523	1661	8286	27721	652
Eu-155	330	215	160	2100	111	255	520	629	3021	13784	268
Percentage of pure β-emitters*	96 %	95 %	97 %	76 %							

Table 9: Comparison of the activity in the samples AVR-1 to AVR-8/AVR-G-19

	Activity [Bq/g]								
• Sample	AVR-1	AVR-2	AVR-3	AVR-4	AVR-5	AVR-6	AVR-7	AVR-8	• AVR-G-19*
• Co-60	12040	14030	10693	11620	13050	11921	16610	17210	18642
Sb-126	n. meas.	n. meas.	n. meas.	n. meas.	n. meas.	n. meas.	n. meas.	n. meas.	EKG (15)
Ba-133	1425	1331	1431	1477	1420	1385	1585	1400	984.86
Cs-134	169	202	190	111	230	165	110	180	186.37
Cs-137	3623	2421	2204	4065	2252	2285	2810	3157	2728.3
Eu-152	<30	<30	<30	<30	<30	<30	<30	<30	EKG (25)
Eu-154	632	664	518	522	605	517	564	650	475.44
Eu-155	166	189	148	151	154	138	142	176	151.54
Ho-166m	n. meas.	n. meas.	n. meas.	n. meas.	n. meas.	n. meas.	n. meas.	n. meas.	EKG (10)

*The decay of the radionuclides contained in sample AVR-G-19 was taken into account

Measuring data: 18.07.2000 for AVR-G-19, 18.06.2004 for AVR-1 to AVR-8

Table 10: Analysis results from ICP/MS measurements for AVR-G-19

Element	Concentration [µg/g]	• Error [%]
Li	0.14	15
B	EKG (0.85)	
K	1.2	24
Ca	1.3	20
Fe	86	15
Co	0.0086	15
Ni	0.79	30
Nb	0.0024	15
Mo	0.11	15
Sn	EKG (0.14)	
Cs	EKG (0.0001)	
Ba	1.5	15
Sm	EKG (0.003)	
Ho	EKG (0.001)	

Table 11: Tare, gross and net weight of the measuring tubes or samples before the test (AVR)

	Solvent	Tare [g] before	Gross [g]	Net [g]	Tare [g] after	Δ before - after [g]
AVR-1	6 M HCl	2.7918	2.8308	0.039	2.7926	0.0008
AVR-2	6 M HCl	2.6851	2.7227	0.038	2.6859	0.0008
AVR-3	7 M HNO_3	2.6495	2.6862	0.037	2.6503	0.0008
AVR-4	7 M HNO_3	2.6984	2.7354	0.037	2.6993	0.0009
AVR-5	6 M CH_3COOH	2.6728	2.716	0.043	2.6735	0.0007
AVR-6	6 M CH_3COOH	2.6582	2.6973	0.039	2.6588	0.0006
AVR-7	4 M H_2SO_4	2.6877	2.729	0.041	2.6884	0.0007
AVR-8	4 M H_2SO_4	2.6785	2.7199	0.041	2.6794	0.0009

Table 12: Tare, gross and net weight of the measuring tubes or samples after the test (AVR)

Test-No.	Solvent	Tare [g]	Gross [g]	Net [g]
AVR-1	6 M HCl	2.7926	2.8168	0.0242
AVR-2	6 M HCl	2.6859	2.7174	0.0315
AVR-3	7 M HNO_3	2.6503	2.6823	0.032
AVR-4	7 M HNO_3	2.6991	2.7291	0.03
AVR-5	6 M CH_3COOH	2.6734	2.7065	0.0331
AVR-6	6 M CH_3COOH	2.6588	2.6917	0.0329
AVR-7	4 M H_2SO_4	2.684	2.7114	0.0274
AVR-8	4 M H_2SO_4	2.6794	2.7151	0.0357

Table 13: Result of the γ spectrometry Cs-137 separation using AMP (AVR)

Bq / 0.5mL		
Sample No.	**Cs-137**	**Co-60**
AMP1	< 0.01	0.71
AMP2	< 0.01	1.29
AMP3	< 0.01	< 0.01
AMP4	< 0.01	< 0.01
AMP5	< 0.01	0.89
AMP6	< 0.01	0.82
AMP7	< 0.01	< 0.01
AMP8	< 0.01	0.03
AMP9	< 0.01	1.06
AMP10	< 0.01	0.75
AMP11	< 0.01	0.02
AMP12	< 0.01	< 0.01
AMP13	< 0.01	< 0.01
AMP14	< 0.01	0.04
AMP15	< 0.01	0.12
AMP16	< 0.01	0.16

Table 14: Comparison of the activity of the nuclides with the permissible limits for disposal (Merlin)

	Measured values [Bq/g]				Permitted limit for removal** [Bq/g]
Nuclide	A of the sample at t=0		A of the sample at t=40a		
	TS 10/1	TS 10/2	TS 10/1	TS 10/2	
H-3	4700	4760	496.0	426.6	1000
C-14	505	449	502.4	502.2	2000
Fe-55	0.05	0.003	0.000	0.000	10000
Co-60	983	956	5.1	3.4	4
Ba-133	5.83	4.71	0.4	0.3	30
Eu-152	986	959	127.2	108.8	8
Eu-154	89.8	88.3	3.6	2.8	7
Eu-155	5.74	5.51	0.0	0.0	100

Table 15: Comparison of the activity of the nuclides with the permissible limits for disposal (AVR)

Nuclide	Permitted limit for removal	AVR-G-19	
	Bq/g	T = 0	T = 40a
Co-60	4	31193	162
Ba-133	30	1275	91
Cs-134	6	694	0
Cs-137	10	2986	1188
Eu-154	7	652	26
Eu-155	100	268	1

Table 16: AVR leaching results

No.	Test-No.	Solvents	mL		Scintillator	tSIE	[cps]	[Bq]/ mL	[Bq]	[Bq] Flask	Graphite [g]	Bq/g Graphite
199	AVR-1	6 M HCl	0.50	acidic	Instagel Plus	337	9.95	18.33	9.17	811.30	0.0384	21128
201	AVR-2	6 M HCl	0.50	acidic	Instagel Plus	337	7.67	13.76	6.88	573.70	0.0377	15217
202	AVR-3	6 M HCl	0.50	acidic	Instagel Plus	333	1.83	2.09	1.05	102.25	0.0384	2663
203	AVR-4	6 M HCl	0.50	acidic	Instagel Plus	333	1.44	1.31	0.66	59.16	0.0377	1569
204	AVR-5	6 M CH3COOH	0.50	acidic	Instagel Plus	369	5.94	10.31	5.16	465.16	0.0364	12779
205	AVR-6	6 M CH3COOH	0.50	acidic	Instagel Plus	367	6.11	10.65	5.33	430.35	0.0371	11600
206	AVR-7	6 M CH3COOH	1.00	acidic	Instagel Plus	371	1.70	0.92	0.92	44.88	0.0364	1233
207	AVR-8	6 M CH3COOH	1.00	acidic	Instagel Plus	371	1.64	0.86	0.86	39.27	0.0371	1059
208	AVR-9	7 M HNO3	0.50	acidic	Instagel Plus	250	10.40	19.23	9.62	851.92	0.0425	20045
209	AVR-10	7 M HNO3	0.50	acidic	Instagel Plus	255	6.55	11.53	5.77	532.76	0.0387	13766
210	AVR-11	7 M HNO3	0.50	acidic	Instagel Plus	259	1.00	0.43	0.22	20.80	0.0425	489
211	AVR-12	7 M HNO3	0.50	acidic	Instagel Plus	258	0.99	0.41	0.21	19.76	0.0387	511
212	AVR-13	4 M H2SO4	1.00	acidic	Instagel Plus	327	11.81	11.03	11.03	530.98	0.0408	13014
213	AVR-14	4 M H2SO4	1.00	acidic	Instagel Plus	324	59.51	58.73	58.73	2739.10	0.0408	67135
214	AVR-15	4 M H2SO4	1.00	acidic	Instagel Plus	337	2.96	2.18	2.18	119.97	0.0408	2940
215	AVR-16	4 M H2SO4	1.00	acidic	Instagel Plus	333	4.37	3.59	3.59	199.03	0.0408	4878

G. References

1. Barnes, M.J., DiPrete, D.P., Hobbs, D.T., et al. (2004) Effects of Ammonium Molybdophosphate (AMP) on Strontium, Actinides, and RCRA Metals in SRS Simuleted Waste

2. Becker, H. Sicherheitsbericht für den Forschungsreaktor FRJ-1 (Merlin) Landesamt für Forschung 1960

3. Bergerfurth, A. Spannungsanalyse eines HTR-Deckenreflektors am Beispiel des AVR-Reaktors (Juli 1987) Berichte der Kernforschungsanlage Jülich Jül-2147

4. Billington D.S., Crawford J.H., Radiation Damage in Solids (1961) Princeton University Press

5. Bisplinghoff, B. (2000) AVR-Analytik - Ergebnisbericht – Institut für Sicherheitsforschung und Reaktortechnik des Forschungszentrum Jülich

6. Borchardt, G. (1973) Ergebnisse der Flussdichtemessungen in den Experimentier-Positionen des FRJ-1 und des FRJ-2 nach Leistungserhöhung auf 10 bzw. 25 MW. Berichte der Kernforschungsanlage Jülich Jül-1022

7. Cordewiner, H.J. (1979) Numerische Berechnung des Tritium-Verhaltens von Kugelhaufenreaktoren am Beispiel des AVR-Reaktors. Berichte der Kernforschungsanlage Jülich Jül-1607

8. Delle, W. (1983) Technische Notiz IRW-TN-43/83, Zum Bestrahlungsverhalten des Reflektorgraphits im AVR, AVR/AMT der Firma Sigri Elektrographit GmbH, Institut für Reaktorwerkstoffe, KFA Jülich

9. Delle, W. (1983) Technische Notiz IRW-TN-87/83, Vergleich der bestrahlungsinduzierten Dimensionsänderungen des AVR-Reflektormaterials mit dem britischen Nukleargraphit P.G.A., Institut für Reaktorwerkstoffe, KFA Jülich

10. Fassbender, J., Münch, E., Nutbohm, D., Thamm, G. (1973) Die gegenwärtige und zukünftige Nutzung der Forschungsreaktoren FRJ-1 (Merlin) und FRJ-2 (DIDO) der Kernforschungsanlage Jülich. Bericht der Zentralabteilung Forschungsreaktoren

11. Fiege, A., (Juli 1992) Tritium KfK 5055 Berichte des Kernforschungszentrum Karlsruhe

12. Fischer, P.G., Verhalten von Tritium in Reaktorgraphiten (1975) Berichte der Kernforschungsanlage Jülich Jül-1238

13. Gaus, H., Hensel, W., Hoinkis, E., Stritzke, D. (1979) Untersuchungen zum Cäsium-Transport in Graphit Berichte des Hahn-Meitner-Institut Berlin HMI-B 315

14. Gerbhardt, E., Thümmler, F., (1969) Reaktorwerkstoffe Band 1 Keramische und Pulvermetallurgische Werkstoffe. B.G. Teubner Verlag Stuttgart

15. Gerbhardt, E., Thümmler, F., (1969) Reaktorwerkstoffe Band 2 Keramische und Pulvermetallurgische Werkstoffe. B.G. Teubner Verlag Stuttgart

16. Greenwood, N.N., Earnshaw, A., Chemie der Elemente, 1.Auflage 1988, VCH

17. Haag, G. (Juli 1973) Über die Graphitierung polykristalliner Kohlenstoffe bei Bestrahlung mit schnellen Neutronen. Berichte der Kernforschungsanlage Jülich, Jül-959-RW

18. Holland, D., Quade, U., Bach, F.W., Wilk, P., A German Research Project about Applicable Graphite Cutting Techniques - Proceedings for the Technical Committee Meeting in Manchester, U.K. 1999.

19. Hollemann, A.F., Wiberg, E., (1985) Lehrbuch der Anorganischen Chemie, 91.-100., verbesserte und stark erweiterte Auflage, deGruyter

20. Jander, G., Blasius, E., Einführung in das anorganisch chemische Praktikum einschließlich der quantitativen Analyse 13., neu bearbeitete Auflage Hirzel Stuttgart 1990

21. Küster, F.W., Thiel, A., Ruland, A., Rechentafeln für die chemische Analytik, 104. bearbeitete Auflage 1993, de Gruyter Berlin

22. Kugeler, K., Schulten, R., Hochtemperaturreaktortechnik HTR 1.Auflage 1989, Springer-Verlag Berlin Heidelberg

23. Lederer, J.L., Wildberg W.D., Reaktorhandbuch 2. Neubearbeitete Auflage 1992, Carl Hanser Verlag München Wien

24. Lieser, K.H., Einführung in die Kernchemie, 3. Auflage 1991, VCH-Verlag

25. Lintner, K., Schmid, E., Werkstoffe des Reaktorbaues mit besonderer Berücksichtigung der Metalle, 1.Auflage 1962, Springer Berlin

26. Lochny, M. (2000) AVR-Analytik II – Ergebnisbericht - Interner Bericht des Forschungszentrums Jülich

27. Maischak, S., Fachinger J., Linse, G., Enge, R., Schädlich, W. (2002) α–, β–, γ–spektrometrische Untersuchungen an Graphitproben der Thermischen Säule 1 des FRJ-1 – Analysenbericht - Berichte des Forschungszentrums Jülich Jül-4014

28. Odoj, R., Qualitätskontrolle radioaktiver Abfälle – Methoden und Beispiele – Vortrag im Rahmen des Berufungsverfahren für das ISR am 25.Juni 2004.

29. Römpp Online, Version 2.3. (2004)

30. Schneider, W. (1971) Vorgesehene Flussmessungen in Experimentierpositionen zum Anfahrprogramm des FRJ-1 nach Umbau – Interner Bericht der KFA Jülich

31. Seelmann-Eggebert, W., et al., Karlsruher Nuklidkarte, 5.Auflage, 1981

32. Söder, B. (1988) Der Einfluss von Struktur und Verunreinigungen auf die strahleninduzierte Selbstdiffusion in Graphit. Berichte des Max-Plank-Instituts für Plasmaphysik IPP 9/63

33. Stahn, B., Matela, K., Zehbe, C., Pöppinghaus, J., Cremer J. - Abbau des Reaktorblocks des Forschungsreaktors FRJ-1 (Merlin) atw48, (2003) Heft 6

34. Steinwarz, W. (1987) Tritium in HTR-Anlagen, Berichte der Kernforschungsanlage Jülich, Jül-2138

35. Umbau des AVR – Reaktors zu einer Prozesswärmeanlage - Ergebnisse der Vorplanungsphase (Juni 1985)

36. Yamagishi, H. (1991) Measurement of neutron flux in the AVR, Berichte des Forschungszentrums Jülich Jül-2467

37. Weise, H.-J., Filss, P. (1995) Identifikation von Beta-Nukliden und Analyse von Mehrfach-Beta-Spektren bei Messungen mit dem Flüssigszintillationsspektrometer (LSC)“ Berichte des Forschungszentrums Jülich Jül-3066

38. Zhang, Z.X., (1992) Untersuchungen zum Nachweis der Langzeitsicherheit bei der Endlagerung abgebrannter Hochtemperatur-Brennelemente in untertägigen Gebirgsformationen.

39. Ziegler, A., Lehrbuch der Reaktortechnik, Band 2 Reaktortechnik 1.Auflage 1984 Springer-Verlag Berlin Heidelberg